Brain state regulation during normal development: Changes in simultaneously recorded EEG–fMRI intrinsic neuronal activity fluctuations

Thesis

presented to the Faculty of Arts of the University of Zurich
for the degree of Doctor of Philosophy by

Rafael Lüchinger

Accepted in the autumn semester 2011
on the recommendation of

Prof. Dr. Lutz Jäncke and
Prof. Dr. Daniel Brandeis

Zürich, March 2, 2012

Contents

1 Summary

Adolescence, the transition from childhood to adulthood, is a critical stage in the human lifespan marked by substantial structural and functional brain changes. This neurodevelopmental process is captured by the resting EEG's decreasing low-frequency activity. However, these electrophysiological changes are poorly understood and there are no efforts so far to study the same phenomenon in fMRI. We used simultaneous EEG–fMRI to better understand the developmental changes in the EEG. The first study focused on the age range between 15 and 25 years. The EEG–fMRI correlations revealed frequency and condition specific functional connections between resting EEG activity and fMRI networks. However, these EEG–fMRI correlations were stable and did not change between these age groups, although the age related decrease of low-frequency EEG activity was observed even at this late stage of brain maturation. Thus, the second study comprised a broader age range from 10 to 25 years and additional methods to compare the development in EEG and fMRI. Again, the EEG–fMRI network correlations proved very stable despite dramatic changes in EEG activity. We concluded that the EEG–fMRI correlations measure a distinct aspect of neurophysiological activity that matures earlier and is rather independent of the developmental process responsible for the low-frequency EEG attenuation. Independent from this EEG development, the EEG–BOLD correlations indicated developmental changes in thalamocortical activity. Additionally, the fMRI signal was quantified by the Fourier Transform similar to the EEG to get an equivalent measure of oscillatory activity. This comparison revealed that EEG and fMRI show very similar developmental feature of decreasing spontaneous activity. This functional development is in line with structural and metabolic brain developments which also show decreasing trajectories, and may reflect that neuronal efficiency increases with brain maturation.

Zusammenfassung

Adoleszenz, der Übergang von der Kindheit ins Erwachsenenalter ist eine sensible Phase im Leben einer Person. Das menschliche Gehirn erfährt dabei grundlegende strukturelle und funktionelle Veränderungen. Ein solcher neuronaler Entwicklungsprozess wird im EEG in Form von abnehmender tieffrequenter Aktivität abgebildet. Die elektrophysiologischen Veränderungen sind jedoch kaum verstanden und bisher wurden keine Bemühungen unternommen dasselbe Phänomen im fMRI zu studieren. Wir haben simultanes EEG–fMRI verwendet um die Entwicklungsprozesse im EEG besser zu verstehen. Die erste Arbeit fokussiert auf den Altersbereich von 15 bis 25 Jahren. Die EEG–fMRI Korrelationen brachten eine funktionelle Beziehung zwischen der EEG Ruheaktivität und fMRI Netzwerken zu Tage die von Frequenz und Zustand abhängig ist. Diese EEG-fMRI Korrelationen waren jedoch stabil und zeigten kaum Veränderung mit dem Alter, obwohl der altersabhängige Abnahme der tieffrequenter EEG Aktivität auch zu diesem späten Zeitpunkt der Hirnentwicklung festgestellt werden konnte. So umfasste die zweite Arbeit dann einen breiteren Altersbereich von 10 bis 25 Jahren und zusätzliche Methoden wurden eingeführt um die Entwicklung von EEG und fMRI zu vergleichen. Wiederum erwiesen sich die EEG–fMRI Korrelationen als sehr stabil trotz der dramatischen Veränderung im EEG. Wir folgern, dass die EEG–fMRI Korrelationen einen bestimmten Aspekt neurophysiologischer Aktivität messen, der sich früher entwickelt, und weitgehend unabhängig ist, vom Entwicklungsprozess der mit der Abnahme der tieffrequenten EEG Aktivität einhergeht. Unabhängig von diesem Entwicklungsprozess im EEG, decken die EEG–fMRI Korrelationen Entwicklungsveränderungen der thalamokortikalen Aktivität auf. Zusätzlich wurden die fMRI Daten Fourier-transformiert um ein dem EEG äquivalentes Mass der Aktivität zu erhalten. Dieser Vergleich zeigte, dass EEG und fMRI sehr ähnlich Entwicklungsmerkmale in Form von abnehmender spontaner Aktivität zeigen. Diese funktionelle Entwicklung scheint parallelen aufzuweisen mit strukturellen und metabolischen Daten zur Hirnentwicklung, die ebenfalls abnehmende Entwicklungsverläufe zeigen, und zusammengefasst womöglich die zunehmende neuronale Effizienz während der Hirnentwicklung widerspiegeln.

2 General Introduction

The research reported in this thesis aimed at finding novel markers of healthy human brain maturation. The General Introduction deals with the scientific background of the main topics addressed in this thesis. It follows two original articles reporting the research conducted. These articles build the core of this thesis and are published in the peer-reviewed journal "Neuroimage". A General Discussion will complete the thesis.

2.1 EEG and brain maturation

The electroencephalogram (EEG) measures neuronal brain activity on the scalp. The EEG signal arises from the summed, synchronous electrical activity of large neuron populations, predominantly from extended cortical sources near the scalp (e.g. cortical pyramidal cells) These specifications derive from to the topological and electrical properties of the volume conductor (brain, cerebrospinal fluid, skull, and scalp) (Lopes da Silva, 2010). The rhythmic background activity of the resting state EEG is characterized by oscillatory rhythms of diverse frequencies and amplitudes. The functional significance of these rhythms derives from the fact that the rhythmic compound of the EEG co-varies strongly with different levels of arousal and consciousness (Lopes da Silva, 2010). Although a huge body of literature has aggregated since the dawn of EEG research in the 1930ies, the exact physiological mechanisms for generation of EEG oscillations are not fully understood. As suspected based on their sensitivity to arousal, and confirmed by corresponding intracranial studies in humans and animals, additional structures such as brainstem, thalamus and thalamocortical circuits are involved in the generation and regulation of some oscillations (Brandeis et al., 2009; Lopes da Silva, 2010).

As the brain matures, EEG activity changes too. This change is characterized by dramatic decrease in low frequency activity, indicating a functional reorganization in the developing brain. The low frequency excess is strongest in childhood and decreases in a curvilinear fashion to end in a mature EEG pattern at early adulthood. The EEG's sensitivity for brain maturation was recognized already the pioneering days and has been replicated extensively up to date (Boord et al., 2007; Clarke et al., 2001; Dustman et al., 1999; Eeg-Olofsson, 1970; Gasser et al., 1988; Gibbs and Knott, 1949; Gmehlin et al., 2010; John et al., 1980; Matousek and Petersen, 1973; Matsuura et al., 1985; Somsen et al., 1997). EEG maturation has been suspected to mirror the development of higher cognitive functions (Case, 1992; John et al., 1980; Thatcher, 1994; Wackermann and Matousek, 1998), and deviations from normal development curves have been associated with lagged or abnormal brain maturation (John et al., 1980). Research has been dedicated to

establish normative data of healthy EEG evolution, and of maturation scales that can serve as an objective measure for brain maturation and brain electric abnormalities (Wackermann and Matousek, 1998). The developmental slow wave reduction extends also to sleep (Campbell and Feinberg, 2009; Feinberg and Campbell, 2010) and was replicated using magnetoencephalography (MEG) (Puligheddu et al., 2005); this latter finding corroborates the neurodevelopmental origin due to the insensitivity of MEG to changes in physical properties such as bone conductivity. The electrophysiological maturation has been linked to neuronal pruning and cortical metabolic activity reduction; both showing similar maturational trajectories (see next section).

2.2 EEG maturation parallels structural and metabolic brain maturation

Magnetic Resonance Tomography/Imaging (MRT/MRI) has become the standard technique providing high resolution anatomical brain images in vivo. The neuronal structure of the brain is typically classified into two categories, gray matter and white matter. Gray matter mainly contains cell bodies and neuronal connections associated with neuronal information processing. White matter reflects myelinated axon tracts, the long range wiring integrating remote brain regions. The general pattern for typical brain development in the first 25 years of life is a roughly linear increase in white matter volumes, and regionally specific inverted U-shaped developmental trajectories for gray matter structures, with peak volumes occurring in late childhood or early adolescence (Giedd et al., 2009). Regional specificity mirrors the functional hierarchy of the brain as primary sensory regions mature first, and associative regions and prefrontal cortex follow at a later stage (Gogtay et al., 2004; Gogtay and Thompson, 2010). The adolescent decrease of gray matter presumably reflects synaptic pruning (Bourgeois and Rakic, 1993; Huttenlocher, 1979). Synaptic pruning during adolescence may indicate the elimination of ineffective connections, and a defect in this regressive process has often been liked to adolescent-emerging psychiatric disorders such as schizophrenia (Paus et al., 2008).

Glucose is the obligatory energy substrate for the brain. The regional neuronal energy consumption can be measured with Positron Emission Tomography (PET). The general pattern for typical brain development of absolute cortical glucose uptake is an inverted U-shaped developmental trajectory peaking in late childhood or early adolescence (Chugani, 1998; Chugani et al., 1987). The parallel trajectories of gray matter amounts and absolute glucose metabolism are not unexpected as the major portion of glucose used by the brain is for the maintenance of the resting membrane potentials (Chugani, 1998). A similar absolute quantity of brain metabolism is provided by arterial spin labeling (ASL) MRI providing perfusion images of regional cerebral blood flow (rCBF). These methods revealed similar maturational metabolic decrease during adolescence (Biagi et al., 2007) even if controlling for gray matter density (Taki et al., 2011).

EEG maturation parallels gray matter maturation in the awake resting state (Whitford et al., 2007) as well as during sleep EEG (Buchmann et al., 2010). However, there may

be limitations of this correspondence as EEG maturation is at least partly frequency specific. Taken together these results show strikingly similar trajectories between low frequency EEG amplitudes and structural and metabolic (Boord et al., 2007; Feinberg and Campbell, 2010; Feinberg et al., 1990) brain maturation adumbrating a common mechanism. On a physiological basis, the EEG oscillations may be partly coupled to gray matter density (and metabolic demands) as synaptic density reflects the connectivity and size of neuron populations on which EEG amplitudes partly depend on (Feinberg and Campbell, 2010). Even if partly coupled to structural and metabolic gray matter properties, EEG oscillations represent reorganization in electric brain function rather than in structure or metabolism. A closer link between markers of functional maturation can be established by comparing the EEG with co-registered functional MRI-BOLD signals (see next section). Although fMRI has come to dominate functional neuroscience, there is no study assessing the maturational relationship of EEG amplitudes to the BOLD signal.

2.3 FMRI and brain maturation

Blood-oxygen-level-dependency (BOLD) FMRI (functional MRI) is sensitive to active neurons which cause a regional influx of oxygenated blood in terms of a local overcompensation. This overcompensation causes a change in the local ratio of oxygenated to deoxygenated hemoglobin for which the BOLD signal is sensitive to. The BOLD signal is a slow hemodynamic correlate of neuronal activity (Logothetis et al., 2001; Niessing et al., 2005). BOLD fMRI emerged in the 1990s (Ogawa et al., 1990) and has since been extensively used to image neuronal correlates of mental and behavioral processes. Regarding developmental aspects, fMRI studies on cognitive brain maturation found often inconsistent findings in terms of increased or decreased neuronal activity (Blakemore and Choudhury, 2006). Instead, a shift "from diffuse to focal" activation (Durston et al., 2006) has been suggested as a neuronal correlate of cognitive development, but this proposal has received mixed reactions (Blakemore and Choudhury, 2006; Brown et al., 2006; Dick et al., 2006). The maturational interpretation of increasing or decreasing activity or spatially diverse activity patterns is hampered by confounding factors such as cognitive effort, experience or strategy (Casey et al., 2005).

More recent fMRI research focused on resting state brain activity in terms of functional connectivity (Biswal et al., 1995; Friston, 2002) between brain regions. This branch of research revealed functional connectivity networks or "resting state networks" (RSNs) that are based on the spontaneously fluctuating BOLD signal and can be interpreted on the functional connotation of the anatomical structures that constitute the RSNs (Damoiseaux et al., 2006). In terms of development, the RSNs were found to be established already at the age of 7 - 9 years (Fair et al., 2009; Supekar et al., 2009) but can be identified rudimentary already in infants (Fransson et al., 2010; Fransson et al., 2007). After the age of 7 - 9 years, maturational changes were described as more subtle fine tuning of within and between network connectivity (Dosenbach et al., 2010; Fair et al., 2009; Fair et al., 2007; Jolles et al., 2011; Supekar et al., 2009) In general, beyond predefined

networks, development is typically characterized as increasing long distance connectivity and regional functional specialization (Uddin et al., 2010).

2.4 EEG and fMRI resting state brain activity

Most of the research introduced so far is based on measurements during rest, which means that subject were recorded in the awake resting state in the absence of any task or stimulation. While EEG research recognized the importance of resting state brain activity since its very beginning in the 1930s, it was rather recently that PET (Positron Emission Tomography) and fMRI research started to pay attention to resting state activity after appropriate methods were developed. A key paper published by Marcus Raichle in 2001, suggesting "a default mode of brain function" was followed by an enormous interest and efforts towards the understanding of resting state fMRI brain activity.

At rest, the brain is far from resting. The enormous intrinsic energy consumption exceeds by far the additional costs associated with momentary demands of the environment which may be as little as 0.5 to 1.0 % of the total energy budget (Raichle, 2006). The spontaneous brain activity transiently engages and disengages very similar networks as during induced cognition (Calhoun et al., 2008; Smith et al., 2009). On an arousal continuum, rest can be seen as an intermitted state between sleep and goal-oriented attention. But also during rest, brain activity transiently fluctuates spontaneously between states of higher or lowered arousal. With the use of eyes-open (EO) and eyes-closed (EC) conditions, systematic arousal variations can be induced in the resting state. Both EEG and fMRI reflect arousal related features of resting brain state regulation. In the EEG the sensitivity is reflected by the oscillatory compound (reviewed in (Olbrich et al., 2009; Sadaghiani et al., 2010) such as Alpha (10 Hz) oscillations typically reflect an "idling" state, higher frequencies ($>$ 13 Hz) reflect an increase and lower frequencies ($<$ 8 Hz) a decrease in arousal. Resting state fMRI features two major (and antagonistic) RSNs, the default mode network (DMN) (Raichle et al., 2001; Raichle and Snyder, 2007) and the attention network (ATN) (Fox et al., 2005) which activity reflects shifts along the arousal scale as their engagement relates to rest or attentional task activity. Vigilance and arousal is regulated among others by thalamic activity and thalamocortical circuitry (Llinas et al., 1998; McCormick and Bal, 1997; Steriade et al., 1993).

2.5 Simultaneous EEG–fMRI during resting state

Evidence for thalamocortical activity during rest has been observed noninvasively by simultaneous recording of EEG and fMRI. These studies revealed that activity in the alpha range (10 Hz) is paralleled by BOLD activity in the thalamus, and by deactivation in broad cortical sensory areas (de Munck et al., 2007; Difrancesco et al., 2008; Feige et al., 2005; Goldman et al., 2002; Lüchinger et al., 2011; Moosmann et al., 2003;

Tyvaert et al., 2008). Such functional couplings are typically based on the temporal correlation between hemodynamically convolved EEG spectral power fluctuations and the co-registered regional BOLD signal in eyes-closed resting state. Further functional couplings of EEG oscillations in different frequencies and also in different resting states (eyes-open) were found in regions comprising the DMN (Lüchinger et al., 2011; Scheeringa et al., 2008) and the ATN (Laufs et al., 2006; Laufs et al., 2003; Lüchinger et al., 2011). As simultaneous recording of EEG and fMRI allows localizing functional correlates of EEG oscillations, the approach may improve the understanding of resting state brain function.

2.6 Study aims and hypotheses

The simultaneous recording of EEG and fMRI promises an elucidation of EEG maturation by means of finding a functional correlate. EEG–fMRI correlates have not been used to study brain development so far. We hypothesized that the EEG–BOLD signal couplings change as a consequence of EEG power decrease. In a first study we assessed this issue at a relatively late state of brain maturation between 15 and 25 years. This transition from late adolescence to early adulthood is a critical stage in the human lifespan. Such (post-)adolescent changes are rarely treated as a maturational step of its own and thus tend to be obscured by stronger developmental effects in childhood.

In a second study we included data from children to extend the search for functional correlates of EEG maturation to a wider age range, i.e. between 10 to 25 years of age. This allowed a more comprehensive investigation as the EEG power decrease is strongest in childhood. In addition we included new methods. The BOLD signal was analyzed in terms of spectral power analogous to EEG power. This allowed a direct comparison of the two signals in terms of equivalent measures.

2.7 References

Biagi, L., Abbruzzese, A., Bianchi, M.C., Alsop, D.C., Del Guerra, A., Tosetti, M., 2007. Age dependence of cerebral perfusion assessed by magnetic resonance continuous arterial spin labeling. J Magn Reson Imaging 25, 696-702.

Biswal, B., Yetkin, F.Z., Haughton, V.M., Hyde, J.S., 1995. Functional connectivity in the motor cortex of resting human brain using echo-planar MRI. Magn Reson Med 34, 537-541.

Blakemore, S.J., Choudhury, S., 2006. Brain development during puberty: state of the science. Dev Sci 9, 11-14.

Boord, P.R., Rennie, C.J., Williams, L.M., 2007. Integrating "brain" and "body" measures: correlations between EEG and metabolic changes over the human lifespan. J Integr Neurosci 6, 205-218.

Bourgeois, J.P., Rakic, P., 1993. Changes of synaptic density in the primary visual cortex of the macaque monkey from fetal to adult stage. J Neurosci 13, 2801-2820.

Brandeis, D., Michel, M.C., Amzica, F., 2009. From neuronal activity to scalp potential fields. In: Michel, M.C., Koenig, T., Brandeis, D., Gianotti, L.R.R., Wackermann, J. (Eds.), Electrical Neuroimaging. Cambridge Unversity Press, New York, pp. 1-24.

Brown, T.T., Petersen, S.E., Schlaggar, B.L., 2006. Does human functional brain organization shift from diffuse to focal with development? Dev Sci 9, 9-11.

Buchmann, A., Ringli, M., Kurth, S., Schaerer, M., Geiger, A., Jenni, O.G., Huber, R., 2010. EEG sleep slow-wave activity as a mirror of cortical maturation. Cereb Cortex 21, 607-615.

Calhoun, V.D., Kiehl, K.A., Pearlson, G.D., 2008. Modulation of temporally coherent brain networks estimated using ICA at rest and during cognitive tasks. Hum Brain Mapp 29, 828-838.

Campbell, I.G., Feinberg, I., 2009. Longitudinal trajectories of non-rapid eye movement delta and theta EEG as indicators of adolescent brain maturation. Proc Natl Acad Sci U S A 106, 5177-5180.
Case, R., 1992. The role of the frontal lobes in the regulation of cognitive development. Brain Cogn 20, 51-73.
Casey, B.J., Galvan, A., Hare, T.A., 2005. Changes in cerebral functional organization during cognitive development. Curr Opin Neurobiol 15, 239-244.
Chugani, H.T., 1998. A critical period of brain development: studies of cerebral glucose utilization with PET. Prev Med 27, 184-188.
Chugani, H.T., Phelps, M.E., Mazziotta, J.C., 1987. Positron emission tomography study of human brain functional development. Ann Neurol 22, 487-497.
Clarke, A.R., Barry, R.J., McCarthy, R., Selikowitz, M., 2001. Age and sex effects in the EEG: development of the normal child. Clin Neurophysiol 112, 806-814.
Damoiseaux, J.S., Rombouts, S.A., Barkhof, F., Scheltens, P., Stam, C.J., Smith, S.M., Beckmann, C.F., 2006. Consistent resting-state networks across healthy subjects. Proc Natl Acad Sci U S A 103, 13848-13853.
de Munck, J.C., Goncalves, S.I., Huijboom, L., Kuijer, J.P., Pouwels, P.J., Heethaar, R.M., Lopes da Silva, F.H., 2007. The hemodynamic response of the alpha rhythm: an EEG/fMRI study. Neuroimage 35, 1142-1151.
Dick, F., Leech, R., Moses, P., Saccuman, M.C., 2006. The interplay of learning and development in shaping neural organization. Dev Sci 9, 14-17.
Difrancesco, M.W., Holland, S.K., Szaflarski, J.P., 2008. Simultaneous EEG/functional magnetic resonance imaging at 4 Tesla: correlates of brain activity to spontaneous alpha rhythm during relaxation. J Clin Neurophysiol 25, 255-264.
Dosenbach, N.U., Nardos, B., Cohen, A.L., Fair, D.A., Power, J.D., Church, J.A., Nelson, S.M., Wig, G.S., Vogel, A.C., Lessov-Schlaggar, C.N., Barnes, K.A., Dubis, J.W., Feczko, E., Coalson, R.S., Pruett, J.R., Jr., Barch, D.M., Petersen, S.E., Schlaggar, B.L., 2010. Prediction of individual brain maturity using fMRI. Science 329, 1358-1361.
Durston, S., Davidson, M.C., Tottenham, N., Galvan, A., Spicer, J., Fossella, J.A., Casey, B.J., 2006. A shift from diffuse to focal cortical activity with development. Dev Sci 9, 1-8.
Dustman, R.E., Shearer, D.E., Emmerson, R.Y., 1999. Life-span changes in EEG spectral amplitude, amplitude variability and mean frequency. Clin Neurophysiol 110, 1399-1409.
Eeg-Olofsson, O., 1970. The development of the electroencephalogram in normal children and adolescents from the age of 1 through 21 years. Acta Paediatr Scand Suppl 208, Suppl208:201+.
Fair, D.A., Cohen, A.L., Power, J.D., Dosenbach, N.U., Church, J.A., Miezin, F.M., Schlaggar, B.L., Petersen, S.E., 2009. Functional brain networks develop from a "local to distributed" organization. PLoS Comput Biol 5, e1000381.
Fair, D.A., Dosenbach, N.U., Church, J.A., Cohen, A.L., Brahmbhatt, S., Miezin, F.M., Barch, D.M., Raichle, M.E., Petersen, S.E., Schlaggar, B.L., 2007. Development of distinct control networks through segregation and integration. Proc Natl Acad Sci U S A 104, 13507-13512.
Feige, B., Scheffler, K., Esposito, F., Di Salle, F., Hennig, J., Seifritz, E., 2005. Cortical and subcortical correlates of electroencephalographic alpha rhythm modulation. J Neurophysiol 93, 2864-2872.
Feinberg, I., Campbell, I.G., 2010. Sleep EEG changes during adolescence: an index of a fundamental brain reorganization. Brain Cogn 72, 56-65.
Feinberg, I., Thode, H.C., Jr., Chugani, H.T., March, J.D., 1990. Gamma distribution model describes maturational curves for delta wave amplitude, cortical metabolic rate and synaptic density. J Theor Biol 142, 149-161.
Fox, M.D., Snyder, A.Z., Vincent, J.L., Corbetta, M., Van Essen, D.C., Raichle, M.E., 2005. The human brain is intrinsically organized into dynamic, anticorrelated functional networks. Proc Natl Acad Sci U S A 102, 9673-9678.
Fransson, P., Aden, U., Blennow, M., Lagercrantz, H., 2010. The functional architecture of the infant brain as revealed by resting-state FMRI. Cereb Cortex 21, 145-154.
Fransson, P., Skiold, B., Horsch, S., Nordell, A., Blennow, M., Lagercrantz, H., Aden, U., 2007. Resting-state networks in the infant brain. Proc Natl Acad Sci U S A 104, 15531-15536.
Friston, K., 2002. Beyond phrenology: what can neuroimaging tell us about distributed circuitry? Annu Rev Neurosci 25, 221-250.
Gasser, T., Verleger, R., Bacher, P., Sroka, L., 1988. Development of the EEG of school-age children and adolescents. I. Analysis of band power. Electroencephalogr Clin Neurophysiol 69, 91-99.
Gibbs, F.A., Knott, J.R., 1949. Growth of the electrical activity of the cortex. Electroencephalogr Clin Neurophysiol 1, 223-229.
Giedd, J.N., Lalonde, F.M., Celano, M.J., White, S.L., Wallace, G.L., Lee, N.R., Lenroot, R.K., 2009. Anatomical brain magnetic resonance imaging of typically developing children and adolescents. J Am Acad Child Adolesc Psychiatry 48, 465-470.

Gmehlin, D., Thomas, C., Weisbrod, M., Walther, S., Pfuller, U., Resch, F., Oelkers-Ax, R., 2010. Individual analysis of EEG background-activity within school age: impact of age and sex within a longitudinal data set. Int J Dev Neurosci.

Gogtay, N., Giedd, J.N., Lusk, L., Hayashi, K.M., Greenstein, D., Vaituzis, A.C., Nugent, T.F., 3rd, Herman, D.H., Clasen, L.S., Toga, A.W., Rapoport, J.L., Thompson, P.M., 2004. Dynamic mapping of human cortical development during childhood through early adulthood. Proc Natl Acad Sci U S A 101, 8174-8179.

Gogtay, N., Thompson, P.M., 2010. Mapping gray matter development: implications for typical development and vulnerability to psychopathology. Brain Cogn 72, 6-15.

Goldman, R.I., Stern, J.M., Engel, J., Jr., Cohen, M.S., 2002. Simultaneous EEG and fMRI of the alpha rhythm. Neuroreport 13, 2487-2492.

Huttenlocher, P.R., 1979. Synaptic density in human frontal cortex - developmental changes and effects of aging. Brain Res 163, 195-205.

John, E.R., Ahn, H., Prichep, L., Trepetin, M., Brown, D., Kaye, H., 1980. Developmental equations for the electroencephalogram. Science 210, 1255-1258.

Jolles, D.D., van Buchem, M.A., Crone, E.A., Rombouts, S.A., 2011. A comprehensive study of whole-brain functional connectivity in children and young adults. Cereb Cortex 21, 385-391.

Laufs, H., Holt, J.L., Elfont, R., Krams, M., Paul, J.S., Krakow, K., Kleinschmidt, A., 2006. Where the BOLD signal goes when alpha EEG leaves. Neuroimage 31, 1408-1418.

Laufs, H., Kleinschmidt, A., Beyerle, A., Eger, E., Salek-Haddadi, A., Preibisch, C., Krakow, K., 2003. EEG-correlated fMRI of human alpha activity. Neuroimage 19, 1463-1476.

Llinas, R., Ribary, U., Contreras, D., Pedroarena, C., 1998. The neuronal basis for consciousness. Philos Trans R Soc Lond B Biol Sci 353, 1841-1849.

Logothetis, N.K., Pauls, J., Augath, M., Trinath, T., Oeltermann, A., 2001. Neurophysiological investigation of the basis of the fMRI signal. Nature 412, 150-157.

Lopes da Silva, F.H., 2010. EEG: Origins and Measuremets. In: Mulert, C., Lemieux, L. (Eds.), EEG - fMRI: Physiological Basis, Technique, and Applications. Springer, Berlin, pp. 19-38.

Lüchinger, R., Michels, L., Martin, E., Brandeis, D., 2011. EEG–BOLD correlations during (post-)adolescent brain maturation. Neuroimage 56, 1493-1505.

Matousek, M., Petersen, I., 1973. Automatic evaluation of EEG background activity by means of age-dependent EEG quotients. Electroencephalogr Clin Neurophysiol 35, 603-612.

Matsuura, M., Yamamoto, K., Fukuzawa, H., Okubo, Y., Uesugi, H., Moriiwa, M., Kojima, T., Shimazono, Y., 1985. Age development and sex differences of various EEG elements in healthy children and adults–quantification by a computerized wave form recognition method. Electroencephalogr Clin Neurophysiol 60, 394-406.

McCormick, D.A., Bal, T., 1997. Sleep and arousal: thalamocortical mechanisms. Annu Rev Neurosci 20, 185-215.

Moosmann, M., Ritter, P., Krastel, I., Brink, A., Thees, S., Blankenburg, F., Taskin, B., Obrig, H., Villringer, A., 2003. Correlates of alpha rhythm in functional magnetic resonance imaging and near infrared spectroscopy. Neuroimage 20, 145-158.

Niessing, J., Ebisch, B., Schmidt, K.E., Niessing, M., Singer, W., Galuske, R.A., 2005. Hemodynamic signals correlate tightly with synchronized gamma oscillations. Science 309, 948-951.

Ogawa, S., Lee, T.M., Kay, A.R., Tank, D.W., 1990. Brain magnetic resonance imaging with contrast dependent on blood oxygenation. Proc Natl Acad Sci U S A 87, 9868-9872.

Olbrich, S., Mulert, C., Karch, S., Trenner, M., Leicht, G., Pogarell, O., Hegerl, U., 2009. EEG-vigilance and BOLD effect during simultaneous EEG/fMRI measurement. Neuroimage 45, 319-332.

Paus, T., Keshavan, M., Giedd, J.N., 2008. Why do many psychiatric disorders emerge during adolescence? Nat Rev Neurosci 9, 947-957.

Pulighеddu, M., de Munck, J.C., Stam, C.J., Verbunt, J., de Jongh, A., van Dijk, B.W., Marrosu, F., 2005. Age distribution of MEG spontaneous theta activity in healthy subjects. Brain Topogr 17, 165-175.

Raichle, M.E., 2006. Neuroscience. The brain's dark energy. Science 314, 1249-1250.

Raichle, M.E., MacLeod, A.M., Snyder, A.Z., Powers, W.J., Gusnard, D.A., Shulman, G.L., 2001. A default mode of brain function. Proc Natl Acad Sci U S A 98, 676-682.

Raichle, M.E., Snyder, A.Z., 2007. A default mode of brain function: a brief history of an evolving idea. Neuroimage 37, 1083-1090; discussion 1097-1089.

Sadaghiani, S., Scheeringa, R., Lehongre, K., Morillon, B., Giraud, A.L., Kleinschmidt, A., 2010. Intrinsic connectivity networks, alpha oscillations, and tonic alertness: a simultaneous electroencephalography/functional magnetic resonance imaging study. J Neurosci 30, 10243-10250.

Scheeringa, R., Bastiaansen, M.C., Petersson, K.M., Oostenveld, R., Norris, D.G., Hagoort, P., 2008. Frontal theta EEG activity correlates negatively with the default mode network in resting state. Int J Psychophysiol 67, 242-251.

Smith, S.M., Fox, P.T., Miller, K.L., Glahn, D.C., Fox, P.M., Mackay, C.E., Filippini, N., Watkins, K.E., Toro, R.,

Laird, A.R., Beckmann, C.F., 2009. Correspondence of the brain's functional architecture during activation and rest. Proc Natl Acad Sci U S A 106, 13040-13045.

Somsen, R.J., van't Klooster, B.J., van der Molen, M.W., van Leeuwen, H.M., Licht, R., 1997. Growth spurts in brain maturation during middle childhood as indexed by EEG power spectra. Biol Psychol 44, 187-209.

Steriade, M., McCormick, D.A., Sejnowski, T.J., 1993. Thalamocortical Oscillations in the Sleeping and Aroused Brain. Science 262, 679-685.

Supekar, K., Musen, M., Menon, V., 2009. Development of large-scale functional brain networks in children. PLoS Biol 7, e1000157.

Taki, Y., Hashizume, H., Sassa, Y., Takeuchi, H., Wu, K., Asano, M., Asano, K., Fukuda, H., Kawashima, R., 2011. Correlation between gray matter density-adjusted brain perfusion and age using brain MR images of 202 healthy children. Hum Brain Mapp 32, 1973-1985.

Thatcher, R.W., 1994. Cyclic cortical reorganization: Origins of human cognitive development. In: Fischer, G.D.K.W. (Ed.), Human behavior and the developing brain. Guilford Press, New York, pp. 232-266.

Tyvaert, L., Hawco, C., Kobayashi, E., LeVan, P., Dubeau, F., Gotman, J., 2008. Different structures involved during ictal and interictal epileptic activity in malformations of cortical development: an EEG–fMRI study. Brain 131, 2042-2060.

Uddin, L.Q., Supekar, K., Menon, V., 2010. Typical and atypical development of functional human brain networks: insights from resting-state FMRI. Front Syst Neurosci 4, 21.

Wackermann, J., Matousek, M., 1998. From the 'EEG age' to a rational scale of brain electric maturation. Electroencephalogr Clin Neurophysiol 107, 415-421.

Whitford, T.J., Rennie, C.J., Grieve, S.M., Clark, C.R., Gordon, E., Williams, L.M., 2007. Brain maturation in adolescence: concurrent changes in neuroanatomy and neurophysiology. Hum Brain Mapp 28, 228-237.

3 EEG–BOLD Correlations During (Post-)Adolescent Brain Maturation

Published as: *Lüchinger R, Michels L, Martin E, Brandeis D, (2011) EEG-BOLD correlations during (post-) adolescent brain maturation. Neuroimage, 56, 1493-1505.*

Abstract **- The transition from adolescence to adulthood is a critical stage in the human lifespan during which the brain still undergoes substantial structural and functional change. The changing frequency composition of the resting state EEG reflects maturation of brain function. This study investigated (post)adolescent brain maturation captured by two independently but simultaneously recorded neuronal signals: EEG and fMRI. Data were collected in a 20 min eyes-open/eyes-closed resting state paradigm. EEG, fMRI-BOLD signal and EEG–BOLD correlations were compared between groups of adults, age 25 (n = 18), and adolescents, age 15 (n = 18). A typical developmental decrease of low-frequency EEG power was observed even at this late stage of brain maturation. Frequency and condition specific EEG–fMRI correlations proved robust for multiple brain regions. However, no consistent change in the EEG–BOLD correlations was identified that would correspond to the neuronal maturation captured by the EEG. This result indicates that the EEG–BOLD correlation measures a distinct aspect of neurophysiological activity that presumably matures earlier, since it is less sensitive to late maturation than the neuronal activity captured by low-frequency EEG.**

3.1 Introduction

Adolescence and the transition into adulthood are critical stages in the human lifespan. The typical emergence of some major mental illnesses during adolescence further indicates fundamental maturational reorganization (Paus et al., 2008) and stresses the importance of understanding late brain maturation. Since the major developmental changes occur during infancy and childhood, specific research on late maturation has often been neglected. However, late maturation, during and after adolescence has attracted increasing attention in recent years (Blakemore and Choudhury, 2006; Sisk and Foster, 2004). A growing body of evidence suggests that there are still substantial structural (Paus, 2005) and functional (Luna et al., 2010) changes in the brain during this time. Gray matter loss and white matter increase in adolescence were found to be consistent with the basic processes

of neuronal maturation, i.e. synaptic pruning and myelination (Giedd et al., 1999; Gogtay et al., 2004; Sowell et al., 2001). Apart from these structural aspects, executive functioning commonly associated with changes in the prefrontal cortex undergoes late brain maturation (Luna et al., 2010; Stevens, 2009). Recent brain imaging research has also investigated brain function at rest (where no stimulus or task is involved) to identify resting state networks (RSNs) of functional connectivity (Beckmann et al., 2005; Damoiseaux et al., 2006; van den Heuvel and Hulshoff Pol, 2010). In terms of the development of functional connectivity, basic principles such as successive neural segregation and hierarchical organization have been described (Fair et al., 2007; Stevens, 2009).

Converging evidence for late brain maturation comes from electroencephalogram (EEG) research. The EEG noninvasively measures electrical mass activity of neurons. An advantage over other functional methods such as fMRI is that the EEG measures neuronal activity directly and in absolute terms, i.e. in physical units (microvolts, μV). Consequently EEG research has focused on resting state brain functioning since its discovery (Berger, 1929) long before the advent of fMRI. The resting EEG is typically characterized by oscillations of different amplitudes and frequencies. One of the major findings since the beginning of resting EEG research is that children's EEG is dominated by slower rhythms which diminish with further brain maturation (Boord et al., 2007; Clarke et al., 2001; Dustman et al., 1999; Gasser et al., 1988; Gibbs and Knott, 1949; John et al., 1980; Matousek and Petersen, 1973; Wackermann and Matousek, 1998). This effect also extends to sleep (Campbell and Feinberg, 2009; Feinberg and Campbell, 2010), and has been suspected to mirror the development of higher cognitive functions (Case, 1992; Thatcher, 1994), and deviations from normal oscillatory patterns has been associated with lagged or abnormal brain maturation (John et al., 1980). That these developmental amplitude reductions are frequency specific, and are also found with magnetoencephalography (MEG) which is insensitive to changes in physical properties such as bone conductivity (Puligheddu et al., 2005; Takeshita et al., 2002), corroborates their neurodevelopmental nature. Again, very few studies specifically focused on late maturational changes (Whitford et al., 2007) although many studies investigated (or included) EEG changes during childhood, when most dramatic changes occur. Typically, linear or curvilinear regression analyses are used to assess developmental effects from childhood to adulthood. Overall age-related changes are well captured using such models but the drawback is a lack of sensitivity to changes during specific, short periods. In particular, (post-)adolescent changes are rarely treated as a maturational step of its own and thus tend to be obscured by stronger developmental effects in childhood. For example, several scientists (Boord et al., 2007; Gasser et al., 1988; Whitford et al., 2007) found low-frequency EEG amplitude reduction associated with late maturation, but the curvilinear developmental regression effects appear to be driven mainly by the younger subjects. The specific contribution of the presumably more subtle changes due to late maturation remains unclear unless studied in a smaller age range confined to the specific (post-)adolescent transition from adolescence to adulthood using regression or age group contrasts. Whitford et al. suggested gray matter loss or synaptic pruning as a candidate

to explain developmental EEG amplitude reduction (Whitford et al., 2007). Despite these structural changes that parallel the changes in EEG, the question remains whether there are also functional changes related to the EEG amplitude reduction with increasing age.

In recent years, simultaneous EEG and fMRI has allowed to link electrophysiological scalp-recorded activity more directly to cortical and subcortical regions. The exact physiological relationship between EEG amplitudes and the fMRI blood oxygen-level dependency (BOLD) signal remains unclear (Laufs, 2008). However, the two signals co-vary during rest in terms of their temporal fluctuation (following appropriate convolution to account for the lag and the lower frequency range of the BOLD signal), indicating that they are functionally coupled. Accordingly, the term coupling as used here does not describe the physiological mechanism underlying their coupling, but the correlation reflecting the statistical similarity between their (convolved) time courses. Research groups have repeatedly verified a thalamocortical circuit associated with alpha (8 - 13 Hz) oscillations (de Munck et al., 2007; Difrancesco et al., 2008; Feige et al., 2005; Goldman et al., 2002; Goncalves et al., 2006; Moosmann et al., 2003; Tyvaert et al., 2008). Furthermore, Scheeringa and colleagues found the so-called default mode network (Raichle et al., 2001; Raichle and Snyder, 2007) to be (inversely) correlated with frontal midline theta power (Scheeringa et al., 2008). Other authors found that different EEG rhythms reflect different functional networks (Laufs et al., 2006; Laufs et al., 2003b; Mantini et al., 2007). A consistent finding of concurrent EEG–fMRI studies is that at least for the lower frequencies, EEG power is inversely related to the BOLD signal, indicating that these EEG signals become stronger with decreased neuronal activity in associated brain regions. To our knowledge, research on resting state using simultaneous EEG–fMRI has so far been limited to healthy adults. The coupling of EEG rhythms to the BOLD signal has not been studied in developmental or clinical settings. Furthermore, little is known about the coupling during eyes-open resting state. Although eyes-open/eyes-closed protocols were used in prior EEG–fMRI resting state studies (Ben-Simon et al., 2008; Feige et al., 2005; Henning et al., 2006; Yang et al., 2009) (mainly to induce alpha modulation), none of these studies analyzed the eyes-open condition separately except for the work by Scheeringa et al. (Scheeringa et al., 2008) addressing eyes-open-theta coupling. Also, most of the previous studies exploring the EEG–BOLD coupling during rest were limited to specific components of the EEG such as eyes-closed occipital alpha or eyes-open frontal midline theta power, using selected electrode sites or ICA components. A comprehensive study of resting state EEG–BOLD coupling covering the common spectral frequency bands and resting states has not yet been performed. Such a study is important, because the profile formed by different EEG rhythms is characteristic of different brain states and brain functions, and because eyes-open and eyes-closed states differ substantially in levels of arousal and EEG (Barry et al., 2007; Berger, 1929 ; Bianciardi et al., 2009; Marx et al., 2004; Marx et al., 2003) as well as in fMRI (Bianciardi et al., 2009; Marx et al., 2004; Marx et al., 2003).

The aim of this study was to investigate late maturation of the brain's resting state using simultaneous EEG–fMRI. In particular, we asked whether changes in EEG–BOLD

coupling parallel developmental EEG amplitude decreases. To investigate this question we compare EEG, fMRI and EEG–BOLD coupling differences between adults and adolescents. According to the literature we expected that adolescents have stronger EEG activity, especially in lower frequencies, although at this age the effect was expected to be subtle. We hypothesized that such increased EEG activity would reflect a distinct immature resting state network, and show coupling to different brain regions, or differ in coupling strength, rather than a constant coupling as expected for simple amplitude scaling of the EEG- or BOLD time series. Although differences were mostly expected in lower frequency bands, we included faster oscillations for comparison. Both eyes-open and eyes-closed conditions were included to provide a comprehensive picture of EEG–BOLD coupling and its late development during common resting states.

3.2 Methods

3.2.1 Patricipants

Two sex matched groups participated in this study. The 18 adults (mean age 24.9 ± 3.8 years, 8 males) were recruited by university billboard ads and 18 adolescents (mean age 15.4 ± 1.1 years, 8 males) were recruited in school classes by approaching their teachers. All participants met the MRI safety standards, were healthy with no history of medical or psychiatric disease, and had normal or corrected to normal vision. All were right-hand dominant as assessed by the Edinburgh Handedness Inventory (Oldfield, 1971). All participants, as well as the children's parents, gave written informed consent prior to the investigation. The study was approved by the local ethics committee and was conducted in accordance with the guidelines determined in the Helsinki Declaration.

3.2.2 Procedure

After EEG preparation, participants were introduced to the nature of EEG signals and artifacts produced by movement and muscle tension. EEG and fMRI was recorded simultaneously in two 10 min resting state sessions with a 16 min working memory test (not reported here) in between. Each session consisted of alternating eyes-open (EO) and eyes-closed (EC) blocks of 2.5 min duration. One session started with eyes-open (EO-EC-EO-EC) and one with eyes-closed (EC-EO-EC-EO). The order of the two sessions was counterbalanced across participants by group and sex. A video beamer outside the scanner room projected onto a screen placed in front of the MR table. A mirror mounted on the head coil enabled participants to see through the bore onto the screen. In the eyes-open blocks a fixation star was presented on the screen, and at the end an instruction was given to close the eyes. The instruction to open the eyes after an eyes-closed block was given by a somatosensory stimulus on the left index finger via a pneumatic device. Short stimulation pulses were given already prior to scanning, to prevent subjects from any knee-jerk movements. Participants were instructed to follow the eyes-open/eyes-closed instruction, relax and refrain from any movements. For increased comfort, participants

were fitted with a custom made felt cushion filling the space between the electrodes at the back of the head. The head was immobilized using foam pads and participants were provided with earplugs. Participants were personally checked after each scan session for electrode heating, tiredness or any indisposition.

3.2.3 Data acquisition

The EEG was recorded inside the scanner using 5 kHz sampling rate, 32 mV input range, 0.1 - 250 Hz bandpass filters, and data transmission from two MR-compatible BrainAmp amplifiers (Brain Products, Gilching, Germany) via optic fibers outside the scanner room. Sixty scalp electrodes were recorded using MR-compatible caps (easycap, Munich, Germany) with twisted and fixed electrode cables in three different editions to account for different head sizes of the participants. All electrode positions of the 10-20 system plus the following 10-10 system sites were used: FPz, AFz FCz, CPz, POz, Oz, Iz, F5/6, FC1/2/3/4/5/6, FT7/8/9/10, C1/2/5/6, CP1/2/3/4/5/6, TP7/8/9/10, P5/6, PO1/2/9/10, OI1/2). O1/2 and FP1/2 were placed 2 cm laterally from the standard positions for more even coverage (Brem et al., 2010; Maurer et al., 2007). F1 served as recording reference, F2 was the ground electrode. Two additional electrodes were placed below the outer canthus of each eye and two further electrodes right to the sternum and on the left chest close to the heart to record the electrocardiogram (ECG). Electrode impedances were kept below 20 kΩ. The EEG was monitored while scanning using online correction software (RecView Brain Products, Gilching, Germany) and checked for signal quality and eyes-open/close transitions. FMRI data were acquired on a 3.0 T (GE Healthcare, Milwaukee, WI, USA) whole-body scanner using a standard head coil. Prior to fMRI acquisition a shimming procedure was used to minimize susceptibility distortions due to local static magnetic field inhomogeneities. Functional MR data were acquired with T2*-sensitive multi-slice echo planar imaging (EPI) sequence (TR = 1.815 s; TE = 32 ms; FOV = 22 cm; image matrix = 64 x 64; voxel size = 3.44 x 3.44 x 3.8 mm^3; flip angle = 75°, 33 axial slices covering the whole brain). One session consisted of 336 volumes. The first 6 volumes were excluded to avoid magnetic saturation effects.

3.2.4 EEG processing and analysis

Brain Vision Analyzer software (version 1.05, Brain Products, Gilching, Germany) served for offline processing of the EEG. MR-gradient artifacts were removed by average artifact subtraction (Allen et al., 2000; Allen et al., 1998) as implemented in the software (sliding average over 50 TRs, down sampled to 500 Hz and lowpass filtered at 70 Hz cutoff). To eliminate the ballistocardiogram artifact (BCG) a very similar subtraction procedure was used, with artifact window aligned on QRS complexes detected in ECG traces, templates based on 10 consecutive pulse intervals, and individually estimated time delay for subtraction based on global field power (GFP) distribution (CBC Parameters, Version 1.1). Subsequently, ECG channels were discarded from further analysis (QRS markers were kept). Data was digitally bandpass filtered (0.5 - 70 Hz, 24 dB/oct and 50 Hz

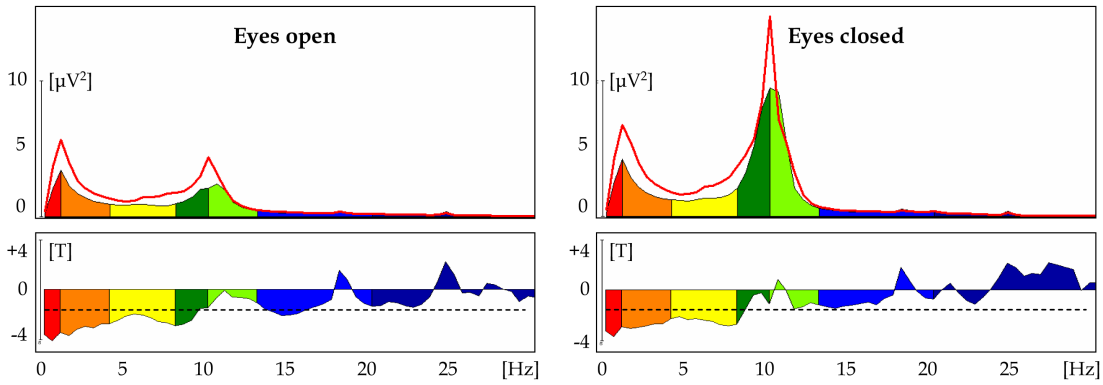

Fig. 1.1 Adolescence is characterized by increased low frequency EEG amplitudes. Group mean of global spectral power (GSP) for adults (colored spectra) and adolescents (red line) separate for eyes-open (left) and eyes-closed (right) condition. Lower panels: t-values of the group contrast. Dashed line: level of significance ($t(34) = 1.69$, $p < 0.05$, one-tailed, uncorrected for multiple comparison).

Notch) and downsampled to 256 Hz. An infomax ICA (Delorme and Makeig, 2004) was calculated on the concatenated data sets of the two sessions. Movement-related artifacts which may not be suitable for ICA correction were excluded from the unmixing procedure. Components were profiled by their topography, activation time course, spectrogram and contribution to averaged BCG amplitude. Components clearly assigned to either eye blinks (Jung et al., 2000), residual gradient artifacts or residual BCG artifacts were excluded from the back projection. The EEG was then transformed to the average reference (Lehmann and Skrandies, 1980) and segments with remaining artifacts were marked and excluded from successive analysis.

EEG regressor construction: First the EEG of each participant was split into the two separate sessions to evaluate possible session differences, and further divided into eyes-open and eyes-closed condition. The condition onsets were defined individually by the exact time of opening and closing the eyes, as indicated by ICA components activation traces. The data were parsed into contiguous epochs triggered by the scan starts, resulting in 330 time points per session. The data were further parsed into epochs of the length of a TR. Absolute spectral power was estimated for each epoch using Fast Fourier Transformation (FFT, Hanning window: 10 %, zero padded, resolution 0.5 Hz). To estimate the total activity over the scalp, global spectral power (GSP) was calculated for each frequency point as the root mean square across all FFT-transformed scalp channels (Jann et al., 2009; Michels et al., 2010). The mean spectral band value was calculated for delta (1 - 3 Hz), theta (4 - 7.5 Hz), alpha1 (8 - 10 Hz), alpha2 (10 - 13 Hz), beta1 (14 - 19 Hz) and beta2 (20 - 30 Hz). GSP estimates for artifactual segments (see above) were linearly interpolated. The GSP time series were normalized and thus recruited for fMRI model specification (see below). Additional regional EEG regressors were built based on subsets of electrodes in order to account for conventional locally defined EEG rhythms. For the delta and theta band frontal electrodes AFz, Fz, F3/4 and FCz were used. For alpha1 and alpha2 occipital electrodes O1/2, and for alpha2 and beta1 central electrodes C3/4 were used.

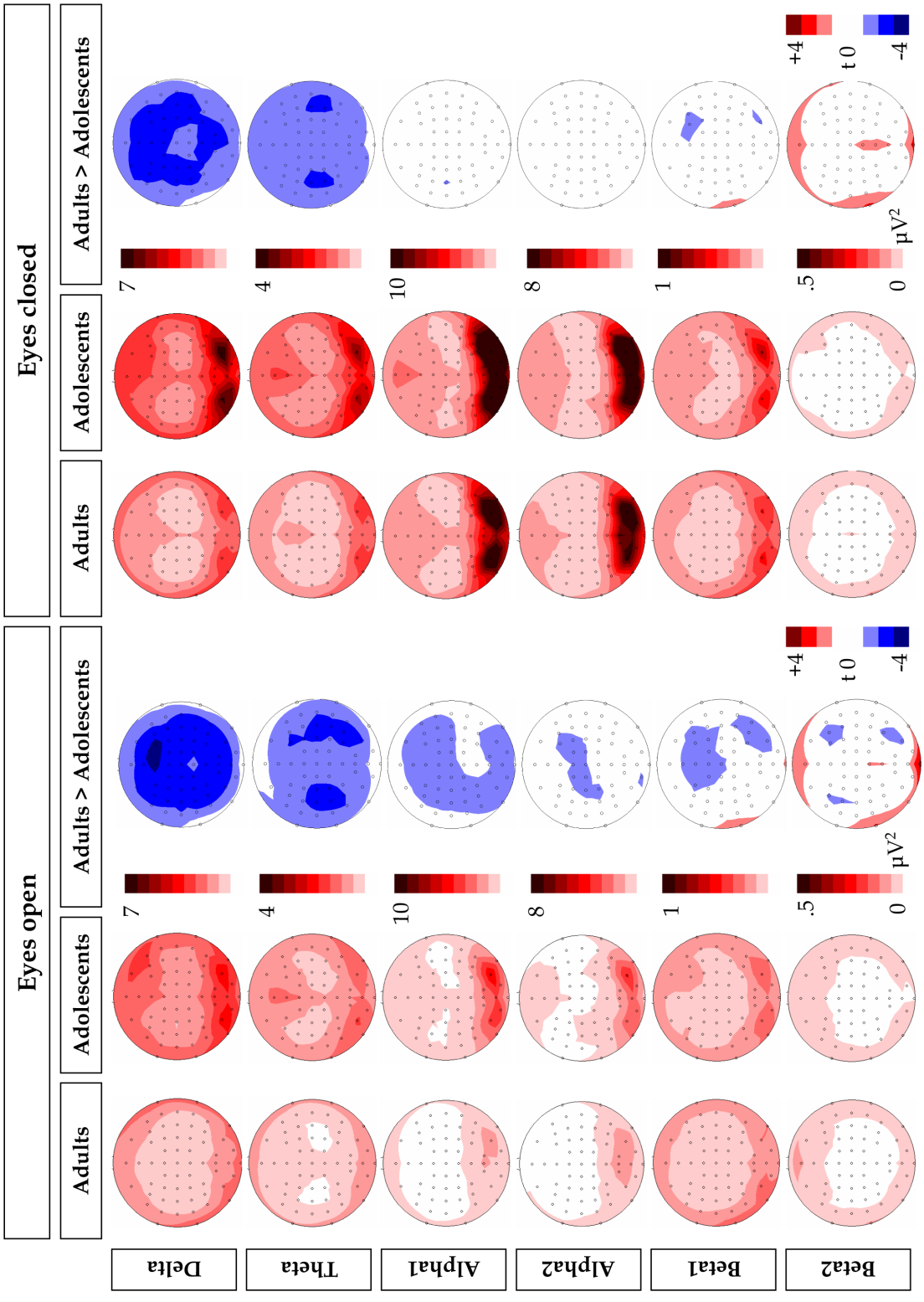

Fig. 1.2 Group mean power maps for adults and adolescents with group difference, separately for eyes-open and eyes-closed. Scaling bars indicate power values in μV^2 for each frequency band. The t-maps have common scaling (-4 to +4 t) and one color step represents a step of $\pm$ 1 t-value. Particularly in lower frequencies adolescents showed increased EEG activity.

The EEG was analyzed in terms of GSP as well as electrode-wise to conserve topographic information. For each condition separately, spectral power values were averaged across FFT epochs and averaged within the above frequency bands. Group means were compared using t-statistics.

3.2.5 FMRI processing and analysis

Preprocessing and statistical analysis of fMRI data was done with SPM5 (Wellcome Department of Cognitive Neurology, London, UK). The two sessions were preprocessed separately. Images were realigned to the first scan to correct for head motion, and motion parameters were later included in the statistical model. No participant needed to be excluded due to extensive head motions (i.e. motion > 2 mm or $> 2°$). To prepare for group analysis, images were normalized to the Montreal Neurological Institute (MNI) standard brain, resampled to isotropic 3 mm^3 voxels and smoothed with a Gaussian kernel (isotropic FWHM of 9 mm). A standard HRF was used for convolution of model regressors. To account for serial correlations, an autoregressive model of the first order was used. Highpass filtering with standard 128 s cutoff eliminated slow signal drifts. Both sessions were analyzed separately to test for session differences. If session differences were not of interest, individual contrast images were calculated from session average. In any case session specific motion parameters were modeled as confounds.

The fMRI analysis modeled BOLD fluctuation, explained by EEG power fluctuations, using a general linear model (GLM). Eyes-open and eyes-closed GSP regressors of each frequency band (see EEG processing above) were used as parametric modulation of the eyes-open and eyes-closed blocks. The transitions between eyes-open and eyes-closed blocks were modeled in separate regressors of no interest, since motor activity and strong visual input is seen here as confounding both EEG and fMRI resting-state signals. In the main analysis, each frequency band was analyzed in a separate model. In a second analysis, focusing only on frequency-specific coupling, all frequency bands were entered into one common GLM. Separate models reveal the complete correlation pattern of a frequency whereas a common model reveals the partial correlation pattern of a frequency at the single subject level. By definition, the latter is only a part of the former. A disadvantage of the common model is that it is blind to the common variance among all regressors (i.e., their covariance) that will not be attributed to any of the partial collinear regressors (e.g. general power increase by eyes-closing, stimulation or even during rest). The common model may increase specificity (Tyvaert et al., 2008) and may therefore be of much interest, but separate models remain essential to detect less frequency-specific effects. Individual contrast images were calculated for eyes-open and eyes-closed GSP modulation regressors and used for random effects analysis. For the main analysis as well as for the common GLM analysis, a 2 x 2 x 6 analysis of variance (ANOVA) with factors group (adults, adolescents), condition (eyes-open, eyes-closed) and frequency (delta, theta, alpha1, alpha2, beta1, beta2) was applied to calculate group statistics. Because the ANOVA revealed strong main effects of condition and frequency of secondary interest (see Results section), EEG–BOLD coupling patterns were reported as post-hoc t-tests (in both directions). Since only condition and frequency specific t-contrasts allow

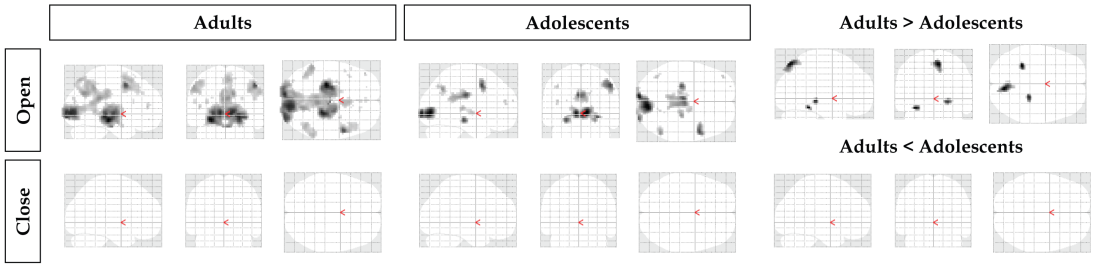

Fig. 1.3 Conventional fMRI analysis without EEG regressors. Group means of individual 'eyes-open > eyes-closed' ("open") and 'eyes-open < eyes-closed' ("close") contrasts are shown at $p < 0.05$ FWE corrected. Group difference thresholded at $p < 0.001$ uncorrected, corrected with minimal cluster size of 25 voxels.

connect to the existing literature on EEG–BOLD coupling, these ANOVA results are attached in supplementary Fig. 1. 1. The three regional EEG regressors (frontal delta and theta, occipital alpha1 and alpha2, central alpha2 and beta1) were calculated in separate random effects analysis.

Conventional fMRI analysis aimed to analyze eyes-open and eyes-closed condition independent from EEG. The model was identical to the one described above except no EEG modulation was included. This model was calculated using a 128 s highpass filter, and in a post-hoc analysis also with a 600 s filter. The first model is analogous to the EEG-informed models, whereas the second uses the adequate filter length to retain also the very slow eyes-open/eyes-closed paradigm cycles of 600 s. Random statistics were calculated based on the individual eyes-open versus eyes-closed contrast image.

Group mean statistics are reported at the $p < 0.05$ significance level, controlled for the family wise error rate (FWE) to account for the problem of multiple comparisons. For the purpose of interpretation only clusters contain at least 20 significant voxels are reported. The second analysis using a common model for all frequencies reached less statistical power and was reported at $p < 0.001$ corrected for multiple comparisons by minimal cluster extent of 25 voxels (Forman et al., 1995; Slotnick et al., 2003). Because group differences did not reach significance at the a priori threshold, results are shown at an uncorrected voxel-threshold of $p < 0.001$ (explanation in results and in discussion). Regions of interest (ROIs) were functionally defined from these group differences to plot local group mean contrast values.

3.3 Results

We did not identify significant differences between the two sessions, neither for EEG, fMRI, nor EEG–fMRI coupling data. Thus we report on data pooled from both recording sessions.

3.3.1 EEG results

Results from both groups replicated the typical resting state EEG characterized by a sharp alpha peak (around 10 Hz), with occipital topography, which was reduced in strength with eyes open. T-tests between the two age groups revealed higher power values for adolescents in lower frequencies (< 10 Hz), as hypothesized (Fig. 1.1 and 1.2). Higher frequencies did not substantially distinguish between the two groups, and the difference even tended to invert. This held for GSP (Fig. 1.1) as well as for the power maps (Fig. 1.2), while the effect was equivalent in both eyes-open and eyes-closed condition.

3.3.2 FMRI results

Conventional fMRI results during eyes-open indicated that the thalamus, visual cortex and frontal eye fields were activated (Fig. 1.3). The adolescent group showed very similar activation within the visual system. During eyes-closed no regions of increased activation were found. Comparing the two groups, some regions were more activated in adults but none were more activated in adolescents. Interestingly, recalculating this analysis using a 600 s highpass filter to accommodate also very slow sustained BOLD effects turned out to yield very similar activations.

3.3.3 EEG–BOLD correlation results

The ANOVA results (supplementary Fig. 1.1) indicated strong and wide-spread main effects of condition and frequency. Therefore t-contrasts by frequency and condition are reported to specify these global effects and relate them to the existing literature on EEG–BOLD coupling. The main effect of group was small compared to the effects of the other factors. The group differences were restricted to visual areas peaking at [18, -84, 15] xyz MNI-coordinate. This difference arose mainly from the eyes-open beta1 band as clarified by t-contrasts with a local maximum in the same region (Fig. 1.4) and region of interest (ROI) analysis (Fig. 1.6), both described below. Interactions did not reach significance at the a priori statistical threshold (except for a few isolated voxels).

Patterns of EEG–BOLD coupling differed between frequencies, conditions and groups (Fig. 1.4 and Fig. 1.5). In all frequency bands, negative correlations were more prominent than positive ones. During eyes-open, more frequency bands showed BOLD correlates than during eyes-closed (Table 1.1).

During eyes-open delta band power correlated negatively with the BOLD signal in the adolescent group in the right inferior parietal lobe. Theta power was negatively correlated with left inferior parietal lobe BOLD in both groups. In adults, theta power and BOLD was also coupled in the right inferior parietal lobe and superior and middle frontal gyrus, both of which are commonly associated with the DMN (see also Fig. 1.6). Both alpha bands are associated to similar brain regions in occipital, parietal and frontal lobes. Beta1 power revealed a very distinct coupling pattern in both groups

in parietal and frontal cortices commonly associated as attention network (Fox et al., 2005).

During eyes-closed the alpha2 band was linked to a thalamocortical pattern in adults and adolescents. Group differences were not significant, but for adolescents alone, the positive correlation with the thalamus did not survive the strict statistical threshold. This correlation is displayed in more detail in Fig. 1.6. The beta1 and alpha2 bands elicited similar coupling, as the thalamus was again positively correlated in adults and the broad negative correlations were already present in adolescents.

The direct group comparison using a two-sample t-test did not reveal any group differences at the a priori threshold. When lowering the statistical threshold, differences first appeared in eyes-open alpha2 and beta bands and eyes-closed beta2 at $p < 0.001$ uncorrected for multiple comparisons, as shown in Fig. 1.4 and 2.5. For these effects, the directions of the EEG–BOLD correlation of both groups are shown in Fig. 1.7.

EEG–BOLD correlations with all frequencies in one common model are shown in supplementary Fig. 1.2 and 2.3. In the ANOVA, the main effects were significant only for factor frequency. Group by frequency interaction reached significance in a few left temporal and right parietal/superior temporal and lateral prefrontal clusters. Condition and frequency interacted in the thalamus, along the precentral and medial frontal gyri, in the parahippocampal gyrus and in the precuneus. Compared to separate GLMs, the common model produced a frequency main effect that was similarly distributed but more diffuse. It eliminated the main effects of group and condition as well as the group by condition interaction, but yielded more group x frequency interactions and differently distributed condition by frequency interactions.

Post-hoc t-tests of the common model correlations yielded only few correlations if corrected by FWE method and were displayed at a more lenient threshold (supplementary Fig. 1.3). Low frequencies delta and theta showed partially similar patterns in both conditions, including positively correlated occipital cortex/precuneus, pre- and postcentral gyri, anterior cingulate cortex and temporal and frontal lobe regions along the Sylvian fissure and negatively correlated clusters in DMN-associated areas including medial prefrontal cortex, posterior cingulated cortex and inferior parietal lobe. During eyes-open predominantly negative correlations were found in occipital cortex/precuneus for alpha2 and in attention-control-network-related areas in lateral parietal/frontal lobes in beta1. During eyes-closed, positive thalamic correlations reached significance in beta1 in adults and adolescents and in beta2 in adults. Negative eyes-closed correlations appeared in alpha2, beta1 and beta2 in occipital, parietal, temporal or pre-/postcentral regions, together reflecting the formerly established thalamocortical pattern. All three higher frequencies accounted partially for this pattern but the frequency specificity appeared not robust when comparing the two groups. Compared to separate GLMs, the common model demonstrated less overall statistical power. The low frequency delta and theta negative DMN association did not change between the two analyses. In contrast, broad positive correlations appeared in these frequencies in regions similar to the negative correlated part of the thalamocortical pattern. This low frequency pattern was specific to both delta

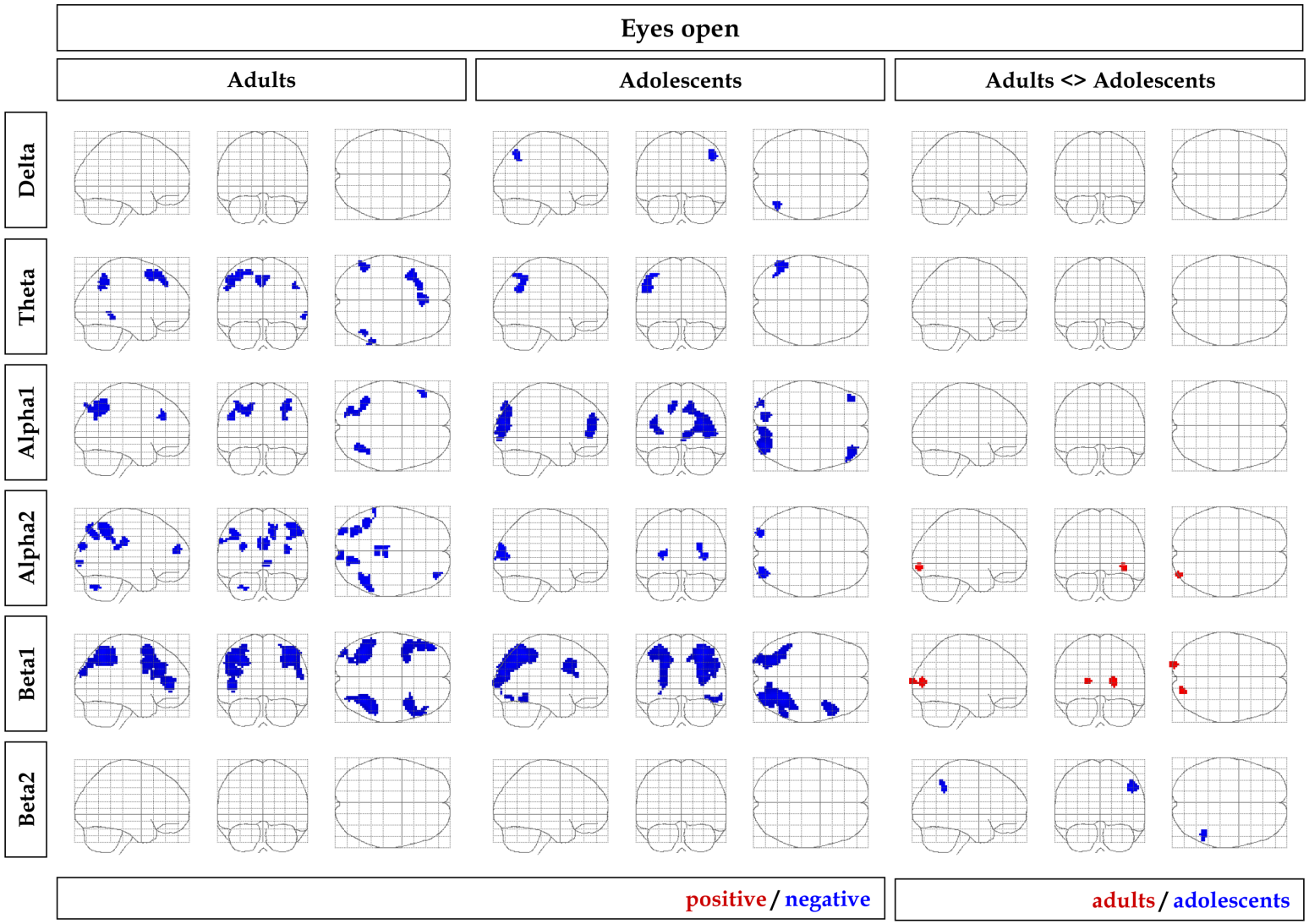

Fig. 1.4 EEG-BOLD correlations during eyes-open. Each row represents one frequency band as labeled on the left. Voxels reaching statistical significance are visualized as maximum intensity projections on sagittal, coronal and axial views. The t-tests are plotted on a 'glass brain'; signs are distinguished by red and blue color (overlay appears in pink). For group means, positive correlations are colored red, negative correlations are colored blue. For group differences both contrasts 'adults > adolescents' and 'adolescents > adults' are overlaid, red color indicating the first and blue the latter contrast. Statistics are thresholded at $p < 0.05$ FWE corrected. For simplification, only clusters > 20 voxels are plotted for group means. The direct group contrast is thresholded at $p < 0.001$ uncorrected, corrected with minimal cluster size of 25 voxels.

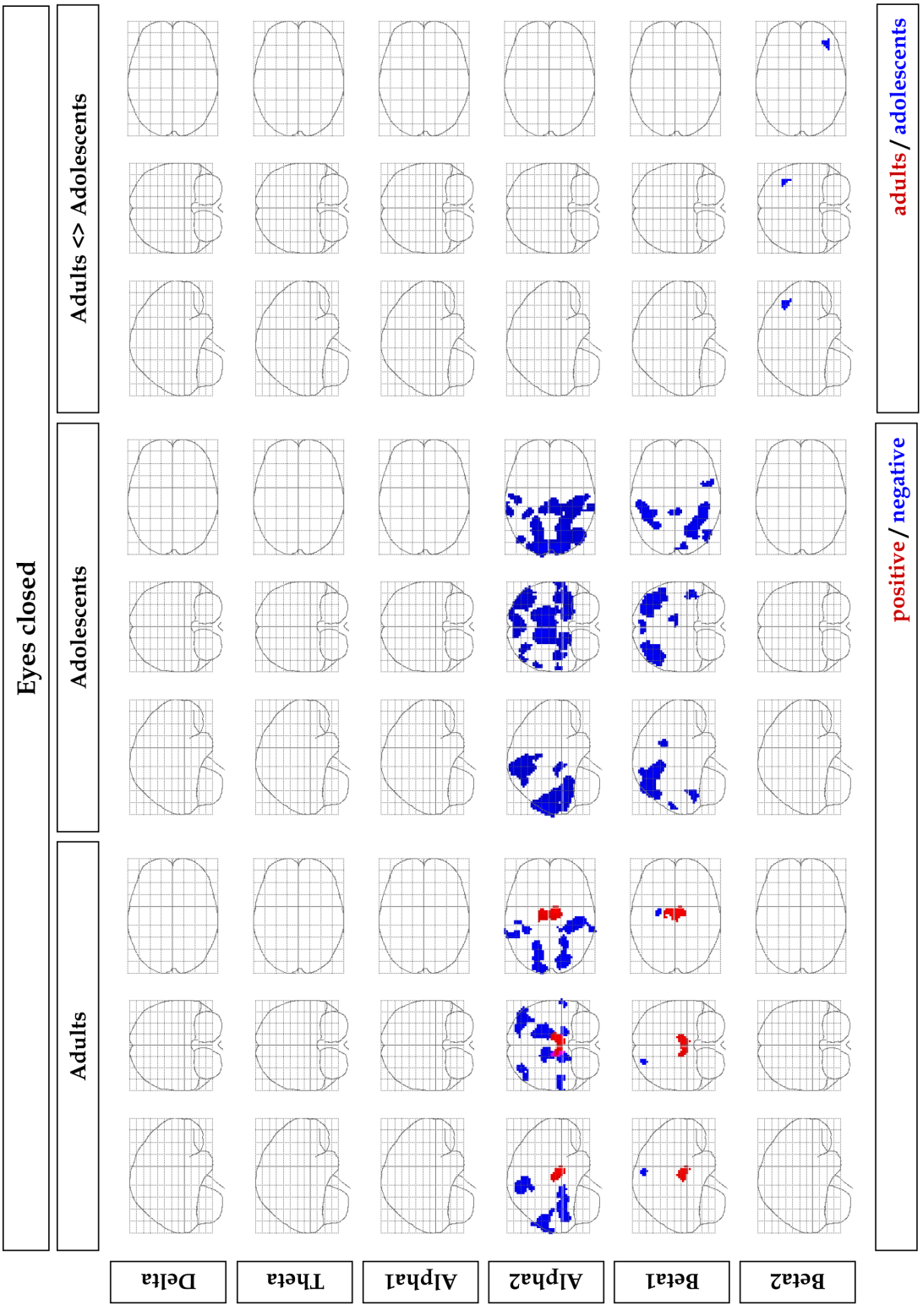

Fig. 1.5 EEG-BOLD correlations during eyes-closed. figure annotation as in Fig. 1.4.

and theta bands, appeared quite robust between adults and adolescents and sustained the alternating conditions. The former redundancy between eyes-open alpha1, alpha2 and beta1 was eliminated in the common model attributing occipital correlations specifically to alpha2 and the attention-control network correlations specifically to beta1. Compared to separate GLMs, the eyes-closed thalamocortical pattern was split up the between all three upper frequency bands by the partial correlation approach. Group differences did not reach significance in this analysis, except for a small cluster in eyes-open alpha1 in right cingulated at [18, -45, 24] peak xyz MNI-coordinate and eyes-closed delta in right inferior parietal lobe at [57, -54, 36] that did not spatially overlap with the correlation pattern of the corresponding frequency.

3.4 Discussion

Characteristic maturational EEG amplitude reduction of low-frequency oscillations were found after age 15, although this effect was less prominent in absolute terms than the decreases reported during infancy, childhood and early adolescence. Unlike studies focusing on adolescents of a similar mean age but including younger, pre-adolescent participants driving the decrease (Gasser et al., 1988; Whitford et al., 2007), we directly compared groups of older adolescents and young adults. Although, based on the literature, only subtle spectral EEG differences could be expected between these groups, we still found substantial reduction of low-frequency EEG amplitudes at this late stage of brain maturation. Despite this EEG age effect, both groups revealed the typical resting state EEG characteristics of strong posterior alpha oscillations with eyes-closed. For theta, a frontal component could also be distinguished. The developmental low frequency power reductions tended to be similar across scalp regions (Fig. 1.2., see also Whitford et al. 2007). Therefore the global GSP measure seems to appropriately summarize (post-)adolescent EEG maturation in one comprehensive measure (Fig. 1.1).

The conventional fMRI results (independent of EEG activity) revealed no such age related group differences (Fig. 1.3). During eyes-open, the visual pathway including thalamus, geniculate laterale nuclei and visual cortex together with frontal eye fields were activated in both groups. These activations can be expected since open eyes produce a stimulation of the visual system which is not the case if the eyes are closed. Furthermore the result is in line with other fMRI studies contrasting eyes-open and eyes-closed states (Marx et al., 2004; Marx et al., 2003). The eyes-closed condition did not elicit any regions of greater activation. Although the standard highpass filter eliminated sustained paradigm induced variance, the reanalysis using less filtering (not shown) did not affect the results. Hence BOLD signal fluctuations responsible for the condition difference mainly consist of faster fluctuations than those sustained over the full eyes-open or eyes-closed periods (300 s each). While the fMRI indicated increased activity during eyes-open, the EEG activity in contrast (in particular within alpha band, consistent with the classical observation of Berger, 1929) was increased during eyes-closed. This result is in line with other observations that synchronization of background EEG is often correlated with states of lower arousal or suppression of brain areas (Barry et al., 2007;

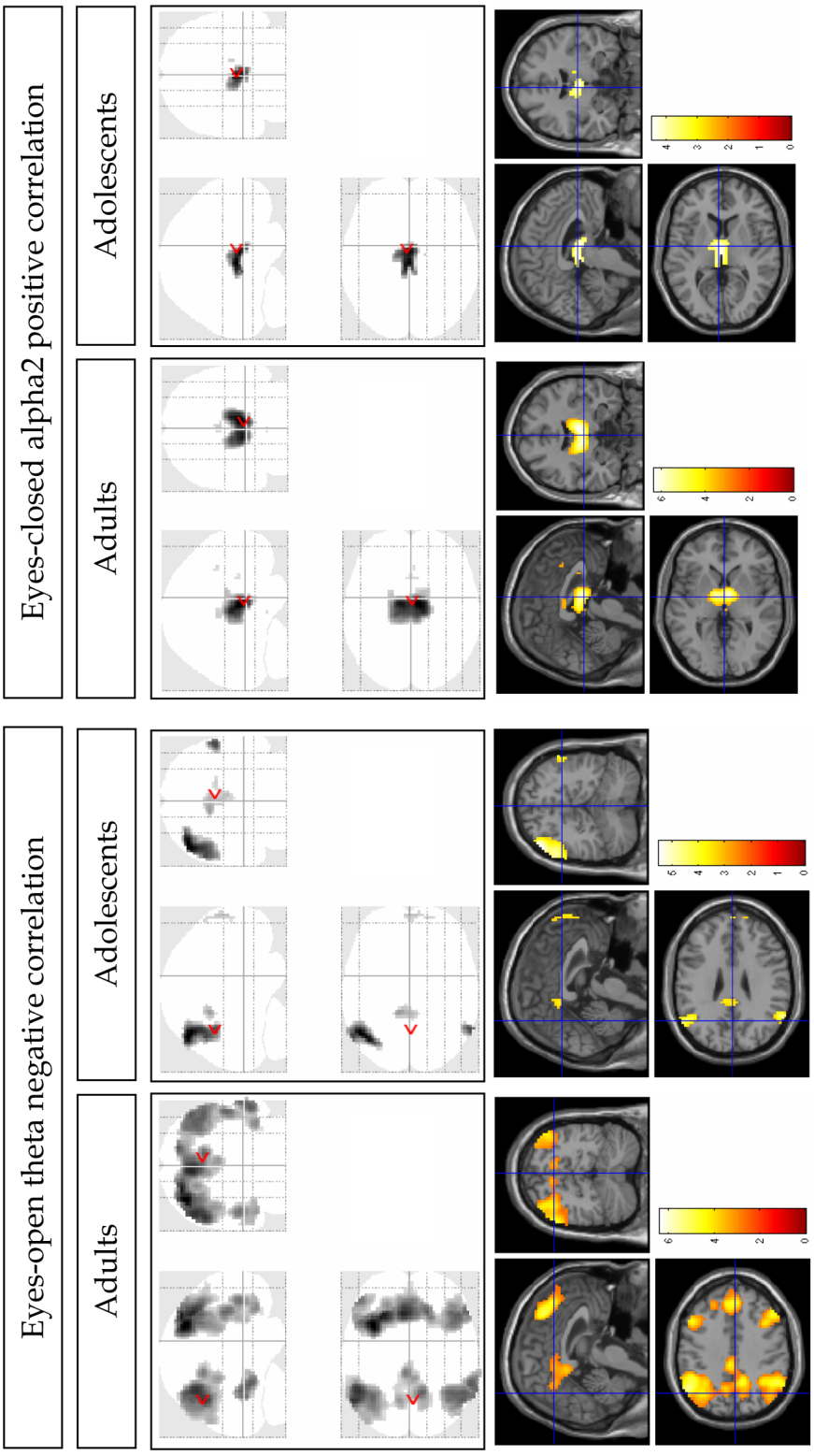

Fig. 1.6 Replication of EEG-BOLD correlations in more detail (random effects). Equivalent to Scheeringa et al., 2008, eyes-open theta negative correlation is shown at $p < 0.05$ FDR corrected, $k = 50$ at spatial coordinates $x = 4$, $y = -66$, $z = 40$. Eyes-closed alpha2 positive correlation is shown at $p < 0.001$, uncorrected, $k = 0$ spatial coordinates $x = 2$, $y = -8$, $z = 1$.

Pfurtscheller, 2001), and illustrates the inverse relationship between lower frequency EEG and fMRI.

The EEG–BOLD correlation results of adults correspond well to the existing literature. Many core findings of previous studies were found replicated: (i) EEG power correlations with the BOLD signal were predominantly negative (de Munck et al., 2007; Feige et al., 2005; Goldman et al., 2002; Laufs et al., 2003a; Moosmann et al., 2003; Ritter et al., 2009; Tyvaert et al., 2008). This inverse relationship is in contrast to studies that find local field potentials (LFP) positively associated with the BOLD signal (Logothetis et al., 2001; Nir et al., 2007; Viswanathan and Freeman, 2007). A possible explanation is that in contrast to LFP at least some EEG rhythms reflect a local deactivation of brain functioning through phasing neuron populations (Pfurtscheller, 2001). (ii) During eyes-open the DMN was anticorrelated with theta power. The adult pattern found here overlaps with previous work in several regions, including right middle temporal gyri, bilaterally inferior parietal lobule and bilaterally inferior frontal gyri (Scheeringa et al., 2008). Scheeringa and colleagues used a spatially constrained theta power represented by a single ICA component. In contrast GSP as used in this study includes signals from all scalp sites without weighting by statistical independence (Jann et al., 2009; Michels et al., 2010). Accordingly our coupling pattern can be interpreted as the global features of theta EEG power. This correlation is displayed in more detail in Fig. 1.6. (iii) During eyes-closed alpha power was negatively correlated in occipital and parietal cortices and positively correlated with the thalamus (de Munck et al., 2007; Difrancesco et al., 2008; Feige et al., 2005; Goldman et al., 2002; Goncalves et al., 2006; Moosmann et al., 2003; Tyvaert et al., 2008). It has been suggested that posterior alpha power represents down-regulation of the primary visual system during eyes-closed with the thalamus partly driving this process (de Munck et al., 2007; Feige et al., 2005; Goldman et al., 2002). However some alpha-BOLD correlation studies could not reveal a positive correlation of the thalamus (Jann et al., 2009; Laufs et al., 2003a). This inconsistency may be explained by the typical large variability of the EEG between individuals (Goncalves et al., 2006). The correlation pattern in our data extended from occipital to pericentral regions, and the thalamocortical pattern extended to the beta1 band. Positive thalamic BOLD correlation in beta band was reported before (de Munck et al., 2009; Moosmann et al., 2003). One reason for this robust pattern may be the inclusion of "rolandic" alpha (Gastaut, 1952; Salmelin and Hari, 1994) and beta (Pfurtscheller, 1981; Salmelin and Hari, 1994) rhythms in GSP. Similar to visual-related posterior alpha, these rhythms which relate to the thalamocortical regulation of motor and somatosensory systems were also found inversely correlated to the BOLD signal (Ritter et al., 2009). During eyes-closed, alpha2 and beta1 were the only frequencies correlated with the BOLD signal. To also account for specific, well defined local EEG rhythms (frontal midline theta, occipital alpha, central alpha and beta), separate analyses were carried out, based on regional sets of electrodes (supplementary Fig. 1.4 and 1.5). The correlation pattern from these local rhythms overlapped to a high degree with the GSP correlation pattern, but tended to be weaker than the latter.

Including both common variants of the resting state paradigm – eyes-open and eyes-

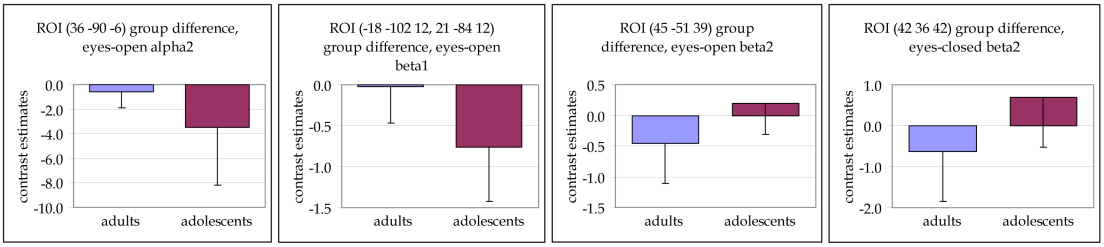

Fig. 1.7 Contrast estimates in regions of interest (ROI) defined by significant group differences as shown in Fig. 1.4 and Fig. 1.5 for eyes-open alpha2, beta1, beta2 and eyes-closed beta2. The ROI's center is given in xyz-coordinates in the panel titles. In the first two panels adolescents have stronger negative EEG-BOLD coupling than adults. In the latter two panels, adolescents have positive but adults have negative coupling.

closed – as well as all major EEG frequency bands, we were able to draw a more comprehensive picture of resting state EEG–BOLD coupling than reported so far. This is important because the two resting conditions do differ substantially in both EEG (Barry et al., 2007; Berger, 1929) and fMRI (Bianciardi et al., 2009; Marx et al., 2004; Marx et al., 2003). Indeed our results were highly condition and partly frequency specific. Interestingly, the eyes-open condition – although somewhat neglected by researchers so far – elicited even more robust EEG–BOLD coupling patterns than the eyes-closed condition. During eyes-open the two alpha bands elicited similar correlations in parietal and frontal lobes. In contrast, during eyes-closed, splitting the alpha band elicited strikingly different results. A conspicuous pattern during eyes-open in the beta1 frequency range was robustly found in both groups. Beta1 GSP correlated negatively in extended bilateral parietal and frontal lobe regions forming the attention network (Fox et al., 2005). Overall we found four main EEG–BOLD coupling patterns in our eyes-open/eyes-closed resting state paradigm, corresponding to (i) the DMN; (ii) occipital cortex; (iii) the attention network; and (iv) a thalamocortical network. Our EEG–BOLD coupling pattern proved robust when based on random effects analysis corrected for multiple comparisons, allowing for reliable generalization to the population level. This contrasts with previous reports of EEG–BOLD coupling where a lack of significant results in random effect analyses was attributed to substantial inter-subject variability of EEG data (Goncalves et al., 2006; Laufs et al., 2006).

We also included an alternative EEG–BOLD coupling analysis to disentangle frequency specific effects. To this end we performed an additional common GLM analysis with all frequency bands entered simultaneously. This ANOVA based on the common model supported our conclusion regarding frequency specific coupling, as the main effect of frequency resembled the one obtained using separate GLMs. The common model analysis eliminated the main effects of group and condition. Consistent with its selective sensitivity to frequency specific effects, some of the condition effects in the separate models analysis appeared as condition by frequency interactions in the common model. The band-wise t-statistics revealed lower overall statistical power in the common model than in separate models. This probably reflects the loss of common variance across frequencies. The common model produced far more positive correlations, particularly in the low frequencies, which can be interpreted as relative rather than absolute increases in coupling.

Further, the common GLM confirmed that the DMN is coupled to both, theta and delta independently, leading to the conclusion that DMN is coupled to low frequency EEG in general. This DMN-low frequency coupling appeared to be the most general EEG–fMRI resting state feature as it occurred independently of condition. The attention-control network related negative correlation during eyes-open was specific for the beta1 band. The common model produced some similarities with the separate models for the alpha and beta bands. However, the positive alpha-BOLD correlation in the thalamus during eyes closed - a landmark EEG–BOLD correlation - was eliminated by the common model. This suggests that the thalamic correlation was partly shared with other frequencies and therefore no longer attributed to alpha2 in the common GLM. Positive thalamic beta correlations were replicated in the common model, suggesting that thalamocortical beta coupling is more frequency specific. Positive thalamic BOLD correlation in beta band was reported before (de Munck et al., 2009; Moosmann et al., 2003). In the common GLM, all higher frequencies became partly sensitive to the negative correlation of the thalamocortical pattern but these correlations appeared not very robust across the two groups. Group differences of the common model analysis were even fewer and appeared in different frequencies than in the separate models analysis. Interestingly, eyes-closed delta was less negative coupled in adults than in adolescents in a small cluster associated with the negatively correlated DMN. This effect was model dependent as it was not evident in separate frequency correlations (next paragraph). Hence it is questionable if this small difference manifests a direct correspondence to the absolute power difference emerging in EEG maturation.

No study so far investigated EEG–BOLD coupling from a developmental perspective in general, or for late maturation in particular. Motivated by the late neurodevelopmental effect of decreasing slow oscillatory power, the primary goal was to investigate corresponding effects in the EEG–BOLD coupling. However, adults and adolescents did not differ in EEG–BOLD correlation in any frequency band. Accordingly, the mean coupling patterns of adults and adolescents overlapped to a high degree. Because of the centrality of this question, we explored trends for corresponding developmental differences of EEG–BOLD coupling using a lenient statistical thresholding ($p < 0.001$, uncorrected for multiple comparisons). Although these trends must be interpreted with caution, adolescents tended towards slightly stronger coupling of occipital regions with the alpha2 and beta1 bands (Fig. 1.4 and 1.5). This trend for stronger coupling parallels a more pronounced occipital EEG topography in these frequency bands in adolescents. However, these subthreshold effects emerged at higher frequencies, and therefore are likely to be unrelated to the significant power decrease during and after late adolescence in low frequencies. This observation held even if thresholded more liberally (i.e. $p < 0.005$ uncorrected, not shown), and even for the frequency specific supplementary analysis. Similarly none of the local EEG rhythms differed in their BOLD correlation pattern between adults and adolescents at the strict statistical threshold (supplementary Fig. 1.4 and 1.5). A minor trend emerged, but again not in the delta and theta bands, and thus not corresponding to the EEG maturation effects. Interestingly however, adolescents tended to have stronger (negative) correlation in post the central sulcus region for the

Table. 1.1 Anatomical regions corresponding to the significant main results in Fig. 1.4 and Fig. 1.5. Listed are cluster size, coordinates in MNI space, peak t-value, corresponding anatomical region and Brodmann Area.

			Adults							Adolescents						
condition	frequency	contrast	cluster size	MNI coordinate (x,y,z)			t-value	anatomical structure	BA	cluster size	coordinates (x,y,z)			t-value	anatomical structure	BA
Eyes-open	Delta	negative								54	48	-63	48	5.51	Right Inferior Parietal Lobule	BA 40
	Theta	negative	124	-36	15	54	5.93	Left Superior Frontal Gyrus	BA 8	263	-48	-57	36	5.35	Left Inferior Parietal Lobule	BA 40
			94	0	33	48	5.32	Left Superior Frontal Gyrus	BA 8							
			97	-48	-54	45	5.27	Left Inferior Parietal Lobule	BA 40							
			24	63	-45	-3	5.01	Right Middle Temporal Gyrus	BA 21							
			10	57	30	18	4.97	Right Inferior Frontal Gyrus	BA 46							
			11	-48	42	3	4.83	Left Inferior Frontal Gyrus	BA 46							
			20	48	-54	39	4.77	Right Inferior Parietal Lobule	BA 40							
			5	45	18	51	4.56	Right Middle Frontal Gyrus	BA 8							
	Alpha1	negative	41	-48	33	30	5.69	Left Middle Frontal Gyrus	BA 46	434	30	-81	21	6.42	Right Middle Occipital Gyrus	BA 19
			18	-48	45	6	5.36	Left Inferior Frontal Gyrus		150	48	48	12	5.64	Right Middle Frontal Gyrus	BA 10
			144	-33	-54	42	5.32	Left Inferior Parietal Lobule	BA 40	55	-15	-84	45	5.39	Left Precuneus	BA 7
			144	33	-63	45	5.21	Right Superior Parietal Lobule	BA 7	42	-33	-90	12	5.09	Left Middle Occipital Gyrus	BA 19
			11	-63	-42	33	5.09	Left Inferior Parietal Lobule	BA 40	55	-45	45	21	5.02	Left Middle Frontal Gyrus	BA 46
			10	12	-72	45	4.54	Right Precuneus	BA 7	12	66	-39	33	4.79	Right Inferior Parietal Lobule	BA 40
										7	-24	-81	21	4.64	Left Precuneus	BA 31
										5	-6	-99	6	4.53	Left Cuneus	BA 18
	Alpha2	negative	171	45	-51	54	5.55	Right Inferior Parietal Lobule	BA 40	203	33	-81	12	5.00	Right Middle Occipital Gyrus	BA 19
			85	15	-72	42	5.34	Right Precuneus	BA 7	41	-30	-93	15	4.83	Left Middle Occipital Gyrus	BA 19
			84	-39	-51	42	5.30	Left Inferior Parietal Lobule	BA 40	14	3	-93	-3	4.76	Right Lingual Gyrus	BA 17
			99	6	-24	33	5.30	Right Cingulate Gyrus	BA 23							
			45	-30	-87	24	5.29	Left Cuneus	BA 19							
			40	-27	-66	-39	5.22	Left Pyramis								
			37	36	57	21	5.15	Right Superior Frontal Gyrus	BA 10							
			14	6	-36	48	4.96	Right Precuneus	BA 7							
			35	6	-93	0	4.82	Right Cuneus	BA 17							
			5	6	15	69	4.77	Right Superior Frontal Gyrus	BA 6							
			5	-24	-27	0	4.76	Left Thalamus								
			8	30	-87	27	4.64	Right Cuneus	BA 19							
	Beta1	negative	485	36	-57	57	6.80	Right Superior Parietal Lobule	BA 7	988	33	-51	51	6.66	Right Precuneus	BA 7
			502	-33	-57	45	6.53	Left Inferior Parietal Lobule	BA 40	577	-24	-69	36	6.03	Left Precuneus	BA 7
			534	-45	42	6	6.46	Left Middle Frontal Gyrus	BA 46	195	48	15	33	5.41	Right Middle Frontal Gyrus	BA 9
			292	39	12	57	5.49	Right Middle Frontal Gyrus	BA 6	52	54	-54	-18	5.34	Right Inferior Temporal Gyrus	BA 20
			7	48	42	-6	4.67	Right Middle Frontal Gyrus	BA 47	21	42	-75	-12	5.03	Right Inferior Occipital Gyrus	BA 19
										14	-42	-63	-9	4.88	Left Middle Temporal Gyrus	BA 37
										9	-18	-90	-6	4.75	Left Lingual Gyrus	BA 17
										16	45	51	3	4.71	Right Inferior Frontal Gyrus	BA 10
										6	-51	27	30	4.68	Left Middle Frontal Gyrus	BA 46
										5	15	-84	-9	4.64	Right Lingual Gyrus	BA 18
	Beta2	negative	44	48	-51	39	4.67	Right Inferior Parietal Lobule	BA 40							
			83	-6	-33	33	4.51	Left Cingulate Gyrus	BA 31							
			28	-48	-57	45	4.37	Left Inferior Parietal Lobule	BA 40							
Eyes-closed	Alpha2	positive	186	9	-6	3	5.79	Right Thalamus								
				-9	-6	3	5.23	Left Thalamus								
				-12	-18	12	4.79	Left Thalamus								
	Alpha2	negative	196	-18	-57	0	5.40	Left Lingual Gyrus	BA 18	2218	-9	-93	33	6.79	Left Cuneus	BA 19
			220	21	-78	24	5.39	Right Precuneus	BA 31	873	45	-18	60	5.74	Right Precentral Gyrus	BA 4
			70	-48	-42	3	5.32	Left Middle Temporal Gyrus	BA 22	43	66	-27	6	5.15	Right Superior Temporal Gyrus	BA 22
			242	54	-21	57	5.15	Right Postcentral Gyrus	BA 3	70	-42	-75	6	5.07	Left Middle Occipital Gyrus	BA 19
			63	21	-51	-3	5.09	Right Parahippocampal Gyrus	BA 30	68	-30	-36	54	5.07	Left Postcentral Gyrus	BA 3
			74	-33	-36	60	4.99	Left Postcentral Gyrus	BA 3	19	60	3	-12	4.95	Right Middle Temporal Gyrus	BA 21
			121	-15	-87	27	4.95	Left Cuneus	BA 19	30	-60	-33	6	4.93	Left Superior Temporal Gyrus	BA 42
			22	66	-36	0	4.80	Right Middle Temporal Gyrus	BA 21	32	-45	-18	63	4.87	Left Precentral Gyrus	BA 4
			13	9	-21	54	4.69	Right Medial Frontal Gyrus	BA 6	6	-36	-27	69	4.79	Left Precentral Gyrus	BA 4
			16	60	-12	39	4.67	Right Precentral Gyrus	BA 6	25	-57	-12	39	4.76	Left Precentral Gyrus	BA 6
			5	18	-72	-9	4.52	Right Lingual Gyrus	BA 18							
	Beta1	positive	138	0	-9	3	5.51	Left Thalamus								
	Beta1	negative	24	-24	-6	66	5.13	Left Middle Frontal Gyrus	BA 6	431	-42	-42	54	5.77	Left Inferior Parietal Lobule	BA 40
										543	27	-60	63	5.67	Right Superior Parietal Lobule	BA 7
										74	48	-66	-6	5.10	Right Inferior Temporal Gyrus	BA 37
										48	57	9	36	4.90	Right Inferior Frontal Gyrus	BA 9
										52	-6	-36	66	4.86	Left Paracentral Lobule	BA 6
										12	-21	-75	45	4.81	Left Precuneus	BA 7
										37	12	-84	24	4.74	Right Cuneus	BA 18
										8	30	-3	72	4.73	Right Superior Frontal Gyrus	BA 6

condition	frequency	contrast	cluster size	MNI coordinate (x,y,z)			t-value	anatomical structure	BA
Eyes-open	Alpha1	adults > adolescents	30	36	-90	-6	3.72	Right Middle Occipital Gyrus	BA 18
	Beta1	adults > adolescents	40	21	-84	12	3.8	Right Cuneus	BA 17
			28	-18	-102	12	3.48	Left Middle Occipital Gyrus	BA 18
	Beta2	adults > adolescents	62	45	-51	39	4.11	Right Inferior Parietal Lobule	BA 40
Eyes-closed	Beta2	adults > adolescents	28	42	36	42	3.58	Right Middle Frontal Gyrus	BA 9

central beta1 rhythm (eyes-closed) than adults. We conclude that, in contrast to the developmental decrease of low frequency EEG activity, the frequency specific EEG–BOLD correlations do not change substantially at this late stage of brain maturation. Contrary to our initial hypothesis that a distinct network reflects late immaturity, but consistent with the simpler scaling hypothesis, the EEG–BOLD correlation pattern between the two signals remains largely the same despite changing magnitude of the low frequency EEG signal. This result indicates that the correlation pattern of EEG and fMRI signals mature earlier than the EEG amplitudes. In order to test whether the subthreshold coupling differences between adolescents and adults reflect genuine but asymptotic developmental effects, it will be necessary to contrast these data to data from younger children. However, the fact that the EEG–BOLD coupling does not mirror the neurodevelopmental process captured by the EEG, suggests that the two domains capture partly different aspects of brain functioning (Laufs, 2008).

The predominantly inverse relationships between EEG and fMRI signals in our data using the separate model may suggest that synchronized neuronal activity, at least for the lower frequency range up to the alpha band, is related to states of lower arousal, lower neural activity, and lower metabolic consumption: (i) EEG power fluctuations are negative correlated to the BOLD signal; (ii) EEG power is increased during eyes-closed whereas the BOLD signal is increased during eyes-open; (iii) EEG power mainly decreases with brain development, whereas the conventional fMRI analysis rather indicates an increasing trend with brain development.

3.5 Conclusion

In this study we investigated spectral EEG power changes between adolescence and adulthood for corresponding differences in the BOLD signal using simultaneously recorded fMRI during rest with eyes-open and eyes-closed periods. First, low-frequency EEG power continued to decrease beyond mid-adolescence. Second, similar robust EEG–BOLD coupling pattern was identified in adults and adolescents. Power in most EEG bands correlated negatively with the BOLD signal in areas of DMN and attention network during eyes-open, and in a thalamocortical network during eyes-closed. However, no robust changes in EEG–BOLD coupling corresponding to the decrease in low-frequency EEG power were identified. Our results indicate that the most prominent changes in EEG amplitudes are independent of the correlation with the BOLD signal during late maturation. To clarify at which developmental stage the mature pattern of EEG–BOLD coupling at rest emerges, future work needs to include younger participants.

3.6 Acknowledgements

This work was supported by the University Research Priority Program on Integrative Human Physiology. We like to thank Thomas Koenig for ICA implementation and Christian Gaser for some MATLAB code advice.

3.7 References

Allen, P.J., Josephs, O., Turner, R., 2000. A method for removing imaging artifact from continuous EEG recorded during functional MRI. Neuroimage 12, 230-239.

Allen, P.J., Polizzi, G., Krakow, K., Fish, D.R., Lemieux, L., 1998. Identification of EEG events in the MR scanner: the problem of pulse artifact and a method for its subtraction. Neuroimage 8, 229-239.

Barry, R.J., Clarke, A.R., Johnstone, S.J., Magee, C.A., Rushby, J.A., 2007. EEG differences between eyes-closed and eyes-open resting conditions. Clin Neurophysiol 118, 2765-2773.

Beckmann, C.F., DeLuca, M., Devlin, J.T., Smith, S.M., 2005. Investigations into resting-state connectivity using independent component analysis. Philos Trans R Soc Lond B Biol Sci 360, 1001-1013.

Ben-Simon, E., Podlipsky, I., Arieli, A., Zhdanov, A., Hendler, T., 2008. Never resting brain: simultaneous representation of two alpha related processes in humans. PLoS One 3, e3984.

Berger, H., 1929 Über das Elektrenkephalogramm des Menschen. European Archives of Psychiatry and Clinical Neuroscience 87, 527-570.

Bianciardi, M., Fukunaga, M., van Gelderen, P., Horovitz, S.G., de Zwart, J.A., Duyn, J.H., 2009. Modulation of spontaneous fMRI activity in human visual cortex by behavioral state. Neuroimage 45, 160-168.

Blakemore, S.J., Choudhury, S., 2006. Brain development during puberty: state of the science. Dev Sci 9, 11-14.

Boord, P.R., Rennie, C.J., Williams, L.M., 2007. Integrating "brain" and "body" measures: correlations between EEG and metabolic changes over the human lifespan. J Integr Neurosci 6, 205-218.

Brem, S., Bach, S., Kucian, K., Guttorm, T.K., Martin, E., Lyytinen, H., Brandeis, D., Richardson, U., 2010. Brain sensitivity to print emerges when children learn letter-speech sound correspondences. Proc Natl Acad Sci U S A 107, 7939-7944.

Campbell, I.G., Feinberg, I., 2009. Longitudinal trajectories of non-rapid eye movement delta and theta EEG as indicators of adolescent brain maturation. Proc Natl Acad Sci U S A 106, 5177-5180.

Case, R., 1992. The role of the frontal lobes in the regulation of cognitive development. Brain Cogn 20, 51-73.

Clarke, A.R., Barry, R.J., McCarthy, R., Selikowitz, M., 2001. Age and sex effects in the EEG: development of the normal child. Clin Neurophysiol 112, 806-814.

Damoiseaux, J.S., Rombouts, S.A., Barkhof, F., Scheltens, P., Stam, C.J., Smith, S.M., Beckmann, C.F., 2006. Consistent resting-state networks across healthy subjects. Proc Natl Acad Sci U S A 103, 13848-13853.

de Munck, J.C., Goncalves, S.I., Huijboom, L., Kuijer, J.P., Pouwels, P.J., Heethaar, R.M., Lopes da Silva, F.H., 2007. The hemodynamic response of the alpha rhythm: an EEG/fMRI study. Neuroimage 35, 1142-1151.

de Munck, J.C., Goncalves, S.I., Mammoliti, R., Heethaar, R.M., Lopes da Silva, F.H., 2009. Interactions between different EEG frequency bands and their effect on alpha-fMRI correlations. Neuroimage 47, 69-76.

Delorme, A., Makeig, S., 2004. EEGLAB: an open source toolbox for analysis of single-trial EEG dynamics including independent component analysis. J Neurosci Methods 134, 9-21.

Difrancesco, M.W., Holland, S.K., Szaflarski, J.P., 2008. Simultaneous EEG/functional magnetic resonance imaging at 4 Tesla: correlates of brain activity to spontaneous alpha rhythm during relaxation. J Clin Neurophysiol 25, 255-264.

Dustman, R.E., Shearer, D.E., Emmerson, R.Y., 1999. Life-span changes in EEG spectral amplitude, amplitude variability and mean frequency. Clin Neurophysiol 110, 1399-1409.

Fair, D.A., Dosenbach, N.U., Church, J.A., Cohen, A.L., Brahmbhatt, S., Miezin, F.M., Barch, D.M., Raichle, M.E., Petersen, S.E., Schlaggar, B.L., 2007. Development of distinct control networks through segregation and integration. Proc Natl Acad Sci U S A 104, 13507-13512.

Feige, B., Scheffler, K., Esposito, F., Di Salle, F., Hennig, J., Seifritz, E., 2005. Cortical and subcortical correlates of electroencephalographic alpha rhythm modulation. J Neurophysiol 93, 2864-2872.

Feinberg, I., Campbell, I.G., 2010. Sleep EEG changes during adolescence: an index of a fundamental brain reorganization. Brain Cogn 72, 56-65.

Forman, S.D., Cohen, J.D., Fitzgerald, M., Eddy, W.F., Mintun, M.A., Noll, D.C., 1995. Improved assessment of significant activation in functional magnetic resonance imaging (fMRI): use of a cluster-size threshold. Magn Reson Med 33, 636-647.

Fox, M.D., Snyder, A.Z., Vincent, J.L., Corbetta, M., Van Essen, D.C., Raichle, M.E., 2005. The human brain is intrinsically organized into dynamic, anticorrelated functional networks. Proc Natl Acad Sci U S A 102, 9673-9678.

Gasser, T., Verleger, R., Bacher, P., Sroka, L., 1988. Development of the EEG of school-age children and adolescents. I. Analysis of band power. Electroencephalogr Clin Neurophysiol 69, 91-99.

Gastaut, H., 1952. [Electrocorticographic study of the reactivity of rolandic rhythm.]. Rev Neurol (Paris) 87, 176-182.

Gibbs, F.A., Knott, J.R., 1949. Growth of the electrical activity of the cortex. Electroencephalogr Clin Neurophysiol 1, 223-229.

Giedd, J.N., Blumenthal, J., Jeffries, N.O., Castellanos, F.X., Liu, H., Zijdenbos, A., Paus, T., Evans, A.C., Rapoport, J.L., 1999. Brain development during childhood and adolescence: a longitudinal MRI study. Nat Neurosci 2, 861-863.

Gogtay, N., Giedd, J.N., Lusk, L., Hayashi, K.M., Greenstein, D., Vaituzis, A.C., Nugent, T.F., 3rd, Herman, D.H., Clasen, L.S., Toga, A.W., Rapoport, J.L., Thompson, P.M., 2004. Dynamic mapping of human cortical development during childhood through early adulthood. Proc Natl Acad Sci U S A 101, 8174-8179.

Goldman, R.I., Stern, J.M., Engel, J., Jr., Cohen, M.S., 2002. Simultaneous EEG and fMRI of the alpha rhythm. Neuroreport 13, 2487-2492.

Goncalves, S.I., de Munck, J.C., Pouwels, P.J., Schoonhoven, R., Kuijer, J.P., Maurits, N.M., Hoogduin, J.M., Van Someren, E.J., Heethaar, R.M., Lopes da Silva, F.H., 2006. Correlating the alpha rhythm to BOLD using simultaneous EEG/fMRI: inter-subject variability. Neuroimage 30, 203-213.

Henning, S., Merboldt, K.D., Frahm, J., 2006. Task- and EEG-correlated analyses of BOLD MRI responses to eyes opening and closing. Brain Res 1073-1074, 359-364.

Jann, K., Dierks, T., Boesch, C., Kottlow, M., Strik, W., Koenig, T., 2009. BOLD correlates of EEG alpha phase-locking and the fMRI default mode network. Neuroimage 45, 903-916.

John, E.R., Ahn, H., Prichep, L., Trepetin, M., Brown, D., Kaye, H., 1980. Developmental equations for the electroencephalogram. Science 210, 1255-1258.

Jung, T.P., Makeig, S., Westerfield, M., Townsend, J., Courchesne, E., Sejnowski, T.J., 2000. Removal of eye activity artifacts from visual event-related potentials in normal and clinical subjects. Clin Neurophysiol 111, 1745-1758.

Laufs, H., 2008. Endogenous brain oscillations and related networks detected by surface EEG-combined fMRI. Hum Brain Mapp 29, 762-769.

Laufs, H., Holt, J.L., Elfont, R., Krams, M., Paul, J.S., Krakow, K., Kleinschmidt, A., 2006. Where the BOLD signal goes when alpha EEG leaves. Neuroimage 31, 1408-1418.

Laufs, H., Kleinschmidt, A., Beyerle, A., Eger, E., Salek-Haddadi, A., Preibisch, C., Krakow, K., 2003a. EEG-correlated fMRI of human alpha activity. Neuroimage 19, 1463-1476.

Laufs, H., Krakow, K., Sterzer, P., Eger, E., Beyerle, A., Salek-Haddadi, A., Kleinschmidt, A., 2003b. Electroencephalographic signatures of attentional and cognitive default modes in spontaneous brain activity fluctuations at rest. Proc Natl Acad Sci U S A 100, 11053-11058.

Lehmann, D., Skrandies, W., 1980. Reference-free identification of components of checkerboard-evoked multichannel potential fields. Electroencephalogr Clin Neurophysiol 48, 609-621.

Logothetis, N.K., Pauls, J., Augath, M., Trinath, T., Oeltermann, A., 2001. Neurophysiological investigation of the basis of the fMRI signal. Nature 412, 150-157.

Luna, B., Padmanabhan, A., O'Hearn, K., 2010. What has fMRI told us about the development of cognitive control through adolescence? Brain Cogn 72, 101-113.

Mantini, D., Perrucci, M.G., Del Gratta, C., Romani, G.L., Corbetta, M., 2007. Electrophysiological signatures of resting state networks in the human brain. Proc Natl Acad Sci U S A 104, 13170-13175.

Marx, E., Deutschlander, A., Stephan, T., Dieterich, M., Wiesmann, M., Brandt, T., 2004. Eyes open and eyes closed as rest conditions: impact on brain activation patterns. Neuroimage 21, 1818-1824.

Marx, E., Stephan, T., Nolte, A., Deutschlander, A., Seelos, K.C., Dieterich, M., Brandt, T., 2003. Eye closure in darkness animates sensory systems. Neuroimage 19, 924-934.

Matousek, M., Petersen, I., 1973. Automatic evaluation of EEG background activity by means of age-dependent EEG quotients. Electroencephalogr Clin Neurophysiol 35, 603-612.

Maurer, U., Brem, S., Bucher, K., Kranz, F., Benz, R., Steinhausen, H.C., Brandeis, D., 2007. Impaired tuning of a fast occipito-temporal response for print in dyslexic children learning to read. Brain 130, 3200-3210.

Michels, L., Bucher, K., Lüchinger, R., Klaver, P., Martin, E., Jeanmonod, D., Brandeis, D., 2010. Simultaneous EEG–fMRI during a working memory task: modulations in low and high frequency bands. PLoS One 5, e10298.

Moosmann, M., Ritter, P., Krastel, I., Brink, A., Thees, S., Blankenburg, F., Taskin, B., Obrig, H., Villringer, A., 2003. Correlates of alpha rhythm in functional magnetic resonance imaging and near infrared spectroscopy. Neuroimage 20, 145-158.

Nir, Y., Fisch, L., Mukamel, R., Gelbard-Sagiv, H., Arieli, A., Fried, I., Malach, R., 2007. Coupling between neuronal firing rate, gamma LFP, and BOLD fMRI is related to interneuronal correlations. Curr Biol 17, 1275-1285.

Oldfield, R.C., 1971. The assessment and analysis of handedness: the Edinburgh inventory. Neuropsychologia 9, 97-113.

Paus, T., 2005. Mapping brain maturation and cognitive development during adolescence. Trends Cogn Sci 9, 60-68.

Paus, T., Keshavan, M., Giedd, J.N., 2008. Why do many psychiatric disorders emerge during adolescence? Nat Rev Neurosci 9, 947-957.

Pfurtscheller, G., 1981. Central beta rhythm during sensorimotor activities in man. Electroencephalogr Clin Neurophysiol 51, 253-264.

Pfurtscheller, G., 2001. Functional brain imaging based on ERD/ERS. Vision Res 41, 1257-1260.

Puligheddu, M., de Munck, J.C., Stam, C.J., Verbunt, J., de Jongh, A., van Dijk, B.W., Marrosu, F., 2005. Age distribution of MEG spontaneous theta activity in healthy subjects. Brain Topogr 17, 165-175.

Raichle, M.E., MacLeod, A.M., Snyder, A.Z., Powers, W.J., Gusnard, D.A., Shulman, G.L., 2001. A default mode of brain function. Proc Natl Acad Sci U S A 98, 676-682.

Raichle, M.E., Snyder, A.Z., 2007. A default mode of brain function: a brief history of an evolving idea. Neuroimage 37, 1083-1090; discussion 1097-1089.

Ritter, P., Moosmann, M., Villringer, A., 2009. Rolandic alpha and beta EEG rhythms' strengths are inversely related to fMRI-BOLD signal in primary somatosensory and motor cortex. Hum Brain Mapp 30, 1168-1187.

Salmelin, R., Hari, R., 1994. Characterization of spontaneous MEG rhythms in healthy adults. Electroencephalogr Clin Neurophysiol 91, 237-248.

Scheeringa, R., Bastiaansen, M.C., Petersson, K.M., Oostenveld, R., Norris, D.G., Hagoort, P., 2008. Frontal theta EEG activity correlates negatively with the default mode network in resting state. Int J Psychophysiol 67, 242-251.

Sisk, C.L., Foster, D.L., 2004. The neural basis of puberty and adolescence. Nat Neurosci 7, 1040-1047.

Slotnick, S.D., Moo, L.R., Segal, J.B., Hart, J., Jr., 2003. Distinct prefrontal cortex activity associated with item memory and source memory for visual shapes. Brain Res Cogn Brain Res 17, 75-82.

Sowell, E.R., Thompson, P.M., Tessner, K.D., Toga, A.W., 2001. Mapping continued brain growth and gray matter density reduction in dorsal frontal cortex: Inverse relationships during postadolescent brain maturation. J Neurosci 21, 8819-8829.

Stevens, M.C., 2009. The developmental cognitive neuroscience of functional connectivity. Brain Cogn 70, 1-12.

Takeshita, K., Nagamine, T., Thuy, D.H., Satow, T., Matsuhashi, M., Yamamoto, J., Takayama, M., Fujiwara, N., Shibasaki, H., 2002. Maturational change of parallel auditory processing in school-aged children revealed by simultaneous recording of magnetic and electric cortical responses. Clin Neurophysiol 113, 1470-1484.

Thatcher, R.W., 1994. Cyclic cortical reorganization: Origins of human cognitive development. In: Fischer, G.D.K.W. (Ed.), Human behavior and the developing brain. Guilford Press, New York, pp. 232-266.

Tyvaert, L., Hawco, C., Kobayashi, E., LeVan, P., Dubeau, F., Gotman, J., 2008. Different structures involved during ictal and interictal epileptic activity in malformations of cortical development: an EEG–fMRI study. Brain 131, 2042-2060.

van den Heuvel, M.P., Hulshoff Pol, H.E., 2010. Exploring the brain network: a review on resting-state fMRI functional connectivity. Eur Neuropsychopharmacol 20, 519-534.

Viswanathan, A., Freeman, R.D., 2007. Neurometabolic coupling in cerebral cortex reflects synaptic more than spiking activity. Nat Neurosci 10, 1308-1312.

Wackermann, J., Matousek, M., 1998. From the 'EEG age' to a rational scale of brain electric maturation. Electroencephalogr Clin Neurophysiol 107, 415-421.

Whitford, T.J., Rennie, C.J., Grieve, S.M., Clark, C.R., Gordon, E., Williams, L.M., 2007. Brain maturation in adolescence: concurrent changes in neuroanatomy and neurophysiology. Hum Brain Mapp 28, 228-237.

Yang, L., Liu, Z., Rios, C., Yuan, H., He, B., 2009. Electrophysiological neuroimaging: cortical correlates of alpha rhythm modulation. Conf Proc IEEE Eng Med Biol Soc 2009, 1934-1936.

3.8 Supplementary material

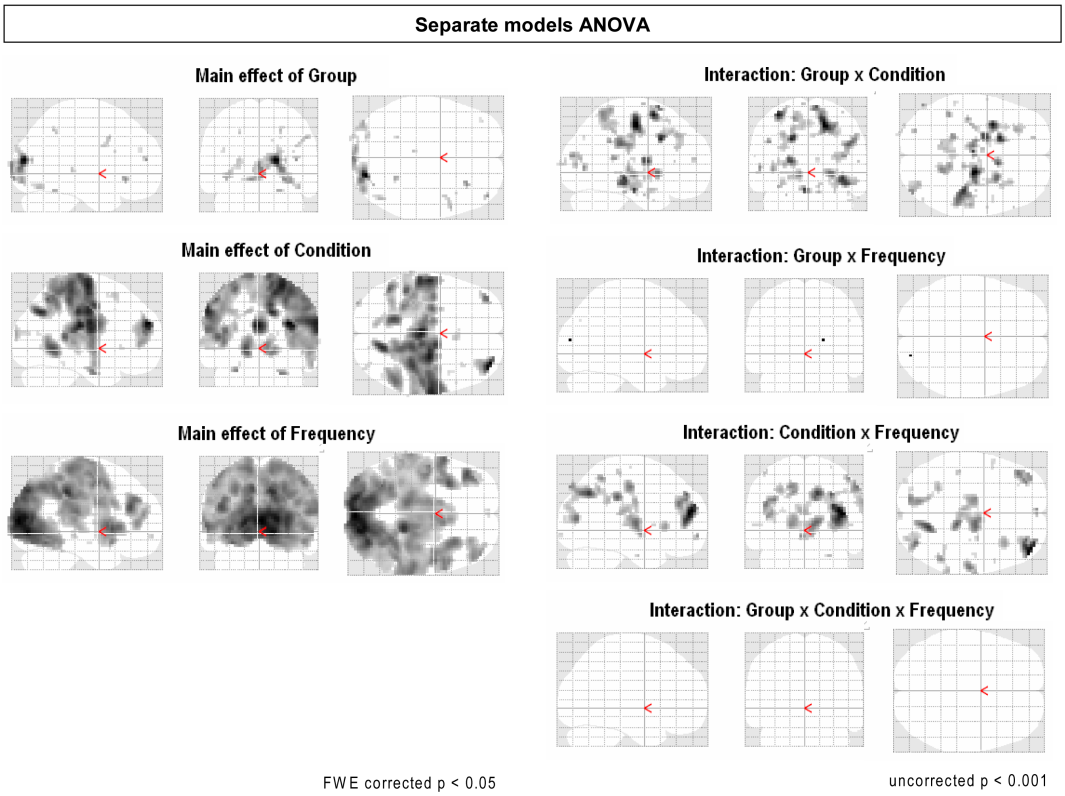

Suplementary Fig. 1.1 ANOVA results of the separate models analysis with main effects and interactions of the Group (adults, adolescents) x Condition (eyes-open, eyes-closed) x Frequency (delta, theta, alpha1, alpha2, beta1, beta2). Main effects are thresholded at $p < 0.05$, FWE corrected. Interactions did not survive FWE correction and are shown at $p < 0.001$, uncorrected ($k = 0$).

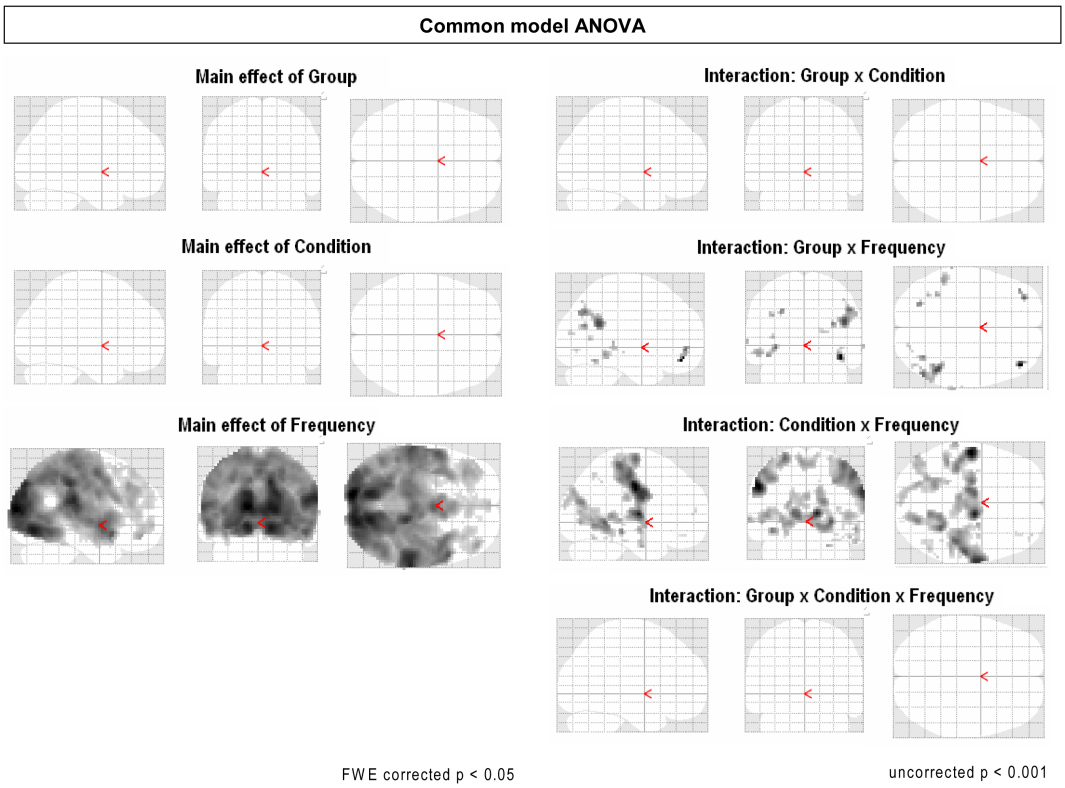

Suplementary Fig. 1.2 ANOVA results for common model analysis with main effects and interactions of the Group (adults, adolescents) x Condition (eyes-open, eyes-closed) x Frequency (delta, theta, alpha1, alpha2, beta1, beta2). Main effects are thresholded at $p < 0.05$, FWE corrected. Interactions did not survive FWE correction and are shown at $p < 0.001$, uncorrected ($k = 0$).

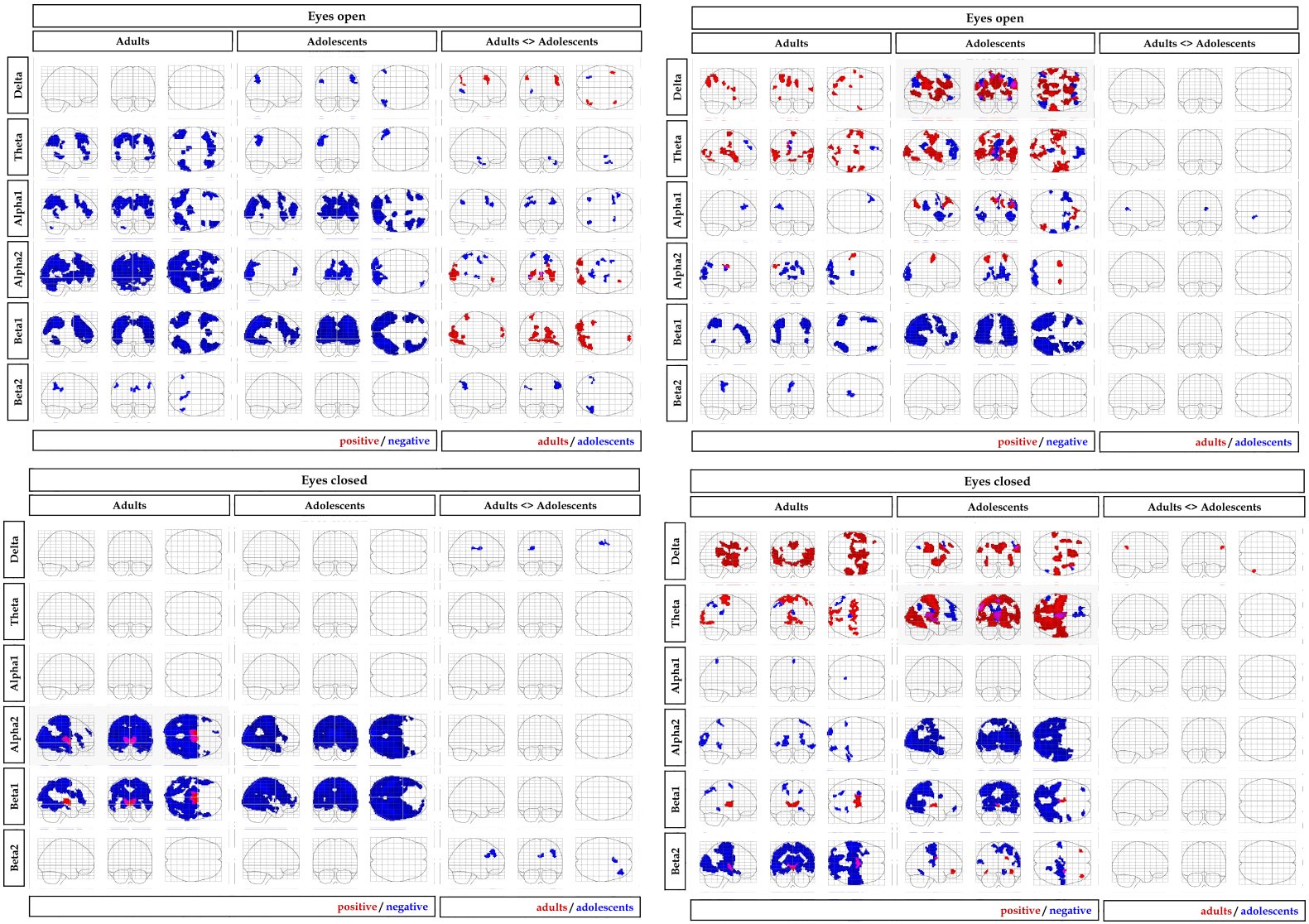

Suplementary Fig. 1.3 Common GLM results (right side). For direct comparison, separate models results identical to Fig. 1.4 and 1.5 are displayed on the left side. For the common model results, both group means and group differences are thresholded at $p < 0.001$, corrected by minimal cluster size of $k = 25$ voxels.

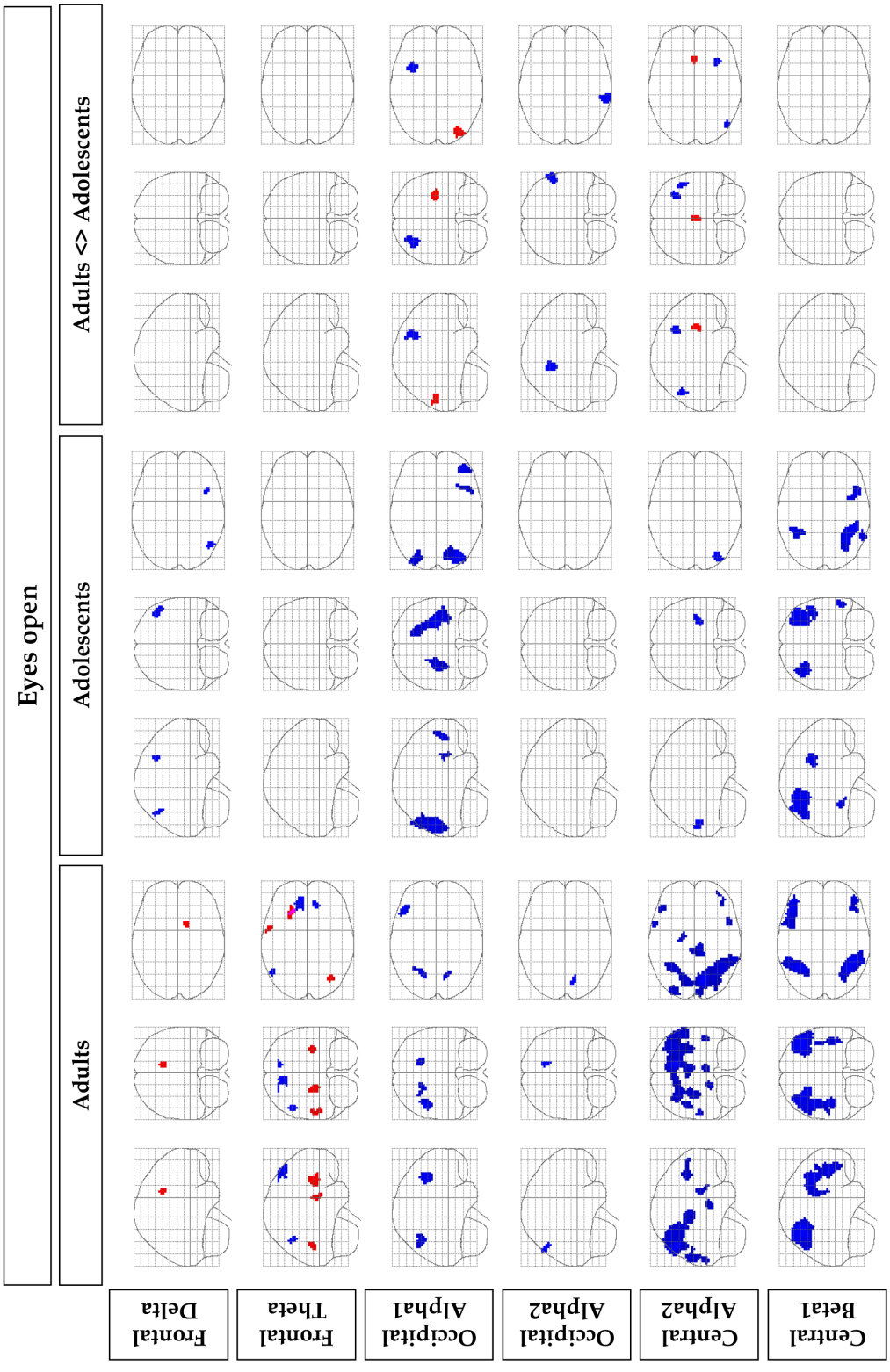

Suplementary Fig. 1.4 EEG-BOLD signal correlations during eyes-open for topographically constrained EEG signals. Frontal electrode set: AFz, Fz, F3/4, FCz. Occipital electrode set: O1/2. Central electrode set: C3/4. Group means are displayed at $p < 0.05$, FWE corrected, $k = 20$. Group differences did not reach significance and are shown at $p < 0.001$, uncorrected, $k = 25$.

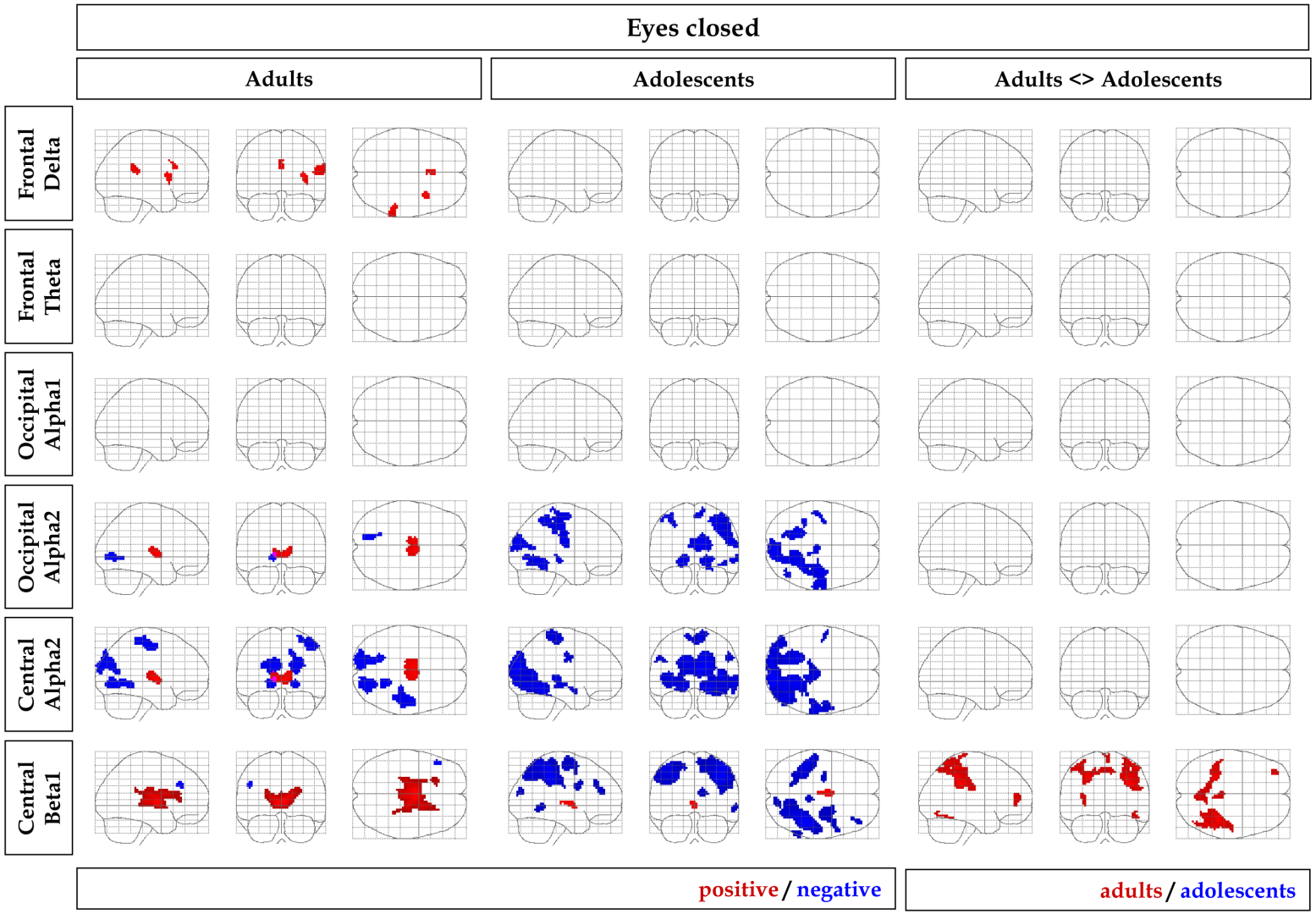

Suplementary Fig. 1.5 EEG-BOLD signal correlations during eyes-closed for topographically constrained EEG signals. Figure annotation as in Supplementary Fig. 1.4.

4 Brain State Regulation During Normal Development: Intrinsic Activity Fluctuations In Simultaneous EEG–FMRI

Published as: *Lüchinger R, Michels L, Martin E, Brandeis D, (2012). Brain state regulation during normal development: Intrinsic activity fluctuations in simultaneous EEG-fMRI. Neuroimage, 60, 1426-1439.*

Abstract **- Brain maturation in adolescence is mirrored by the EEG as a pronounced decrease in low frequency activity. This EEG power attenuation parallels reductions of structural and metabolic markers of neuronal maturation (i.e., gray matter loss and decrease of absolute cerebral glucose utilization). However, it is largely unknown what causes these electrophysiological changes, and how this functional reorganization relates to other functional measures such as the fMRI BOLD signal. In this study, we used simultaneously recorded EEG and fMRI to localize hemodynamic correlates of fluctuating EEG oscillations and to study the development of this EEG–BOLD coupling. Furthermore, the maturational EEG power attenuation was directly compared to BOLD signal power maturation. Both analyses were novel in their developmental perspective and aimed at providing a functional lead to EEG maturation. Data from 19 children, 18 adolescents and 18 young adults were acquired in 10 min eyes-open/eyes-closed resting states. Our results revealed that both EEG and BOLD amplitudes strongly decrease between childhood and adulthood, but their functional coupling remains largely unchanged. The global reduction of absolute amplitude of spontaneous slow BOLD signal fluctuation is a novel marker for brain maturation, and parallels the globally decreasing trajectories of EEG amplitudes, gray matter and glucose metabolism during adolescence. Further, the absence of thalamocortical EEG–BOLD coupling in children together with age-related normalized thalamic BOLD power increase indicated maturational changes in brain state regulation.**

4.1 Introduction

Human brain maturation is mirrored by changes in the resting electroencephalogram (EEG). The EEG power decreases between late childhood and early adulthood as a curvilinear function of age, most prominently in low frequencies which have been documented

extensively for over 60 years (Boord et al., 2007; Dustman et al., 1999; Eeg-Olofsson, 1970; Gasser et al., 1988; Gibbs and Knott, 1949; Matousek and Petersen, 1973; Matsuura et al., 1985; Somsen et al., 1997) and have been related to cognitive maturation (Case, 1992; John et al., 1980; Thatcher, 1994; Wackermann and Matousek, 1998). The maturational power decrease is a global phenomenon (Whitford et al., 2007); typically affecting all scalp sites, although its effect in additional topographical features has been noted (Gasser et al., 1988).

Oscillatory activity in the EEG at rest (i.e. in the absence of task or stimulation) demonstrates that the brain is far from resting. The enormous intrinsic energy consumption exceeds by far the additional costs associated with momentary demands of the environment (which may be as little as 0.5 to 1.0 % of the total energy budget) (Raichle, 2006). EEG oscillations arise from synchronized mass activity of mainly cortical neuron populations. Resting state EEG oscillations are typically subdivided into different bands such as low frequencies delta (1 - 4 Hz) and theta (4 - 8 Hz) and higher frequencies alpha (8 - 12 Hz) and beta (13 - 30 Hz). In general, increased low frequency power is a typical phenomenon in lower arousal functional states such as sleep (Cajochen et al., 2002; Campbell and Feinberg, 2009), neuropathology (Llinas et al., 2005; Llinas et al., 1999) or sedation (John et al., 2001). During resting states, the oscillatory compound reflects changes in brain states as indicated by shifts in arousal and alertness (Klimesch, 1999).

It is largely unknown which neuronal process guides the partly low-frequency-specific decrease in the EEG. Despite evidence that synchronized postsynaptic mass activity of aligned cortical neurons is the main source of the EEG, and that inhibitory activity and different cell types may contribute to higher frequencies, the exact generation and functional mechanisms of EEG oscillations are not fully understood (Brandeis et al., 2009). EEG changes, therefore, have been related to other neuronal measures. Brain development roughly shows a linear increase in global white matter volumes and an inverted U-shaped developmental trajectory for global gray matter structures, with peak volumes occurring in late childhood or early adolescence (Giedd et al., 1999; Gogtay and Thompson, 2010). Gray matter loss is a global phenomenon with lower order cortices maturing prior to higher order cortices (Gogtay et al., 2004). State independent, general mechanisms are also implicated by the fact that global EEG power decrease parallels maturational trajectories in sleep (Buchmann et al., 2011) and awake resting state (Whitford et al., 2007). Gray matter decrease reflects synaptic pruning (Bourgeois and Rakic, 1993; Huttenlocher, 1979), which presumably eliminates redundant connections and may be disrupted in adolescent psychiatric diseases (Paus et al., 2008). Physiologically, synaptic density may affect EEG power, as synaptic density reflects the connectivity and size of neuron populations from which EEG power partly derives (Boord et al., 2007; Feinberg and Campbell, 2010). Synaptic density also affects glucose metabolism, as the major portion of glucose maintains resting potentials (Chugani, 1998). Hence, absolute metabolic rates were found to parallel gray matter maturation in terms of cortical glucose uptake (Chugani, 1998; Chugani et al., 1987) and cerebral hemodynamic perfusion (Biagi et al., 2007), even though some maturational changes remain evident

after controlling statistically for gray matter density (Taki et al., 2011). The common global maturational decrease in electrical activity, neuronal density and metabolic energy budget has been highlighted (Boord et al., 2007; Feinberg and Campbell, 2010; Feinberg et al., 1990) referring to a general neuroregressive phenomenon (Chugani, 1998; Cowan et al., 1984). Metabolism is more closely related to the EEG in that it reflects brain function rather than structure. A close functional relation has also been demonstrated between electrophysiology and fMRI (Logothetis et al., 2001). Although BOLD-fMRI (blood-oxygen-level-dependency functional magnetic resonance imaging) has come to dominate human functional neuroscience, there is no study assessing the maturation of the relationship between EEG amplitudes and BOLD signals (neither in terms of the covariation of the fluctuating signals nor in quantitative terms of absolute signal amplitudes).

The fMRI BOLD signal is a slow hemodynamic correlate of activation that increases where neuronal activity increases (Logothetis et al., 2001; Niessing et al., 2005; Nir et al., 2007). Conventional fMRI studies report both increases as well as decreases in local BOLD activity as maturational correlate of cognitive functions (Blakemore and Choudhury, 2006), depending on the specific task, brain region and developmental phase. A general developmental trend "from diffuse to focal" may better account for the findings (Blakemore and Choudhury, 2006; Brown et al., 2006; Dick et al., 2006; Durston et al., 2006). Still, the maturational interpretation of increasing or decreasing activity or spatially diverse activity patterns is limited by confounding factors such as cognitive effort, experience or strategy (Casey et al., 2005). More recent fMRI research has focused on resting state brain activity in terms of functional connectivity (Biswal et al., 1995; Friston, 2002) between brain regions. This research approach has revealed resting state networks (RSNs) which are based on the spontaneously yet coherently fluctuating BOLD signal, and which are interpreted on the functional connotation of the anatomical structures that constitute the RSNs (Damoiseaux et al., 2006). In terms of development, the RSNs in awake children were found to be established as early as the age of 7 - 9 years (Fair et al., 2009; Supekar et al., 2009). After this age, maturational changes were described as more subtle fine tuning of within- and between-network connectivity (Dosenbach et al., 2010; Fair et al., 2009; Fair et al., 2007; Jolles et al., 2011; Supekar et al., 2009).

Large-scale networks of coherently fluctuating BOLD signals, of which now up to ten have been consistently identified (Damoiseaux et al., 2006; Deco et al., 2011), were first observed during passive rest but their activity continues during cognitive engagement (e.g. task or stimulation) with a high topographical correspondence (Calhoun et al., 2008; Mennes et al., 2010; Smith et al., 2009; Thomason et al., 2008). On an arousal continuum, rest can be seen as an intermittent state between sleep and attention, which itself transiently fluctuates subtly along the arousal scale. Both EEG and fMRI reflect arousal-related features of resting brain state regulation. In the EEG, the sensitivity is reflected by the oscillatory composition (Olbrich et al., 2009; Sadaghiani et al., 2010). Resting state fMRI features two major (and antagonistic) RSNs, the default mode network (DMN) (Raichle et al., 2001; Raichle and Snyder, 2007) and the attention

network (ATN) (Fox et al., 2005) the activity of which reflects shifts along the arousal scale as their engagement relates to rest or attentional task activity. The physiological mechanism that regulates vigilance/arousal/alertness states is associated with thalamic activity and thalamocortical circuitry (Llinas et al., 1998; McCormick and Bal, 1997; Steriade et al., 1993). Evidence for human thalamocortical activity during rest has been obtained noninvasively by simultaneous recording of EEG and fMRI. These studies revealed that activity in the alpha range (10 Hz) is accompanied by BOLD activity in a thalamocortical network (TCN) with thalamus positively correlated and sensory areas negatively correlated (de Munck et al., 2007; Difrancesco et al., 2008; Feige et al., 2005; Goldman et al., 2002; Lüchinger et al., 2011; Moosmann et al., 2003; Tyvaert et al., 2008). Such functional coupling is typically based on temporal correlation of frequency-specific EEG power fluctuations (convolved with the slow hemodynamic response function) with the co-registered regional BOLD signal in eyes-closed resting state. Functional coupling of EEG oscillations in different frequencies was also found in regions comprising the DMN (Lüchinger et al., 2011; Scheeringa et al., 2008) and the ATN (Laufs et al., 2006; Laufs et al., 2003; Lüchinger et al., 2011). Both resting with eyes-open (EO) or eyes-closed (EC) refer to passive baseline activity (Gusnard and Raichle, 2001). EO condition increases arousal more than EC condition (Barry et al., 2009; Barry et al., 2007) inducing an arousal gradient that allows for differentiation between state-dependent and state-independent effects. As simultaneous recording of EEG and fMRI allows for localizing functional correlates of EEG oscillations, it adds to the understanding of resting state brain function and may even reveal a functional correlate of EEG maturation. Apart from our own recent study on late maturation, EEG–fMRI correlates have not been studied from a developmental perspective. We hypothesize that the EEG–BOLD signal couplings differ between children and adults as a result of the drastic power decrease in the EEG.

We further compare for the first time EEG maturation to BOLD signal maturation in terms of absolute amplitudes. This appears to be the most logical and direct approach in terms of equivalent measures. In contrast to EEG–BOLD signal correlations, which only consider normalized fluctuations of activity, spectral power provides an absolute measure of activity. The spectral range of the spontaneously fluctuating BOLD signal that is associated with neuronal activity is about 0.01 to 0.1 Hz (Biswal et al., 1995; Cordes et al., 2001), corresponding to the activity range of RSNs (Fox and Raichle, 2007). In resting state fMRI, the spectral power has recently attracted a great deal of interest (e.g. Baria et al., 2011; Biswal et al., 2010; Duff et al., 2008; Horovitz et al., 2008; Yang et al., 2007; Zuo et al., 2010). While the BOLD signal power is usually normalized to reduce inter-subject variability, here we used absolute power to detect possible decreases in activity relating to development. We also used absolute power for an equivalent contrast to EEG power (relative power was examined in a subsidiary analysis). To our knowledge, maturation of BOLD amplitude has not been investigated yet. Despite the lack of literature, we anticipate a power decrease from childhood to adulthood. We base this expectation on the aforementioned decreasing neurodevelopmental trend that is common to structural and functional measures which likely relate to the BOLD signal.

In this study we thus examined EEG power and fMRI BOLD signal fluctuations for their functional coupling (i.e., temporal correlation), and compared their absolute signal amplitudes (i.e., spectral power). Both approaches are novel in the developmental context and aimed to capture markers of normal healthy brain development. We investigated the major EEG frequency bands and both resting states (EO/EC), as they proved to be important factors in EEG–BOLD signal correlations (Lüchinger et al., 2011), and allows to distinguish between state-dependent and state-independent developmental mechanisms.

4.2 Methods

4.2.1 Patricipants

We used the same groups of adults and adolescents as described in our previous report (Lüchinger et al., 2011) and additionally recruited a group of children. The original sample sizes used for analysis were reduced due to technical issues during scanning (3 adults, 2 adolescents), excessive head motion ($>$ 3 mm, 1 adolescent) and unsuccessful artifact rejection (1 child), resulting in 18 adults (mean age 25.3 $\pm$ 3.8 years, 8 males), 18 adolescents (mean age 15.9 $\pm$ 1.1 years, 8 males) and 19 children (mean age 10.6 $\pm$ 1.3 years, 8 males). The age statistics deviate slightly from the earlier publication due to more precise age calculation (monthly vs. years). All participants were right-hand dominant (Oldfield, 1971), had normal or corrected-to-normal vision, met the MRI safety standards and were healthy with no history of neurological or psychiatric disease. They were not taking drugs or medication currently, and they were asked to refrain from caffeine and nicotine consumption during the day of scanning. All participants, as well as the children's parents, gave written, informed consent prior to the investigation. The study was approved by the local ethics committee and was conducted in accordance with the guidelines determined in the Helsinki Declaration.

4.2.2 Procedure and recordings

The procedure, devices and data recording followed our published protocol (Lüchinger, Michels et al. 2011), and consisted of 10 min resting state simultaneous EEG–fMRI recording with alternating EO/EC blocks of 2.5 min. In contrast to the previous report, only the 10 min first session was analyzed in this study because not all children completed the 2nd session following our extended measurement protocol (up to this session, protocols were identical among the groups).

4.2.3 EEG analysis

EEG preprocessing and analysis were done using BrainVision Analyzer 1.05 (BrainProducts, Gilching, Germany). Gradient artifacts were removed by average artifact subtraction (Allen et al., 2000; Allen et al., 1998), lowpass-filtered at 70 Hz cutoff and downsampled from 5 kHz to 500 Hz. The ballistocardiogram artifact was attenuated using a very

similar subtraction method with artifact windows aligned on QRS complexes detected in ECG traces (Allen et al., 2000; Allen et al., 1998), using maximal covariance method, templates based on 10 consecutive pulse intervals, and individually estimated time delay for subtraction based on global field power (GFP) distribution (CBC Parameters, Version 1.1).

EEG was digitally bandpass-filtered (0.5 - 70 Hz, 24 dB/oct and 50 Hz Notch) and further downsampled to 256 Hz. Using ICA decomposition (Delorme and Makeig, 2004) with selective back projection, eye blinks (Jung et al., 2000) and residual gradient and ballistocardiogram artefacts were eliminated. The residual MR-gradient artefacts components were identified by their spectral peaks and their non-physiological topography (sharp asymmetry along the sagittal midline; scanner and cabling dependent). Residual ballistocardiac artefacts components were also identified by their characteristic topography (Debener et al., 2008). The same criteria were used for all age groups. Children and adolescents did not differ regarding residual EEG artefacts as judged by the total number of ICA components rejected (25.6 $\pm$ 6.45 versus 27.7 $\pm$ 8.1 out of 62), but fewer ICA components were rejected in adults (17.9 $\pm$ 3.0, $p < 0.01$ for both comparisons). The residual slice artefact at 18 Hz was suppressed by a narrow band rejection filter $\pm$ 0.5 Hz (Sadaghiani et al., 2010). All channels were then transformed to the average reference (Lehmann and Skrandies, 1980) and segments with remaining artefacts were marked for later rejection.

EEG power fluctuation. First, the EEG data set of each participant was parsed into EO and EC conditions. The conditions' onsets were defined individually by the exact time of opening and closing the eyes, as indicated by ICA component activation trace. For each volume acquisition (duration of 1.815 s), the absolute spectral power was calculated on each channel by a Fast Fourier Transformation (FFT) (Hanning window: 10 %, zero padded, 0.5 Hz resolution). Global spectral power (GSP) (Jann et al., 2009; Michels et al., 2010) was calculated for each FFT-transformed epoch as the root mean square across all channels. Hence, GSP is a measure of the total oscillatory activity over the scalp. The mean spectral band value was calculated for six common frequency bands comprising of delta (1 - 3 Hz), theta (4 - 7.5 Hz), alpha1 (8 - 9.5 Hz), alpha2 (10 - 13 Hz), beta1 (14 - 19 Hz) and beta2 (20 - 30 Hz) and the scan-to-scan fluctuation was used for correlation analysis with fMRI data after linear interpolation of epochs priorly marked as artifacts.

EEG mean power. Based on these steps, EEG amplitude was calculated as the mean of each FFT transformed epoch while epochs beforehand marked as artifacts were omitted. Group mean GSP was calculated for each condition and frequency band separately. Two-sample t-tests were used to calculate group differences (considered significant at $p < 0.05$, one-tailed, uncorrected for multiple comparisons). In addition, electrode-wise calculations allowed mapping power to illustrate its scalp topography. Group mean power maps as well as t-maps for group differences were calculated. A t-value of > 3.144 corresponds to $p < 0.05$ for one-sided group differences (Bonferroni corrected for 60 multiple tests within a map).

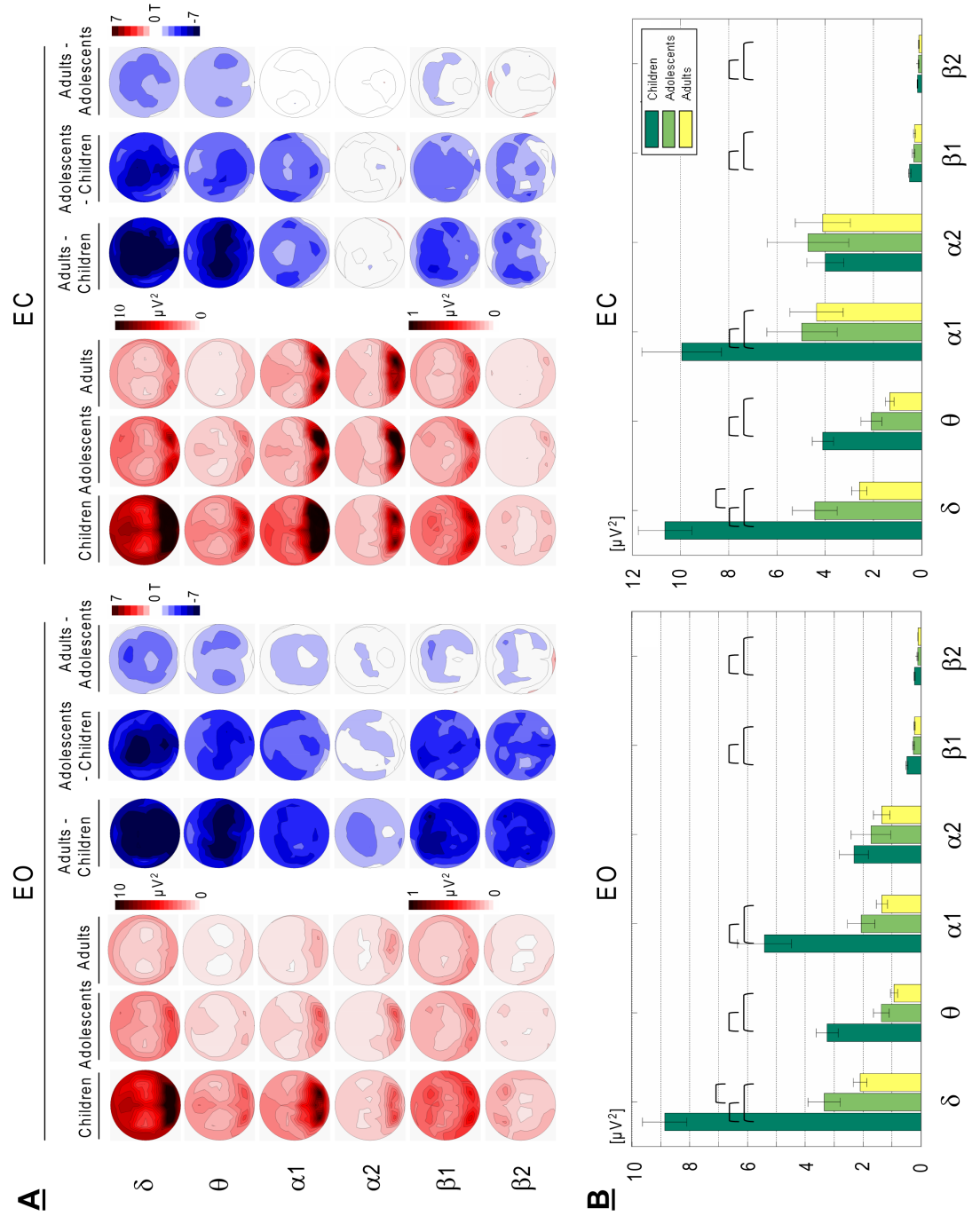

Fig. 2.1 EEG band power results. A: EEG topography and topographical group differences of EO and EC resting states. Group means are shown with color scaling. The spectrum follows a power law (compare B) necessitating a different scaling for beta1 and beta2. Contour lines indicate a step of 0.5 μV^2 and are based on triangulation and linear interpolations of the sixty scalp electrodes. Group differences are shown as t-maps with red (positive) to blue (negative) scaling. All t-maps range from 7 to -7 whereas all differences are calculated as 'younger group - older group'. Contour lines represent a step of ±1 t-value. A t-value of >= 3.144 corresponds to $p < 0.05$ for one-sided group difference, Bonferroni corrected for 60 multiple tests within a map. The top of the maps is anterior. B: The global spectral power (GSP) separated by group, condition and frequency. The bars represent mean power values in μV^2 and error bars reflect the standard error mean. The brackets indicate significant group differences (two-sample t-test, $p < 0.05$, one-tailed, uncorrected for multiple comparisons).

4.2.4 EEG–BOLD signal correlation

FMRI data preprocessing and analysis were done using SPM8 (Wellcome Department of Cognitive Neurology, London, UK). The images were realigned to the first scan by affine transformation and normalized into MNI standard space. They were resampled to 3 mm cubic voxels and spatially smoothed with 8 mm FWHM Gaussian kernel. The six head motion parameters together with mean white matter and cerebrospinal fluid signals were later used as nuisance covariates. Located by thresholded SPM8 template (> 70 %), cerebrospinal fluid was extracted from 5 mm spheres within ventricles [0, 11, 9; 0, -40, -2] (xyz MNI-coordinates) and white matter from anterior and posterior corpus callosum [0, -38, 13; 0, 26, 2].

EEG–BOLD signal correlations were calculated voxel-wise, using the SPM8 general linear model (GLM) approach. Each of the depicted frequency bands was analyzed in a separate model. The model consisted of two boxcar functions modeling EO and EC conditions which were parametrically modulated by the aforementioned GSP fluctuations. The opening and closing of the eyes introduce transition-specific motor and visual activity. This was seen here as confounding both EEG and fMRI resting-state signals, and was modeled in two additional regressors in an event-related manner. The standard hemodynamic response function was used to convolve the model regressors. A first-order autoregressive model accounted for serial correlations and a 128 s highpass filter eliminated very slow drifts. The model always contained the nuisance variables. The model was run for each participant, and the contrast image of the GSP regressor was written for subsequent group statistics.

A 3 x 2 x 6 full factorial design (Analysis of Variance, ANOVA) was used for random effects analysis, with factor group (adults, adolescents, and children), factor condition (EO, EC) and factor frequency (delta, theta, alpha1, alpha2, beta1, beta2). Post-hoc t-tests were calculated separately for groups, conditions and frequencies in both positive and negative directions. Group differences were calculated as simple contrasts between all three groups in both directions (younger $>$ $<$ older). All group differences were inclusively masked by the corresponding group mean correlation patterns of the groups involved in the contrast. This allowed constraining group differences only in regions with significant correlations in any of the two group means involved in a group contrast. However, all group differences were also calculated without masking. The group differences are sensitive to different kinds of maturation effects such as linear or non-linear trajectories (including (inverted) U-shaped trajectories peaking in adolescence). A 2 x 6 full factorial design with factor condition and frequency and the participant's age (monthly) as covariate was calculated to estimate more general, maturation independent EEG–BOLD signal correlation patterns.

In a second analysis (Lüchinger et al., 2011), all six GSP frequency bands were included simultaneously in one common GLM at the subject level. Such a model provides partial correlations and was also used to alternatively test the frequency specificity in the EEG–BOLD signal correlations. The partial correlation patterns resulting from the common GLM were analyzed identically to the main analysis on the group level with a group x condition x frequency ANOVA as well as a condition x frequency ANCOVA with age as

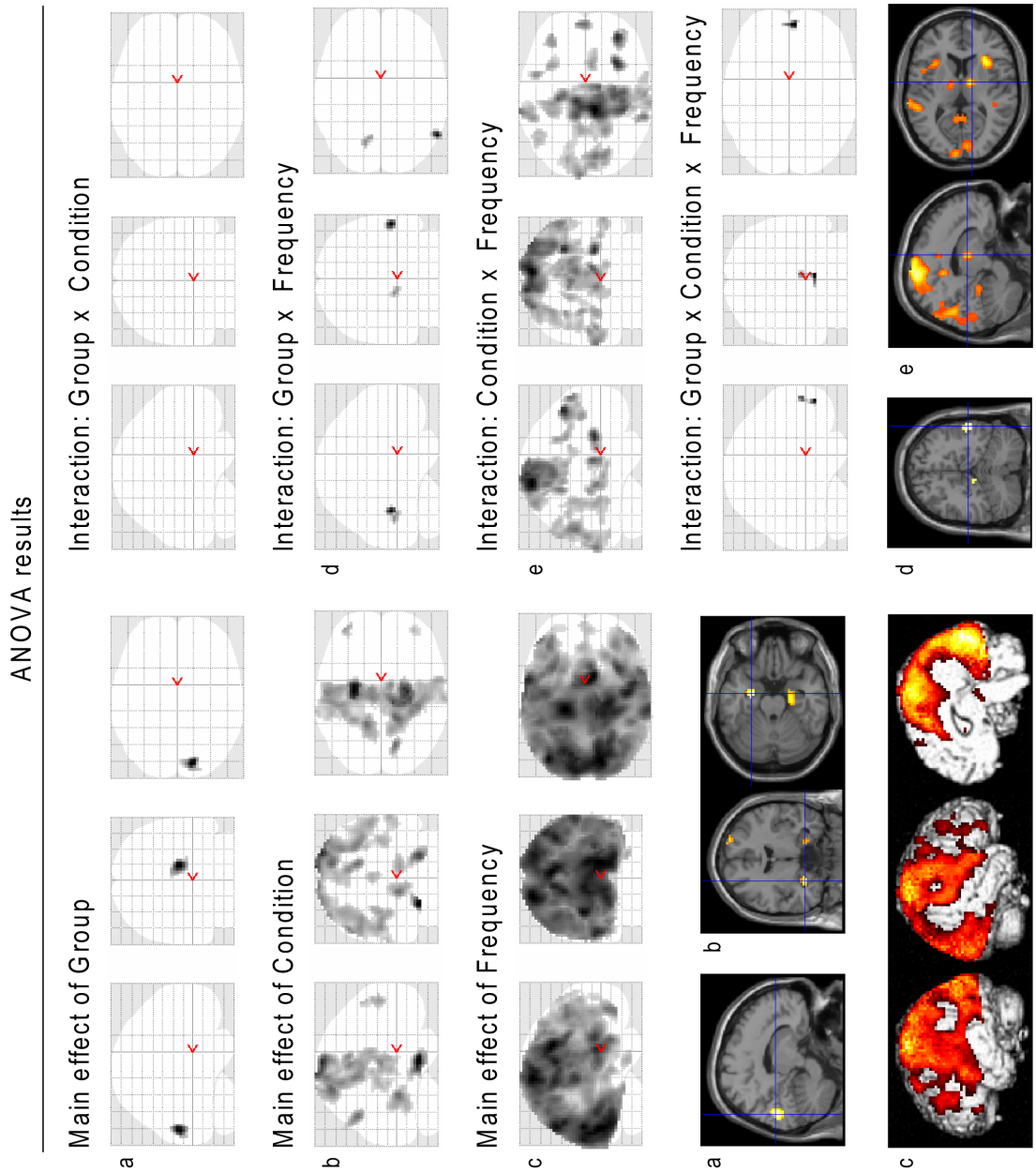

Fig. 2.2 ANOVA main effects and interactions of the EEG-BOLD correlation images resulting from the 3 groups by 2 conditions by 6 frequencies full factorial model. F-values are shown as maximum intensity projection in 'glassbrains' (saggital, coronal and axial views). Statistical height threshold was set to $p < 0.001$, corrected by extent threshold $k = 25$ voxels. To highlight topographical specificity, selected results were overplayed on SPM anatomical templates and labeled accordingly (a - e). Main effects of condition (b) and frequency (c) were thresholded at $p < 0.05$, FWE corrected, $k = 25$.

covariate. Results were considered significant at height threshold $p < 0.001$, corrected for multiple comparison by extent threshold of minimal cluster size of $k = 25$ voxels (Forman et al., 1995). The voxel extent threshold was calculated with Monte Carlo simulation (Slotnick et al., 2003).

4.2.5 BOLD signal spectral power analysis

BOLD signal spectral power was calculated on the same preprocessed images as used for EEG–BOLD signal correlation using REST toolbox V1.3 (http://restfmri.net). Prior to analysis, the six motion parameters were residualized from the images. REST calculates spectral power as ALFF (amplitude of low frequency fluctuation) (Yang et al., 2007; Zang et al., 2007). ALFF is the band average of the square-rooted FFT (taper percent = 0, FFT length = shortest). After removal of the linear trend, ALFF was calculated for the frequency range of 0.01 - 0.08 Hz for each participant separately for each condition. The BOLD spectral power is usually normalized spatially or even spectrally to reduce inter-subject variance. In order to coherently compare the maturing (absolute) EEG amplitudes to absolute amplitudes in the BOLD signal, the raw, non-normalized ALFF was used. However, the spatially normalized ALFF (mALFF = ALFF – mean(ALFF)) is more sensitive to regional differences, and was therefore calculated as well.

Group mean BOLD signal power was calculated for EO and EC conditions separately. Group differences were calculated condition-wise as two sample t-tests in both directions (younger <> older). The statistical threshold was set identically to the EEG–BOLD signal correlation analysis.

4.3 Results

4.3.1 EEG results

All groups' mean power maps revealed the typical resting state feature of pronounced posterior alpha power during EC (Fig. 2.1A) peaking around 10 Hz (Fig. 2.1B). Delta, theta and alpha1 showed a local power increase over middle frontal regions. The band-specific EEG topography appeared similar across groups. The t-maps confirmed the extensive, rather global topography of the power reduction with age, but also indicated a centrally maximal reduction for theta- and a fronto-centrally maximal reduction for delta and beta. This power reduction was most apparent in low frequencies and between children and adults, but extended to higher (beta) bands and was evident among adolescents and adults as well. GSP is a single global measure of frequency-specific EEG activity and was calculated to measure EEG–BOLD signal correlation. GSP profiles yielded the typical resting state's spectral profile (Fig. 2.1B). The t-tests confirmed significant GSP reduction between children and the two older groups for all frequency bands except for alpha2. The GSP reduction was significant between adolescents and adults in the delta band and approached significance in the theta band. Hence, GSP closely mirrored the maturational power decrease and together with the rather global topography of the EEG power decrease, GSP is an appropriate measure of EEG brain

maturation.

4.3.2 EEG–BOLD signal correlation results

The ANOVA main effects revealed that the EEG–BOLD signal correlations differed significantly among groups, conditions and frequencies (Fig. 2.2). Groups differed in one cluster in the occipital cortex. Conditions mainly differed along pre- and postcentral gyri and bilaterally in the hippocampus. Frequency effects were strongest in the occipital cortex, extending along dorsal and ventral streams, in pre- and postcentral gyri and in the lateral frontal cortex. Interactions were most apparent between condition and frequency. These results, which were also marked by distinct hemisphere symmetry, are listed in Supplementary Table S1.

EEG–BOLD signal correlations were subsequently calculated for each factor level separately (Fig. 2.3A). Overall, negative correlations dominated over positive correlations. Between groups, the correlations were robust as they reached significance in similar regions and in the same direction (correlation sign). Despite the weak ANOVA main effect on the groups, some critical patterns differed particularly between children and the older groups (adolescents and adults). In particular, children did not show a positive thalamic correlation in EC higher frequencies (alpha2, beta1, and beta2), not even at a very low statistical threshold. Across frequencies, differing correlation patterns appeared, consistent with the prominent frequency's main effect. Nevertheless, pattern redundancies between neighboring frequency bands emerged in some cases. The common model analysis clarified these redundancies (see below). Distinct differences appeared among lower and higher frequencies. In contrast to higher frequencies, the lower bands contained many more positive correlations. EO and EC conditions yielded different correlation patterns. Some portions appeared complementary between the conditions, such as the pre- and postcentral gyri. This is consistent with the ANOVA main effect of condition yielding the same structures.

Maturation-independent EEG–BOLD signal correlations were obtained by omitting the factor group and instead using age as covariate (Fig. 2.4 and Supplementary Table S3). EO delta power was positively correlated in the anterior cingulate cortex (ACC) and the anterior insula. Very similar correlations were found for EC delta but also for EO and EC theta. The theta band additionally showed widespread positive correlations along pre- and postcentral gyri and the adjacent superior frontal and superior temporal cortices. Visual inspection at lower statistical thresholds suggested that both low frequencies in both conditions share positive correlation to the cinguloopercular network (Dosenbach et al., 2007; Dosenbach et al., 2006). Negative correlations appeared for EO theta in the medial prefrontal cortex (MPFC), posterior cingulate cortex (PCC)/precuneus and bilaterally in inferior/superior lateral parietal cortex, together constituting the DMN, among other regions. Fractions of the DMN also exhibited negative correlations with EC theta and EO/EC delta, but these correlations were much less distinct and also involved other regions such as the middle/superior/inferior frontal gyrus. During EO, all higher frequencies from alpha1 to beta2 were negatively correlated in similar regions comprising portions of the occipital, parietal and frontal cortex and the posterior cingulate. This

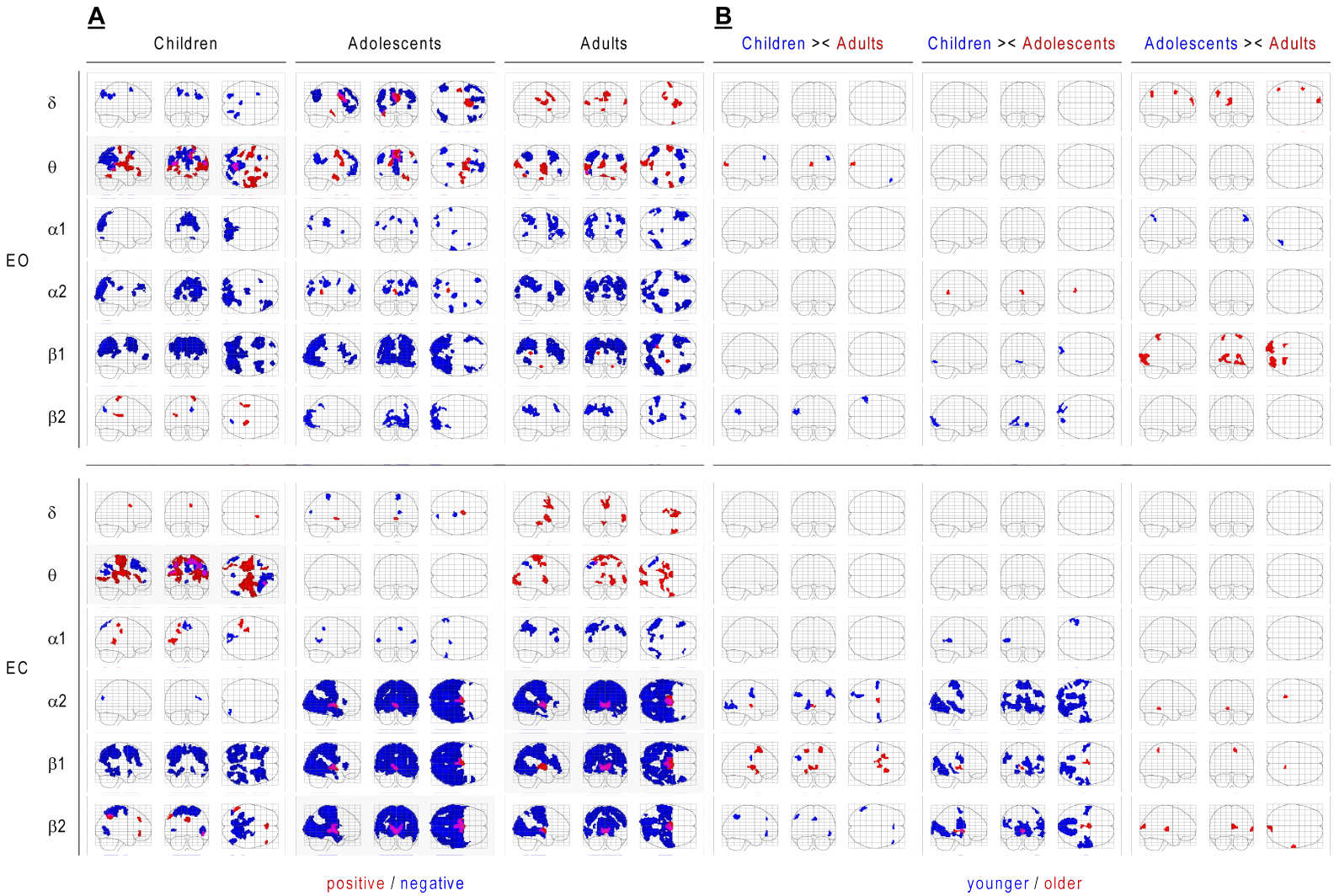

Fig. 2.3 Maturation of EEG-BOLD signal correlations. A: Group means by condition and frequency. T-values are shown as maximum intensity projection in 'glassbrains'. Positive correlations are scaled in red and negative correlations are scaled in blue. An overlay of red and blue colored voxels results in pink in the respective angle. B: Group differences of EEG-BOLD signal correlations separated by condition and frequency. Group differences are shown in both directions 'younger <> older' and color-coded as indicated by the column titles. All group differences were inclusively masked by the corresponding group mean correlation patterns of the groups involved in the contrast. A and B: Statistical height threshold was set to $p < 0.001$, corrected by extent threshold $k = 25$ voxels.

pattern was strongest for EO beta1 and overlaps with the ATN, especially in parietal and frontal areas. The only positive correlations appeared in the hippocampus with alpha1. During EC, the most salient correlation pattern appeared in the higher frequencies alpha2, beta1 and beta2. The pattern involved the positively correlated thalamus together with strong, widespread negative correlations in occipital, temporal, parietal, and frontal lobes. Although widespread, these negative correlations were limited to cortical regions, and excluded, for instance, the cingulate cortex, partly inferior parietal cortex, much of the frontal lobe and most of the sub-lobar regions.

The group differences of the correlation patterns are shown in Fig. 2.3B and listed in Supplementary Table S2. The most salient group difference was found in EC higher frequency bands alpha2, beta1 and beta2. Children had less negative correlations in cortical regions and less positive correlations in the thalamus (compared to adults in alpha2 and beta1, compared to adolescents in beta1 and beta2). Adolescents apparently had the strongest negative correlations. Despite this finding, only a few small, isolated or discontinuous group differences appeared. In order not to miss eventual weak yet more consistent maturation effects, the results were also inspected at a low statistical threshold ($p < 0.01$, $k = 0$, not shown).

The partial correlation patterns yielded similar overall results. The ANOVA (not shown) yielded a few more clusters for the main effect of group than the main analysis. The main effects of condition and frequency, and the condition x frequency interaction were similar in topography to those observed in the main analysis. Age-independent partial correlations are displayed in Fig. 2.4C. The negative DMN correlation appeared to be more specific for theta than for delta. The negative ATN correlation proved more specific for EO beta1 than for the neighboring bands. The low frequencies remained similar among conditions. The EC thalamocortical pattern was confirmed to be specific to all three higher frequency bands. The common model analysis produced more positive correlations across the group's mean patterns than the main analysis and overall reached slightly less statistical power. The group differences (not shown) were even fewer and the thalamocortical pattern no longer differed significantly. The children's negative EC theta-DMN correlation was stronger than in adolescents, but did not differ when compared to adults. Similar to the main analysis, the sparse group differences thus appeared isolated and did not reveal a continuous maturational trend for the correlations that would parallel power decrease in maturational low frequency EEG.

4.3.3 BOLD power results

Absolute BOLD signal power was much higher in gray matter than in white matter or cerebrospinal fluid. The power intensity projection mirrored the brain's gray matter structure (Fig. 2.5A). Topographically, the power distributions were similar across groups and conditions, but children showed higher power values. This group difference was highly significant in the direct group contrasts (Fig. 2.5B). In all comparisons, the younger group always exhibited more BOLD signal power than the older group. The other direction (older > younger) yielded no significant differences. Between children and the older groups, the power differences affected almost all brain regions. Between adolescents

and adults, the more subtle differences yielded a distinct topography with regions in the medial prefrontal cortex, posterior cingulate/precuneus and inferior parietal cortex. Compared to EO, these differences were slightly less pronounced.

The normalized power values revealed a very similar topography corresponding to gray matter anatomy. The group differences were much subtler and demonstrated high spatial specificity (Fig. 2.5C). Children were characterized consistently by significantly lower normalized BOLD power in the thalamus compared to both older groups in both conditions. Similarly, children showed significantly lower normalized power in the medial prefrontal cortex, posterior cingulate and left inferior parietal cortex compared to both older groups, especially during EO.

4.4 Discussion

4.4.1 General findings

The current study extends our earlier findings on late maturation to a younger age range including childhood (Lüchinger et al., 2011), and introduces a more comprehensive methodology including BOLD power analysis (matching the EEG analyses) to developmental fMRI work. Additional aspects of EEG–BOLD coupling maturation established here include generally consistent patterns across age groups but also frequency specific maturational differences.

Specifically, in comparison to (Lüchinger et al., 2011) the current study reveals three new findings. First, the functional coupling of cortical regions between spontaneous EEG power fluctuations and the BOLD signal is not only similar between adults and adolescents but also between school-aged children and older individuals in most frequency bands. Second, the absence of thalamocortical EEG–BOLD coupling in children, together with age-related normalized thalamic BOLD power increase, indicates that the EEG–BOLD coupling is not insensitive to maturation effects per se. Third, the absolute amplitude of spontaneous slow BOLD signal fluctuation reflects a marker for brain maturation, parallel to the globally decreasing trajectories of EEG amplitudes, gray matter and glucose metabolism during adolescence.

4.4.2 Brain development and EEG maturation

The low frequency EEG attenuation has a long tradition as a robust marker for functional brain maturation. Our data, recorded inside the MR scanner, strikingly confirm these findings. Strongest in lower frequencies with t-values up to 10 and higher, the power reduction was similar between EO and EC oscillations. Consistent with other studies (Boord et al., 2007; Kurth et al., 2010), this effect to a lower degree extended also to higher frequencies. According to previous publications, we do not believe that the observed EEG effects are massively influenced by changes of physical properties of the head (e.g., skull conductance or impedance) which change during early development, as these changes appear to be less prominent for the present age range (Hoekema et al., 2003). The fact that our developmental EEG amplitude reductions were frequency specific, and matched

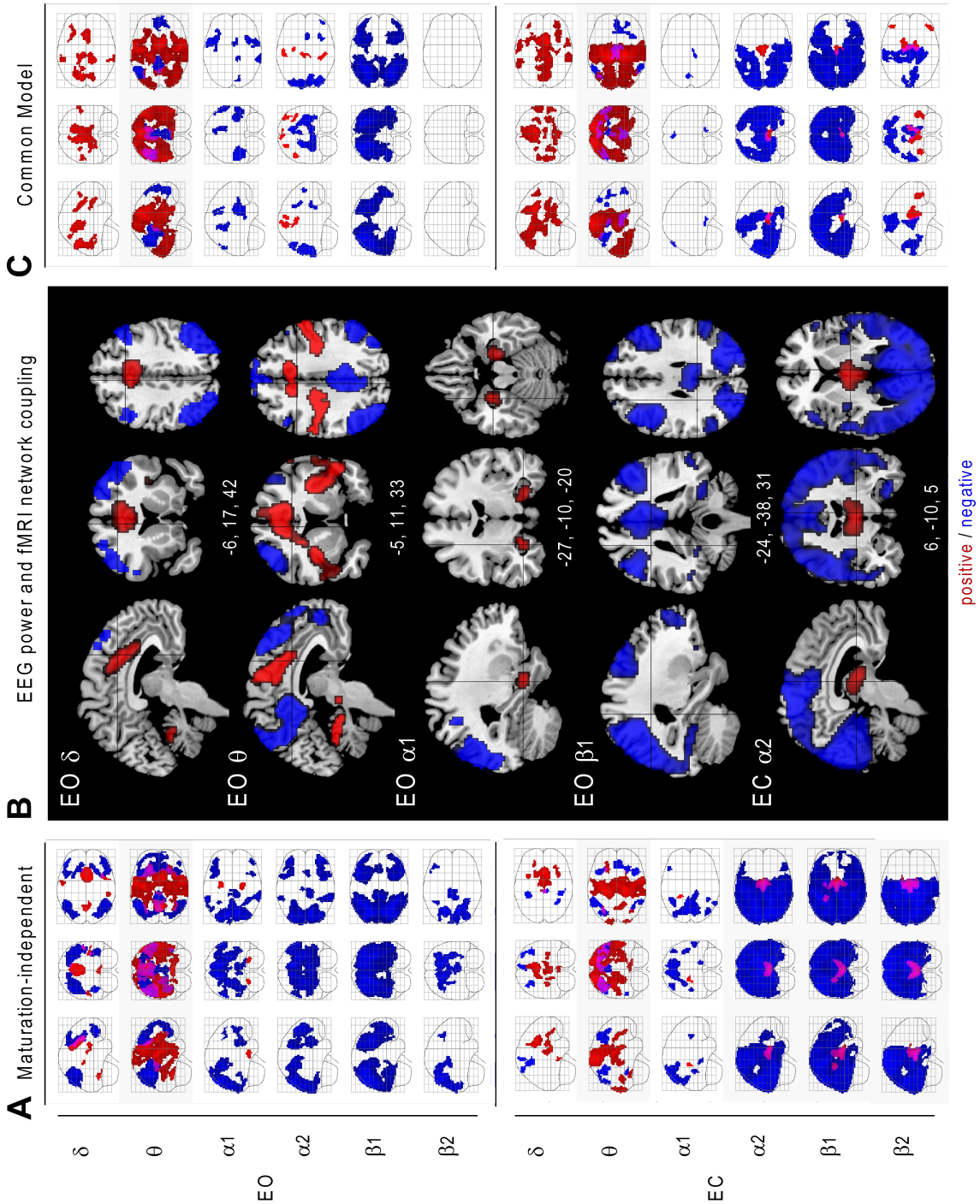

Fig. 2.4 Maturation-independent EEG-BOLD signal correlation results including all 55 participants with age as the covariate. A: Results from the main analysis (separate models). B: Topographical specificity for a selection (entitled accordingly) of the separate models results on anatomical template image (MNI-coordinates specified beneath). C: Maturation-independent partial correlation patterns resulting from the alternative common model analysis. A - C: T-values are shown as maximum intensity projections simultaneously for both positive (red) and negative (blue) correlations. An overlay of red and blue colored voxels in a specific perspective results in pink. Statistical height threshold was set to $p < 0.001$, corrected by extent threshold $k = 25$ voxels.

those found for the same age range with magnetoencephalography, which is insensitive to these changes in physical skull properties (Ciesielski et al., 2010; Pulighеddu et al., 2005), corroborates their neurodevelopmental nature.

EEG power maturation was not confined to a local topographical component but indicates changes in diffuse global scalp oscillatory activity as most electrodes were affected. Thus, GSP reflecting the averaged scalp activity captured EEG maturation well. GSP demonstrated that children's activity had more than 4 times higher power values than those found in adults in delta band (1 - 3.5 Hz) and almost 3 times higher in theta band (4 - 7.5 Hz) (Fig. 2.1B). The EEG signal is generated by synaptic activity of synchronized, mainly cortical neuron populations. Although the exact physiological mechanisms of EEG oscillations are not fully understood, their maturational transformation has been found to parallel changes in brain structure (Buchmann et al., 2011; Whitford et al., 2007). The parallel trajectories of EEG amplitudes and gray matter may have a common physiological background, since synaptic density reflects the connectivity and size of neuron populations which EEG amplitudes partly depend on (Boord et al., 2007; Feinberg and Campbell, 2010). In contrast to these former studies, we investigated the relation of EEG maturation to the functional fMRI-BOLD signal.

4.4.3 EEG–BOLD signal correlations

Resting state EEG and fMRI capture two partly complementary aspects of intrinsic brain activity. The brain's intrinsic BOLD activity reveals a spatially segregated functional architecture consisting of coherent large-scale networks (Raichle, 2006). Our data demonstrated a robust coupling between the different EEG oscillations and such networks. Summarized in a maturation-independent analysis we delineated three basic and robust correlation patterns. All three coupling patterns reflect different states of arousal (DMN, ATN) or mechanisms of arousal regulation (TCN). Arousal is likely the dominant factor in spontaneously fluctuating resting state brain activity.

DMN. EO theta was negatively correlated to the DMN, in line with previous findings (Scheeringa et al., 2008). Positive correlations appeared widespread in and near the cinguloopercular network (Dosenbach et al., 2007; Dosenbach et al., 2006). This pattern was similar across both low frequencies in both conditions (as confirmed by inspection at a lower threshold). The inverse relation of theta and DMN is consistent with their association to cognition as theta power (Inanaga, 1998) increases and DMN activity decreases (Raichle and Snyder, 2007) in response to cognitively demanding mental activity. Similarly, the positive correlation between theta and the cinguloopercular network is consistent with its task-positive role (Dosenbach et al., 2007; Dosenbach et al., 2006; Seeley et al., 2007) .

ATN. EO beta1 was negatively correlated in broad occipital and parieto- frontal cortices. The bilateral fronto-parietal pattern, as has been described before (Laufs et al., 2006; Laufs et al., 2003), comprises regions engaged in task processing (Corbetta and Shulman, 2002) and closely matches the ATN found in resting state data (Fox et al., 2005).

TCN. EC alpha oscillations were positively correlated in the thalamus and negatively

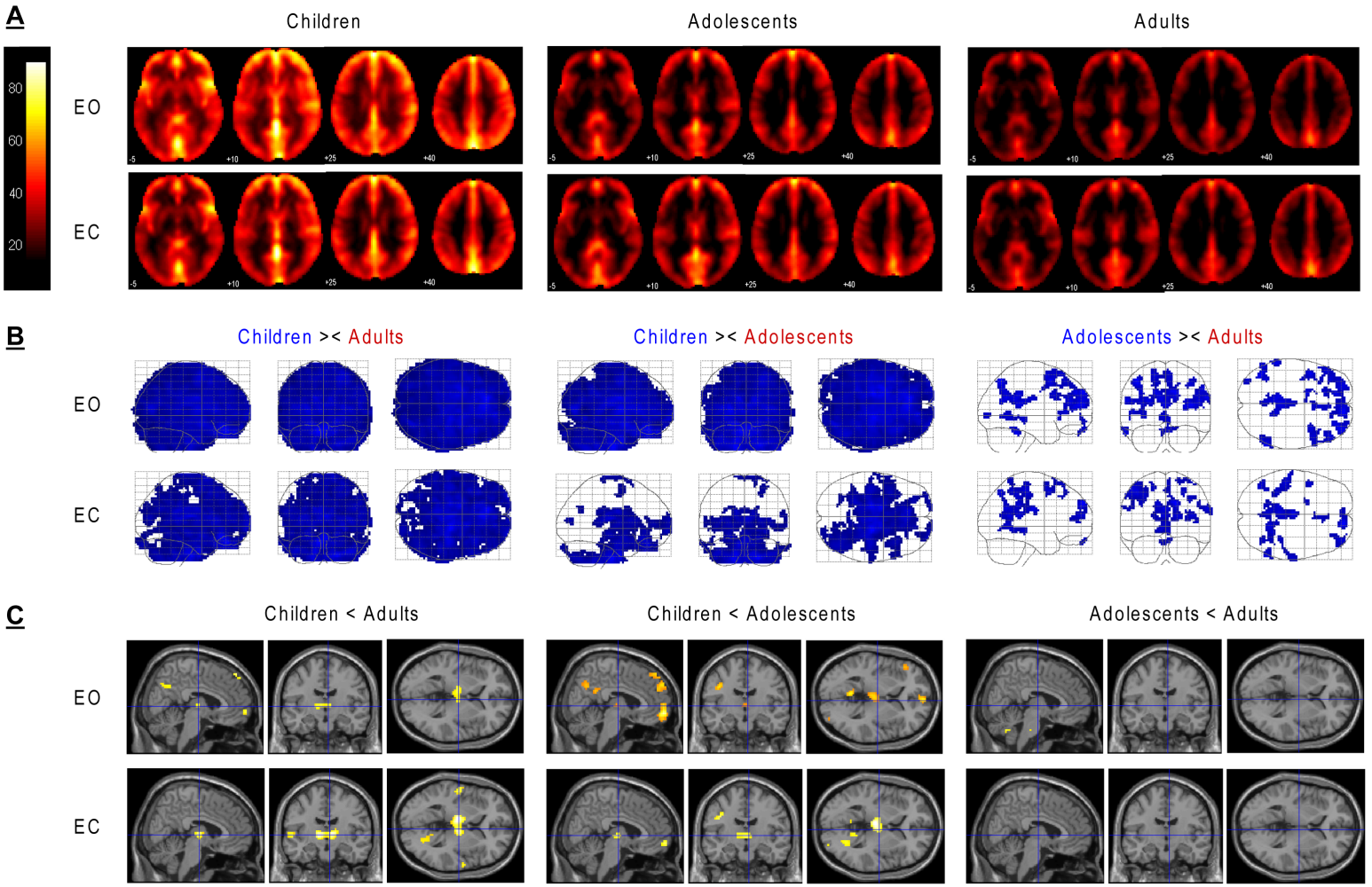

Fig. 2.5 BOLD spectral power analysis. A: Group mean absolute BOLD signal power, separated by condition. Color bar scaling (15 - 90 [arbitrary units]) and slice selection (axial: -5, 10, 25, 40) were kept constant. B: Group differences of absolute BOLD signal power. Contrasts are shown in both directions 'younger <> older' and color-coded as indicated by the column titles. No voxel was observed showing higher BOLD power in the older group. Statistical height threshold was set to $p < 0.001$, corrected by extent threshold $k = 25$ voxels. C: Group differences of normalized BOLD signal power differences separated by condition. T-statistics were superimposed on SPM anatomical template. Slice-coordinates were chosen to highlight the thalamus. Only contrasts 'younger < older' were shown. Statistical height threshold was set to $p < 0.001$, corrected by extent threshold $k = 25$ voxels. The contrast EO 'Children < Adolescents' was thresholded at $p < 0.005$, $k = 25$, to visualize consistency of normalized thalamic power increase with age.

correlated in occipital, parietal and temporal cortex. This replicates the hallmark finding of EEG–fMRI correlations (de Munck et al., 2007; Difrancesco et al., 2008; Feige et al., 2005; Goldman et al., 2002; Goncalves et al., 2006; Lüchinger et al., 2011; Moosmann et al., 2003; Tyvaert et al., 2008) and EEG–PET studies (Sadato et al., 1998; Schreckenberger et al., 2004). This finding corroborates the long standing concept that alpha synchronization reflects an idling state of thalamocortical arousal regulation characterized by cortical down regulation in sensory areas (for review e.g.: Feige et al., 2005). The pattern extended to beta1 and beta2 bands as found before (de Munck et al., 2009; Moosmann et al., 2003). The thalamocortical coupling pattern reported here was not evoked by short-term (e.g. 20 s) alpha reactivity ("Berger effect"), but rather characterizes a more persistent resting state maintenance of 2.5 min.

EO and EC conditions yielded different EEG–BOLD coupling patterns. This suggests that the conditions affect brain function more profoundly than one could expect from the simple blocking of visual input. However, the coupling differences are in line with EEG (Barry et al., 2007; Berger, 1929) and fMRI literature (Bianciardi et al., 2009; Marx et al., 2004; Marx et al., 2003; Yang et al., 2007) reporting EO/EC condition differences. With the increasing interest in resting state brain function, differences between EO and EC have likewise garnered interest, and they also relate to the debate about an optimal 'baseline' (Raichle et al., 2001). The parallel analysis of six major frequency bands ranging from 1 to 30 Hz proofed to be the most important factor influencing the EEG–BOLD correlations. The main effect of frequency was massive and demonstrated that there is substantial variation among frequency bands in spite of the fact that there are moderate inter-frequency dependencies as well. This partly contradicts theoretical models of EEG–fMRI fusion which assume less frequency- and condition-specific transfer functions (Kilner et al., 2005; Rosa et al., 2010).

The band-wise coupling analyses revealed several, at least partly, distinct networks which were both frequency dependent, and varied with arousal states (eyes open versus eyes closed). However, a simple functional interpretation in terms of distinct oscillation speeds of these networks may not be warranted, since we did not examine coupling specifically for the classical fMRI-defined RSN. In addition, coupling with a given frequency does not imply that the network acts as an EEG generator with the given frequency, and the coupling pattern may not converge with the distribution identified by electromagnetic source localization.

Former studies typically used oscillatory activity from a focal component in terms of a subset of electrodes. The robust correlations yielded by GSP suggest that fundamental couplings to DMN, ATN and TCN arise from diffuse rhythms rather than focal components. The previous results for the adult and adolescent groups were replicated using only the first half of the data to equate to the shorter recording duration in children. Such high reliability of the resting EEG–fMRI coupling patterns extends similar findings for separate resting EEG (Buckelmuller et al., 2006; Napflin et al., 2008) and fMRI (Van Dijk et al., 2010) markers.

Common model analysis. Partial correlations were much less frequently reported in the literature (de Munck et al., 2009; Tyvaert et al., 2008), yet explain the portion of

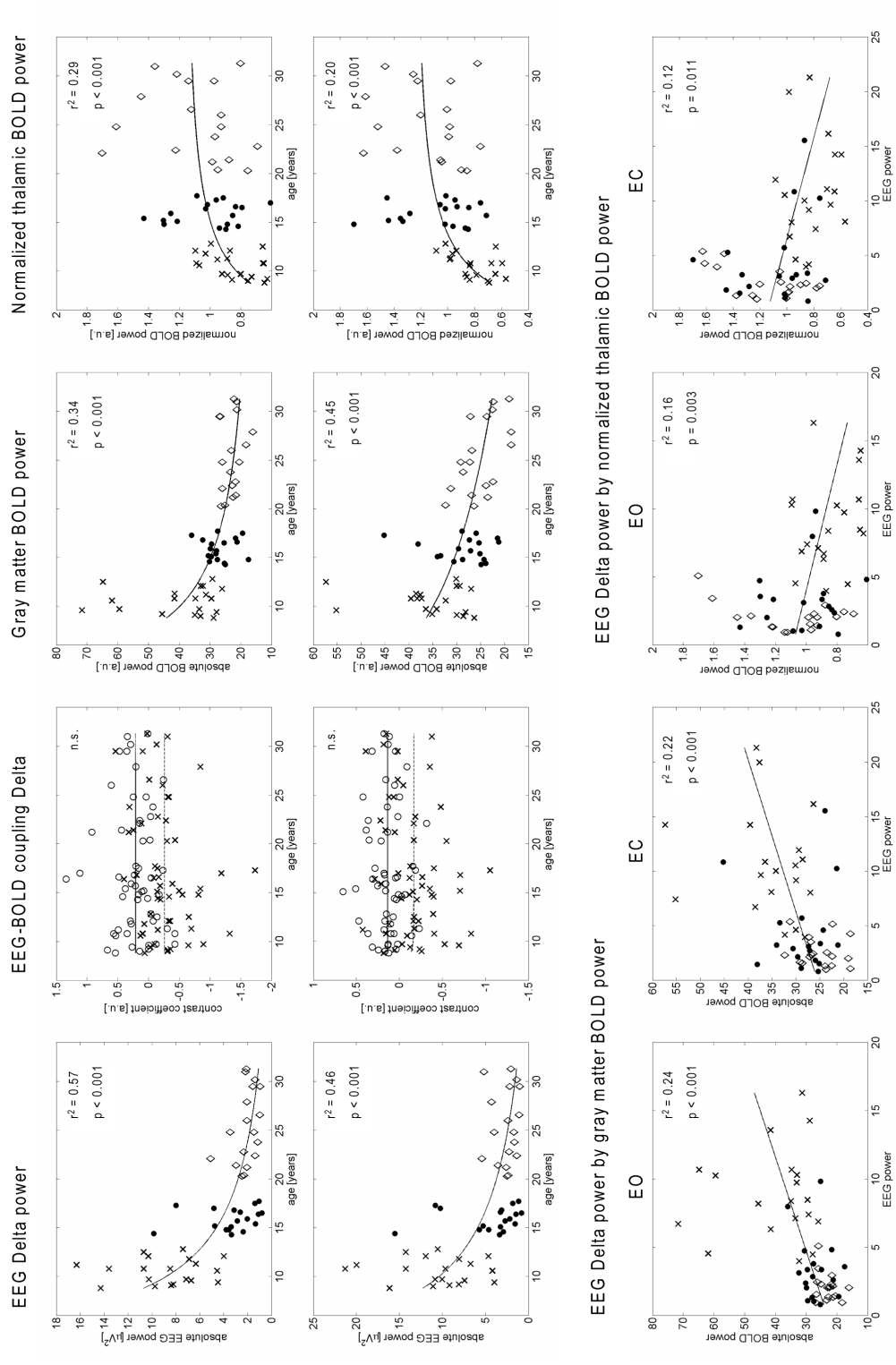

Fig. 2.6 Scatter plots illustrating the main findings. A: EEG power, EEG-BOLD coupling, absolute and normalized BOLD power by age. Markers represent group membership (cross: Children, dot: Adolescents, diamond: Adults). Power curve ($f(x) = a*xb$) was used for data fit. EEG power and EEG-BOLD coupling is represented by delta band GSP. EEG-BOLD correlations are mean values within significant group mean patterns and are shown for both positive (circle, solid slope) and negative (cross, dashed slope) correlations. Absolute BOLD power was averaged within gray matter voxels (SPM template > 40 %). Normalized BOLD power was averaged within thalamic voxels (AAL-ROI). B: Absolute gray matter and normalized thalamic BOLD power by EEG delta power. Linear slope ($f(x) = a+x*b$) was used for data fit. A and B: coefficients r^2 and p were calculated using SPSS 16.

correlation that is unique to a specific frequency band. Accordingly, DMN correlation is specific to theta power rather than to delta power. ATN correlation is more specific to beta1 than to the neighboring bands and the thalamocortical pattern was specific to all three upper frequency bands alpha2, beta1 and beta2. EC theta manifested a coupling very similar to the thalamocortical pattern, yet with opposite correlation signs. This was not evident in the main analysis. Therefore we interpret these results as mainly model driven effects. The frequency fluctuation changes as non-orthogonal regressors enter the model (Andrade et al., 1999), in this case leaving their fingerprints in concurrent frequency bands.

4.4.4 Maturation of EEG–BOLD coupling patterns

Maturational EEG power attenuation was characterized dominantly by lower frequencies in both conditions and followed a continuous trajectory. We hypothesized that a corresponding substrate of this general power reduction needs to be identifiable in an analog pattern across age, condition and frequency. In contrast, inconsistent effects limited to single factor levels hardly explain the power reduction comprehensively. Despite the fact that the EEG signal at the scalp can be generated in many ways, we further hypothesized that the global vanishing of amplitudes is likely related to profound mechanisms, possibly localized in broad areas across the whole cortex, a large-scale network whose activity affects widespread areas across the brain, or a functionally central region projecting to large portions of the cortex. In contrast, few, small and less centrally integrated regions seem rather implausible.

The EEG–BOLD signal coupling did not change profoundly with maturation as revealed by the ANOVA main effect of age. Although the coupling differed significantly in the right visual cortex, this focal, peripheral cluster did not match our scheme to possibly account for global EEG change. The group differences in EEG–BOLD coupling (Fig. 2.3B) revealed no consistent pattern of changes. The few significant differences were neither focused on low frequencies nor did they reoccur between the groups contrasts, which would indicate a continuous maturational track similar to EEG. A consistent meaningful pattern across group, condition and frequency was not identified at very low statistical threshold either. This is important as the power attenuation may be very loosely related to changing correlated activity in brain regions. The lack of a direct correspondence between changing EEG power and retaining EEG–BOLD signal correlations means that the fluctuations driving these correlations are largely independent from the oscillatory magnitude in the EEG signal. The correlation measure reflects the coherence of signal time courses independent from the scales. Therefore, the amplitudes depending on neuronal masses are likely independent from synaptic pruning. The functional coupling reflects a distinct aspect of neurophysiological activity that presumably matures earlier than the neurodevelopmental process responsible for low frequency EEG attenuation. These results are consistent with similar findings in our previous report on late maturation (Lüchinger et al., 2011). EEG oscillations were coupled to RSN's such as the DMN. The significant EEG coupling to these RSNs even at the age of 8 years is plausible as RSN's were found to be established already at the age of 7 - 9 years (Fair et al., 2009; Fair et al., 2007;

Supekar et al., 2009). Our results thus suggest that EEG oscillations of a given frequency keep the same connotation between children and adults in terms of functional correlate to BOLD signal activity, and that most frequency specific BOLD topographies are conserved across development despite changes in EEG frequency composition.

Although we did not find a 'direct' correspondence, we identified robust age-related differences in the thalamocortical coupling pattern. This key feature of EEG–BOLD coupling differed between children and adolescents as well as children and adults significantly in terms of less negative cortical and less positive thalamic correlations. Children did not indicate a coupling of EEG fluctuation to thalamic activity at all (Fig. 2.3A), even at very low statistical threshold. The thalamocortical pattern associated with EC alpha2, beta1 and beta2 matures between the ages of 10 to 16 years. This suggests that the depicted oscillations have a different connotation in children than in adolescents or adults, as their functional coupling to BOLD signal activity is significantly different.

Although this EEG–BOLD coupling maturation was limited to EC higher frequencies, it is tempting to speculate about an 'indirect' relation to the dominantly low frequency power decrease, due to the fundamental role of the thalamus and thalamocortical circuitry for brain state regulation and the generation of scalp electric oscillations. The higher frequency EC correlation to thalamocortical BOLD signal does not imply that the thalamus and thalamocoritcal interaction itself oscillates in this particular frequency range only during EC. Thalamic and thalamocortcial state regulation feature other frequency ranges and are well known to be related to low frequency scalp activity (Brandeis et al., 2009). EEG maturation therefore may be related to thalamic and thalamocortical activity as well. The higher frequency EC EEG–BOLD coupling may reflect only a distinct aspect and small portion of thalamocortical activity limited to state- and frequency-dependent scalp activity. Nevertheless, it yielded the functional maturation in these structures with converging evidence from normalized BOLD power, thus indicating state-independent thalamic maturation (see below). Hence we propose that EEG power decrease may be 'indirectly' related to higher frequency EC EEG–BOLD coupling changes as they could emerge from the same neuronal substrate (the maturational changes in thalamocortical activity). However, (low frequency) EEG power decrease and thalamocortical changes may also be independent phenomena of brain maturation.

This proposal would link brain maturation with other brain states based on the converging feature of low frequency excess, for which the thalamus and thalamocortical circuits are well-established neuronal substrates. Such states are low arousal states like sleep (Steriade et al., 1993; Tsai et al., 2010) or anesthesia (John et al., 2001), and neuropathology (Llinas et al., 1999; Michels et al., 2011a; Michels et al., 2011b; Sarnthein et al., 2003). Low arousal states and neuropathologic conditions can be seen as states of lower brain functioning. Our results suggest that brain immaturity resembles features of lower brain functioning as well. The result is also in line with findings that some EEG and fMRI markers implicate a maturational lag in neurodevelopmental disorders such as Attention Deficit Hyperactivity Disorder (Doehnert et al., 2010; Fair et al., 2010), but

by no means implies that normal immaturity in childhood represents a pathological or under-aroused state.

The EEG–BOLD coupling results might be partly influenced by age-related confounds in physiological noise, such as breathing (which we did not record) or blood-pulse artifact. In developmental EEG and fMRI studies breathing is rarely accounted for. In simultaneous EEG–fMRI the main physiological confound comes from motion-related blood-pulse artifact due to magnetic field strength (Debener et al., 2008). The procedure for blood-pulse artifact reduction was standardized and carefully applied to all groups in the same way. Younger participants tend to have a higher pulse rate, but the performance of the average artifact subtraction is not influenced by the pulse rate. The same BCG artifact ICA components were rejected between the groups as the topography as well as the frequency pattern does not change across age groups. In addition, the number of excluded ICA components which contained residual EEG artifacts did not differ between children and adolescents. Since the major developmental effects on EEG and EEG–BOLD coupling were observed between these two groups, a contribution of differences in EEG quality is thus unlikely. Based on the EEG results shown in Figure 1A and B we conclude that the pulse artifact reduction was well achieved. Some remaining BCG artifact can be seen in the group mean topography but the group differences do not indicate a systematic bias with age.

We describe group differences in EEG–BOLD coupling state dependent in higher (> 10 Hz). The BCG artifact is strongest between 0 and 4 Hz. Group differences caused by confounding BCG artifact would (i) produce group differences in lower frequencies and (ii) affect both resting states similarly, as the age related pulse differences are state-independent. Importantly, the coupling pattern in low frequencies (delta, theta) did not differ between children and older participants. For example the components of the DMN or the cingulo-opercular network appeared in all groups in delta/theta. It would be difficult to explain why remaining BCG would affect the EC high frequency range but not state independent low frequency range. Nevertheless we cannot exclude by definition that the lacking thalamocortical coupling pattern in children could be influenced by remaining BCG contamination. Future studies might include approaches to better account for physiological confounds (Glover et al., 2000).

4.4.5 Maturation of the magnitude of spontaneous BOLD signal fluctuations

BOLD signal power was calculated for a direct comparison to EEG power maturation in terms of equivalent measures. The spontaneous fluctuating BOLD signal reflects the energy demand of the brain at rest (Raichle, 2006). The BOLD signal power was averaged within the low frequency range (0.01 - 0.08 Hz) which drives the functional connectivity and the RSNs, and which is believed to reflect mainly neuronal activity. Our data revealed prominent, global activity decrease in the resting BOLD signal with age (Fig. 2.5B). Strongest in children, the BOLD signal trajectory followed a non-linear decrease very similar to low frequency EEG power (Fig. 2.6A). To our knowledge, this finding is novel and provides a new marker for functional brain maturation. The decrease in hemodynamic

rest activity relates to other markers of structural and functional brain maturation that show similar decreases during adolescence (Boord et al., 2007; Feinberg and Campbell, 2010; Feinberg et al., 1990). The hemodynamic activity fluctuation attenuation also parallels the structural and metabolic maturation spatially, as a global phenomenon, affecting the entire brain. Possibly, the hemodynamic power decrease is coupled with metabolic decrease (Biagi et al., 2007; Chugani, 1998; Chugani et al., 1987; Taki et al., 2011), and both decreases may be guided by synaptic pruning (Giedd et al., 1999; Gogtay et al., 2004; Huttenlocher, 1979). Even if the physiological coupling between the diverse measures is not fully understood, the pattern represents converging evidence for general functional and structural reorganization towards higher efficiency.

The subtraction of the individual mean power level was expected to increase the sensitivity to spatial differences at the cost of sensitivity to global amplitude reductions with maturation. Since this normalized BOLD power was typically used in previous studies, these results connect most directly to the literature. After this normalization the relative BOLD activity was found to increase with age in the thalamus (Fig. 2.5C). This demonstrated the high functional specificity of BOLD signal power measure and directly corresponded to the maturation in the thalamocortical EEG–BOLD coupling. The normalized thalamic BOLD power correlated to the thalamic EC alpha2-BOLD coupling with $r = 0.557$ across participants in a post-hoc calculation. As noted above, this relative activity increase in the thalamus, together with the immature thalamocortical EEG–BOLD coupling provides converging evidence for maturational change in thalamocortical brain state regulation during rest. The thalamic and thalamocortical functions associated with abilities to transiently disconnect from environmental input, regulate sensory or motor distraction, and the maintenance of prolonged mental focus characterize human behavioral maturation.

Conventional fMRI studies report both increases as well as decreases in local BOLD activity as maturational correlate of cognitive functions (Blakemore and Choudhury, 2006), depending on the specific task, brain region and developmental phase. However interpretations of maturational BOLD signal chances are hampered by confounding factors such as cognitive effort, experience and strategy (Casey et al., 2005). Although our results need to be verified in further studies, the resting state BOLD power provides an absolute quantity of functional brain maturation and is less ambiguous in terms of behavioral confounds. Although the BOLD signal power was analyzed in the spectral range thought to reflect neuronal activity (< 0.1 Hz), physiological confounds such as respiration and blood pulse in the higher frequency range (> 0.1 Hz) can affect lower frequency ranges by aliasing (Birn et al., 2008). The spatial patterns of both absolute and normalized BOLD signal power maturation were different from those typically yielded by physiological artifacts.

We hypothesize that these BOLD power decreases with age are related to the gray matter volume decreases, similar to the maturational decreases of slow EEG activity (Whitford et al., 2007) which remain correlated with gray matter reductions even after correcting for whole-brain volume (Buchmann et al., 2011). Therefore, we interpret our results as mainly driven by neuronal maturation, although this needs to be confirmed in

further studies.

4.5 Conclusion

This study demonstrates that global EEG low frequency power decrease from childhood to adulthood (8.8 - 31.3 years) is paralleled by global BOLD signal power decrease, while temporal functional coupling remains largely unchanged. The novel finding of global BOLD signal power decrease is consistent with global decreases in structural and metabolic markers, indicating profound neuronal reorganization during adolescence. Moreover, thalamic and thalamocortical maturation was implicated by EEG–fMRI coupling and normalized BOLD power.

4.6 Acknowledgements

This work was supported by the University Research Priority Program "Integrative Human Physiology" at the University of Zurich. We are grateful for all the participant interest in the study; we especially thank the children and their parents for their commitment.

4.7 References

Allen, P.J., Josephs, O., Turner, R., 2000. A method for removing imaging artifact from continuous EEG recorded during functional MRI. Neuroimage 12, 230-239.

Allen, P.J., Polizzi, G., Krakow, K., Fish, D.R., Lemieux, L., 1998. Identification of EEG events in the MR scanner: the problem of pulse artifact and a method for its subtraction. Neuroimage 8, 229-239.

Andrade, A., Paradis, A.L., Rouquette, S., Poline, J.B., 1999. Ambiguous results in functional neuroimaging data analysis due to covariate correlation. Neuroimage 10, 483-486.

Baria, A.T., Baliki, M.N., Parrish, T., Apkarian, A.V., 2011. Anatomical and Functional Assemblies of Brain BOLD Oscillations. J Neurosci 31, 7910-7919.

Barry, R.J., Clarke, A.R., Johnstone, S.J., Brown, C.R., 2009. EEG differences in children between eyes-closed and eyes-open resting conditions. Clin Neurophysiol 120, 1806-1811.

Barry, R.J., Clarke, A.R., Johnstone, S.J., Magee, C.A., Rushby, J.A., 2007. EEG differences between eyes-closed and eyes-open resting conditions. Clin Neurophysiol 118, 2765-2773.

Berger, H., 1929 Über das Elektrenkephalogramm des Menschen. European Archives of Psychiatry and Clinical Neuroscience 87, 527-570.

Biagi, L., Abbruzzese, A., Bianchi, M.C., Alsop, D.C., Del Guerra, A., Tosetti, M., 2007. Age dependence of cerebral perfusion assessed by magnetic resonance continuous arterial spin labeling. J Magn Reson Imaging 25, 696-702.

Bianciardi, M., Fukunaga, M., van Gelderen, P., Horovitz, S.G., de Zwart, J.A., Duyn, J.H., 2009. Modulation of spontaneous fMRI activity in human visual cortex by behavioral state. Neuroimage 45, 160-168.

Birn, R.M., Murphy, K., Bandettini, P.A., 2008. The effect of respiration variations on independent component analysis results of resting state functional connectivity. Hum Brain Mapp 29, 740-750.

Biswal, B., Yetkin, F.Z., Haughton, V.M., Hyde, J.S., 1995. Functional connectivity in the motor cortex of resting human brain using echo-planar MRI. Magn Reson Med 34, 537-541.

Biswal, B.B., Mennes, M., Zuo, X.N., Gohel, S., Kelly, C., Smith, S.M., Beckmann, C.F., Adelstein, J.S., Buckner, R.L., Colcombe, S., Dogonowski, A.M., Ernst, M., Fair, D., Hampson, M., Hoptman, M.J., Hyde, J.S., Kiviniemi, V.J., Kotter, R., Li, S.J., Lin, C.P., Lowe, M.J., Mackay, C., Madden, D.J., Madsen, K.H., Margulies, D.S., Mayberg, H.S., McMahon, K., Monk, C.S., Mostofsky, S.H., Nagel, B.J., Pekar, J.J., Peltier, S.J., Petersen, S.E., Riedl, V., Rombouts, S.A., Rypma, B., Schlaggar, B.L., Schmidt, S., Seidler, R.D., Siegle, G.J., Sorg, C., Teng, G.J., Veijola, J., Villringer, A., Walter, M., Wang, L., Weng, X.C., Whitfield-Gabrieli, S.,

Williamson, P., Windischberger, C., Zang, Y.F., Zhang, H.Y., Castellanos, F.X., Milham, M.P., 2010. Toward discovery science of human brain function. Proc Natl Acad Sci U S A 107, 4734-4739.

Blakemore, S.J., Choudhury, S., 2006. Brain development during puberty: state of the science. Dev Sci 9, 11-14.

Boord, P.R., Rennie, C.J., Williams, L.M., 2007. Integrating "brain" and "body" measures: correlations between EEG and metabolic changes over the human lifespan. J Integr Neurosci 6, 205-218.

Bourgeois, J.P., Rakic, P., 1993. Changes of synaptic density in the primary visual cortex of the macaque monkey from fetal to adult stage. J Neurosci 13, 2801-2820.

Brandeis, D., Michel, M.C., Amzica, F., 2009. From neuronal activity to scalp potential fields. In: Michel, M.C., Koenig, T., Brandeis, D., Gianotti, L.R.R., Wackermann, J. (Eds.), Electrical Neuroimaging. Cambridge Unversity Press, New York, pp. 1-24.

Brown, T.T., Petersen, S.E., Schlaggar, B.L., 2006. Does human functional brain organization shift from diffuse to focal with development? Dev Sci 9, 9-11.

Buchmann, A., Ringli, M., Kurth, S., Schaerer, M., Geiger, A., Jenni, O.G., Huber, R., 2011. EEG sleep slow-wave activity as a mirror of cortical maturation. Cereb Cortex 21, 607-615.

Buckelmuller, J., Landolt, H.P., Stassen, H.H., Achermann, P., 2006. Trait-like individual differences in the human sleep electroencephalogram. Neuroscience 138, 351-356.

Cajochen, C., Wyatt, J.K., Czeisler, C.A., Dijk, D.J., 2002. Separation of circadian and wake duration-dependent modulation of EEG activation during wakefulness. Neuroscience 114, 1047-1060.

Calhoun, V.D., Kiehl, K.A., Pearlson, G.D., 2008. Modulation of temporally coherent brain networks estimated using ICA at rest and during cognitive tasks. Hum Brain Mapp 29, 828-838.

Campbell, I.G., Feinberg, I., 2009. Longitudinal trajectories of non-rapid eye movement delta and theta EEG as indicators of adolescent brain maturation. Proc Natl Acad Sci U S A 106, 5177-5180.

Case, R., 1992. The role of the frontal lobes in the regulation of cognitive development. Brain Cogn 20, 51-73. Casey, B.J., Galvan, A., Hare, T.A., 2005. Changes in cerebral functional organization during cognitive development. Curr Opin Neurobiol 15, 239-244.

Chugani, H.T., 1998. A critical period of brain development: studies of cerebral glucose utilization with PET. Prev Med 27, 184-188.

Chugani, H.T., Phelps, M.E., Mazziotta, J.C., 1987. Positron emission tomography study of human brain functional development. Ann Neurol 22, 487-497.

Ciesielski, K.T., Ahlfors, S.P., Bedrick, E.J., Kerwin, A.A., Hamalainen, M.S., 2010. Top-down control of MEG alpha-band activity in children performing Categorical N-Back Task. Neuropsychologia 48, 3573-3579.

Corbetta, M., Shulman, G.L., 2002. Control of goal-directed and stimulus-driven attention in the brain. Nat Rev Neurosci 3, 201-215.

Cordes, D., Haughton, V.M., Arfanakis, K., Carew, J.D., Turski, P.A., Moritz, C.H., Quigley, M.A., Meyerand, M.E., 2001. Frequencies contributing to functional connectivity in the cerebral cortex in "resting-state" data. AJNR Am J Neuroradiol 22, 1326-1333.

Cowan, W.M., Fawcett, J.W., O'Leary, D.D., Stanfield, B.B., 1984. Regressive events in neurogenesis. Science 225, 1258-1265.

Damoiseaux, J.S., Rombouts, S.A., Barkhof, F., Scheltens, P., Stam, C.J., Smith, S.M., Beckmann, C.F., 2006. Consistent resting-state networks across healthy subjects. Proc Natl Acad Sci U S A 103, 13848-13853.

de Munck, J.C., Goncalves, S.I., Huijboom, L., Kuijer, J.P., Pouwels, P.J., Heethaar, R.M., Lopes da Silva, F.H., 2007. The hemodynamic response of the alpha rhythm: an EEG/fMRI study. Neuroimage 35, 1142-1151.

de Munck, J.C., Goncalves, S.I., Mammoliti, R., Heethaar, R.M., Lopes da Silva, F.H., 2009. Interactions between different EEG frequency bands and their effect on alpha-fMRI correlations. Neuroimage 47, 69-76.

Debener, S., Mullinger, K.J., Niazy, R.K., Bowtell, R.W., 2008. Properties of the ballistocardiogram artefact as revealed by EEG recordings at 1.5, 3 and 7 T static magnetic field strength. Int J Psychophysiol 67, 189-199.

Deco, G., Jirsa, V.K., McIntosh, A.R., 2011. Emerging concepts for the dynamical organization of resting-state activity in the brain. Nat Rev Neurosci 12, 43-56.

Delorme, A., Makeig, S., 2004. EEGLAB: an open source toolbox for analysis of single-trial EEG dynamics including independent component analysis. J Neurosci Methods 134, 9-21.

Dick, F., Leech, R., Moses, P., Saccuman, M.C., 2006. The interplay of learning and development in shaping neural organization. Dev Sci 9, 14-17.

Difrancesco, M.W., Holland, S.K., Szaflarski, J.P., 2008. Simultaneous EEG/functional magnetic resonance imaging at 4 Tesla: correlates of brain activity to spontaneous alpha rhythm during relaxation. J Clin Neurophysiol 25, 255-264.

Doehnert, M., Brandeis, D., Imhof, K., Drechsler, R., Steinhausen, H.C., 2010. Mapping attention-deficit/hyperactivity disorder from childhood to adolescence–no neurophysiologic evidence for a developmental lag of attention but

some for inhibition. Biol Psychiatry 67, 608-616.
Dosenbach, N.U., Fair, D.A., Miezin, F.M., Cohen, A.L., Wenger, K.K., Dosenbach, R.A., Fox, M.D., Snyder, A.Z., Vincent, J.L., Raichle, M.E., Schlaggar, B.L., Petersen, S.E., 2007. Distinct brain networks for adaptive and stable task control in humans. Proc Natl Acad Sci U S A 104, 11073-11078.
Dosenbach, N.U., Nardos, B., Cohen, A.L., Fair, D.A., Power, J.D., Church, J.A., Nelson, S.M., Wig, G.S., Vogel, A.C., Lessov-Schlaggar, C.N., Barnes, K.A., Dubis, J.W., Feczko, E., Coalson, R.S., Pruett, J.R., Jr., Barch, D.M., Petersen, S.E., Schlaggar, B.L., 2010. Prediction of individual brain maturity using fMRI. Science 329, 1358-1361.
Dosenbach, N.U., Visscher, K.M., Palmer, E.D., Miezin, F.M., Wenger, K.K., Kang, H.C., Burgund, E.D., Grimes, A.L., Schlaggar, B.L., Petersen, S.E., 2006. A core system for the implementation of task sets. Neuron 50, 799-812.
Duff, E.P., Johnston, L.A., Xiong, J., Fox, P.T., Mareels, I., Egan, G.F., 2008. The power of spectral density analysis for mapping endogenous BOLD signal fluctuations. Hum Brain Mapp 29, 778-790.
Durston, S., Davidson, M.C., Tottenham, N., Galvan, A., Spicer, J., Fossella, J.A., Casey, B.J., 2006. A shift from diffuse to focal cortical activity with development. Dev Sci 9, 1-8.
Dustman, R.E., Shearer, D.E., Emmerson, R.Y., 1999. Life-span changes in EEG spectral amplitude, amplitude variability and mean frequency. Clin Neurophysiol 110, 1399-1409.
Eeg-Olofsson, O., 1970. The development of the electroencephalogram in normal children and adolescents from the age of 1 through 21 years. Acta Paediatr Scand Suppl 208, Suppl208:201+.
Fair, D.A., Cohen, A.L., Power, J.D., Dosenbach, N.U., Church, J.A., Miezin, F.M., Schlaggar, B.L., Petersen, S.E., 2009. Functional brain networks develop from a "local to distributed" organization. PLoS Comput Biol 5, e1000381.
Fair, D.A., Dosenbach, N.U., Church, J.A., Cohen, A.L., Brahmbhatt, S., Miezin, F.M., Barch, D.M., Raichle, M.E., Petersen, S.E., Schlaggar, B.L., 2007. Development of distinct control networks through segregation and integration. Proc Natl Acad Sci U S A 104, 13507-13512.
Fair, D.A., Posner, J., Nagel, B.J., Bathula, D., Dias, T.G., Mills, K.L., Blythe, M.S., Giwa, A., Schmitt, C.F., Nigg, J.T., 2010. Atypical default network connectivity in youth with attention-deficit/hyperactivity disorder. Biol Psychiatry 68, 1084-1091.
Feige, B., Scheffler, K., Esposito, F., Di Salle, F., Hennig, J., Seifritz, E., 2005. Cortical and subcortical correlates of electroencephalographic alpha rhythm modulation. J Neurophysiol 93, 2864-2872.
Feinberg, I., Campbell, I.G., 2010. Sleep EEG changes during adolescence: an index of a fundamental brain reorganization. Brain Cogn 72, 56-65.
Feinberg, I., Thode, H.C., Jr., Chugani, H.T., March, J.D., 1990. Gamma distribution model describes maturational curves for delta wave amplitude, cortical metabolic rate and synaptic density. J Theor Biol 142, 149-161.
Forman, S.D., Cohen, J.D., Fitzgerald, M., Eddy, W.F., Mintun, M.A., Noll, D.C., 1995. Improved assessment of significant activation in functional magnetic resonance imaging (fMRI): use of a cluster-size threshold. Magn Reson Med 33, 636-647.
Fox, M.D., Raichle, M.E., 2007. Spontaneous fluctuations in brain activity observed with functional magnetic resonance imaging. Nat Rev Neurosci 8, 700-711.
Fox, M.D., Snyder, A.Z., Vincent, J.L., Corbetta, M., Van Essen, D.C., Raichle, M.E., 2005. The human brain is intrinsically organized into dynamic, anticorrelated functional networks. Proc Natl Acad Sci U S A 102, 9673-9678.
Friston, K., 2002. Beyond phrenology: what can neuroimaging tell us about distributed circuitry? Annu Rev Neurosci 25, 221-250.
Gasser, T., Verleger, R., Bacher, P., Sroka, L., 1988. Development of the EEG of school-age children and adolescents. I. Analysis of band power. Electroencephalogr Clin Neurophysiol 69, 91-99. Gibbs, F.A., Knott, J.R., 1949. Growth of the electrical activity of the cortex. Electroencephalogr Clin Neurophysiol 1, 223-229.
Giedd, J.N., Blumenthal, J., Jeffries, N.O., Castellanos, F.X., Liu, H., Zijdenbos, A., Paus, T., Evans, A.C., Rapoport, J.L., 1999. Brain development during childhood and adolescence: a longitudinal MRI study. Nat Neurosci 2, 861-863.
Glover, G.H., Li, T.Q., Ress, D., 2000. Image-based method for retrospective correction of physiological motion effects in fMRI: RETROICOR. Magn Reson Med 44, 162-167.
Gogtay, N., Giedd, J.N., Lusk, L., Hayashi, K.M., Greenstein, D., Vaituzis, A.C., Nugent, T.F., 3rd, Herman, D.H., Clasen, L.S., Toga, A.W., Rapoport, J.L., Thompson, P.M., 2004. Dynamic mapping of human cortical development during childhood through early adulthood. Proc Natl Acad Sci U S A 101, 8174-8179.
Gogtay, N., Thompson, P.M., 2010. Mapping gray matter development: implications for typical development and vulnerability to psychopathology. Brain Cogn 72, 6-15.
Goldman, R.I., Stern, J.M., Engel, J., Jr., Cohen, M.S., 2002. Simultaneous EEG and fMRI of the alpha rhythm. Neuroreport 13, 2487-2492.

Goncalves, S.I., de Munck, J.C., Pouwels, P.J., Schoonhoven, R., Kuijer, J.P., Maurits, N.M., Hoogduin, J.M., Van Someren, E.J., Heethaar, R.M., Lopes da Silva, F.H., 2006. Correlating the alpha rhythm to BOLD using simultaneous EEG/fMRI: inter-subject variability. Neuroimage 30, 203-213.

Gusnard, D.A., Raichle, M.E., 2001. Searching for a baseline: functional imaging and the resting human brain. Nat Rev Neurosci 2, 685-694.

Hoekema, R., Wieneke, G.H., Leijten, F.S., van Veelen, C.W., van Rijen, P.C., Huiskamp, G.J., Ansems, J., van Huffelen, A.C., 2003. Measurement of the conductivity of skull, temporarily removed during epilepsy surgery. Brain Topogr 16, 29-38.

Horovitz, S.G., Fukunaga, M., de Zwart, J.A., van Gelderen, P., Fulton, S.C., Balkin, T.J., Duyn, J.H., 2008. Low frequency BOLD fluctuations during resting wakefulness and light sleep: a simultaneous EEG–fMRI study. Hum Brain Mapp 29, 671-682.

Huttenlocher, P.R., 1979. Synaptic density in human frontal cortex - developmental changes and effects of aging. Brain Res 163, 195-205.

Inanaga, K., 1998. Frontal midline theta rhythm and mental activity. Psychiatry Clin Neurosci 52, 555-566. Jann, K., Dierks, T., Boesch, C., Kottlow, M., Strik, W., Koenig, T., 2009. BOLD correlates of EEG alpha phase-locking and the fMRI default mode network. Neuroimage 45, 903-916.

John, E.R., Ahn, H., Prichep, L., Trepetin, M., Brown, D., Kaye, H., 1980. Developmental equations for the electroencephalogram. Science 210, 1255-1258.

John, E.R., Prichep, L.S., Kox, W., Valdes-Sosa, P., Bosch-Bayard, J., Aubert, E., Tom, M., di Michele, F., Gugino, L.D., 2001. Invariant reversible QEEG effects of anesthetics. Conscious Cogn 10, 165-183.

Jolles, D.D., van Buchem, M.A., Crone, E.A., Rombouts, S.A., 2011. A comprehensive study of whole-brain functional connectivity in children and young adults. Cereb Cortex 21, 385-391.

Jung, T.P., Makeig, S., Westerfield, M., Townsend, J., Courchesne, E., Sejnowski, T.J., 2000. Removal of eye activity artifacts from visual event-related potentials in normal and clinical subjects. Clin Neurophysiol 111, 1745-1758.

Kilner, J.M., Mattout, J., Henson, R., Friston, K.J., 2005. Hemodynamic correlates of EEG: a heuristic. Neuroimage 28, 280-286.

Klimesch, W., 1999. EEG alpha and theta oscillations reflect cognitive and memory performance: a review and analysis. Brain Res Brain Res Rev 29, 169-195.

Kurth, S., Ringli, M., Geiger, A., LeBourgeois, M., Jenni, O.G., Huber, R., 2010. Mapping of cortical activity in the first two decades of life: a high-density sleep electroencephalogram study. J Neurosci 30, 13211-13219.

Laufs, H., Holt, J.L., Elfont, R., Krams, M., Paul, J.S., Krakow, K., Kleinschmidt, A., 2006. Where the BOLD signal goes when alpha EEG leaves. Neuroimage 31, 1408-1418.

Laufs, H., Kleinschmidt, A., Beyerle, A., Eger, E., Salek-Haddadi, A., Preibisch, C., Krakow, K., 2003. EEG–correlated fMRI of human alpha activity. Neuroimage 19, 1463-1476.

Lehmann, D., Skrandies, W., 1980. Reference-free identification of components of checkerboard-evoked multichannel potential fields. Electroencephalogr Clin Neurophysiol 48, 609-621.

Llinas, R., Ribary, U., Contreras, D., Pedroarena, C., 1998. The neuronal basis for consciousness. Philos Trans R Soc Lond B Biol Sci 353, 1841-1849.

Llinas, R., Urbano, F.J., Leznik, E., Ramirez, R.R., van Marle, H.J., 2005. Rhythmic and dysrhythmic thalamocortical dynamics: GABA systems and the edge effect. Trends Neurosci 28, 325-333.

Llinas, R.R., Ribary, U., Jeanmonod, D., Kronberg, E., Mitra, P.P., 1999. Thalamocortical dysrhythmia: A neurological and neuropsychiatric syndrome characterized by magnetoencephalography. Proc Natl Acad Sci U S A 96, 15222-15227.

Logothetis, N.K., Pauls, J., Augath, M., Trinath, T., Oeltermann, A., 2001. Neurophysiological investigation of the basis of the fMRI signal. Nature 412, 150-157.

Lüchinger, R., Michels, L., Martin, E., Brandeis, D., 2011. EEG–BOLD correlations during (post-)adolescent brain maturation. Neuroimage 56, 1493-1505.

Marx, E., Deutschlander, A., Stephan, T., Dieterich, M., Wiesmann, M., Brandt, T., 2004. Eyes open and eyes closed as rest conditions: impact on brain activation patterns. Neuroimage 21, 1818-1824.

Marx, E., Stephan, T., Nolte, A., Deutschlander, A., Seelos, K.C., Dieterich, M., Brandt, T., 2003. Eye closure in darkness animates sensory systems. Neuroimage 19, 924-934.

Matousek, M., Petersen, I., 1973. Automatic evaluation of EEG background activity by means of age-dependent EEG quotients. Electroencephalogr Clin Neurophysiol 35, 603-612.

Matsuura, M., Yamamoto, K., Fukuzawa, H., Okubo, Y., Uesugi, H., Moriiwa, M., Kojima, T., Shimazono, Y., 1985. Age development and sex differences of various EEG elements in healthy children and adults–quantification by a computerized wave form recognition method. Electroencephalogr Clin Neurophysiol 60, 394-406.

McCormick, D.A., Bal, T., 1997. Sleep and arousal: thalamocortical mechanisms. Annu Rev Neurosci 20, 185-215.

Mennes, M., Kelly, C., Zuo, X.N., Di Martino, A., Biswal, B.B., Castellanos, F.X., Milham, M.P., 2010. Inter-individual differences in resting-state functional connectivity predict task-induced BOLD activity. Neuroimage 50, 1690-1701.

Michels, L., Bucher, K., Brem, S., Halder, P., Lüchinger, R., Liechti, M., Martin, E., Jeanmonod, D., Kroll, J., Brandeis, D., 2011a. Does Greater Low Frequency EEG Activity in Normal Immaturity and in Children with Epilepsy Arise in the Same Neuronal Network? Brain Topogr 5, 78-89.

Michels, L., Bucher, K., Lüchinger, R., Klaver, P., Martin, E., Jeanmonod, D., Brandeis, D., 2010. Simultaneous EEG–fMRI during a working memory task: modulations in low and high frequency bands. PLoS One 5, e10298.

Michels, L., Moazami-Goudarzi, M., Jeanmonod, D., 2011b. Correlations between EEG and clinical outcome in chronic neuropathic pain: surgical effects and treatment resistance. Brain Imaging And Behavior 5, 329-348.

Moosmann, M., Ritter, P., Krastel, I., Brink, A., Thees, S., Blankenburg, F., Taskin, B., Obrig, H., Villringer, A., 2003. Correlates of alpha rhythm in functional magnetic resonance imaging and near infrared spectroscopy. Neuroimage 20, 145-158.

Napflin, M., Wildi, M., Sarnthein, J., 2008. Test-retest reliability of EEG spectra during a working memory task. Neuroimage 43, 687-693.

Niessing, J., Ebisch, B., Schmidt, K.E., Niessing, M., Singer, W., Galuske, R.A., 2005. Hemodynamic signals correlate tightly with synchronized gamma oscillations. Science 309, 948-951.

Nir, Y., Fisch, L., Mukamel, R., Gelbard-Sagiv, H., Arieli, A., Fried, I., Malach, R., 2007. Coupling between neuronal firing rate, gamma LFP, and BOLD fMRI is related to interneuronal correlations. Curr Biol 17, 1275-1285.

Olbrich, S., Mulert, C., Karch, S., Trenner, M., Leicht, G., Pogarell, O., Hegerl, U., 2009. EEG–vigilance and BOLD effect during simultaneous EEG/fMRI measurement. Neuroimage 45, 319-332.

Oldfield, R.C., 1971. The assessment and analysis of handedness: the Edinburgh inventory. Neuropsychologia 9, 97-113.

Paus, T., Keshavan, M., Giedd, J.N., 2008. Why do many psychiatric disorders emerge during adolescence? Nat Rev Neurosci 9, 947-957.

Puligheddu, M., de Munck, J.C., Stam, C.J., Verbunt, J., de Jongh, A., van Dijk, B.W., Marrosu, F., 2005. Age distribution of MEG spontaneous theta activity in healthy subjects. Brain Topogr 17, 165-175.

Raichle, M.E., 2006. Neuroscience. The brain's dark energy. Science 314, 1249-1250.

Raichle, M.E., MacLeod, A.M., Snyder, A.Z., Powers, W.J., Gusnard, D.A., Shulman, G.L., 2001. A default mode of brain function. Proc Natl Acad Sci U S A 98, 676-682.

Raichle, M.E., Snyder, A.Z., 2007. A default mode of brain function: a brief history of an evolving idea. Neuroimage 37, 1083-1090; discussion 1097-1089.

Rosa, M.J., Kilner, J., Blankenburg, F., Josephs, O., Penny, W., 2010. Estimating the transfer function from neuronal activity to BOLD using simultaneous EEG–fMRI. Neuroimage 49, 1496-1509.

Sadaghiani, S., Scheeringa, R., Lehongre, K., Morillon, B., Giraud, A.L., Kleinschmidt, A., 2010. Intrinsic connectivity networks, alpha oscillations, and tonic alertness: a simultaneous electroencephalography/functional magnetic resonance imaging study. J Neurosci 30, 10243-10250.

Sadato, N., Nakamura, S., Oohashi, T., Nishina, E., Fuwamoto, Y., Waki, A., Yonekura, Y., 1998. Neural networks for generation and suppression of alpha rhythm: a PET study. Neuroreport 9, 893-897.

Sarnthein, J., Morel, A., von Stein, A., Jeanmonod, D., 2003. Thalamic theta field potentials and EEG: high thalamocortical coherence in patients with neurogenic pain, epilepsy and movement disorders. Thalamus & Related Systems 2, 231-238.

Scheeringa, R., Bastiaansen, M.C., Petersson, K.M., Oostenveld, R., Norris, D.G., Hagoort, P., 2008. Frontal theta EEG activity correlates negatively with the default mode network in resting state. Int J Psychophysiol 67, 242-251.

Schreckenberger, M., Lange-Asschenfeldt, C., Lochmann, M., Mann, K., Siessmeier, T., Buchholz, H.G., Bartenstein, P., Grunder, G., 2004. The thalamus as the generator and modulator of EEG alpha rhythm: a combined PET/EEG study with lorazepam challenge in humans. Neuroimage 22, 637-644.

Seeley, W.W., Menon, V., Schatzberg, A.F., Keller, J., Glover, G.H., Kenna, H., Reiss, A.L., Greicius, M.D., 2007. Dissociable intrinsic connectivity networks for salience processing and executive control. J Neurosci 27, 2349-2356.

Slotnick, S.D., Moo, L.R., Segal, J.B., Hart, J., Jr., 2003. Distinct prefrontal cortex activity associated with item memory and source memory for visual shapes. Brain Res Cogn Brain Res 17, 75-82.

Smith, S.M., Fox, P.T., Miller, K.L., Glahn, D.C., Fox, P.M., Mackay, C.E., Filippini, N., Watkins, K.E., Toro, R., Laird, A.R., Beckmann, C.F., 2009. Correspondence of the brain's functional architecture during activation and rest. Proc Natl Acad Sci U S A 106, 13040-13045.

Somsen, R.J., van't Klooster, B.J., van der Molen, M.W., van Leeuwen, H.M., Licht, R., 1997. Growth spurts in brain maturation during middle childhood as indexed by EEG power spectra. Biol Psychol 44, 187-209.

Steriade, M., McCormick, D.A., Sejnowski, T.J., 1993. Thalamocortical Oscillations in the Sleeping and Aroused Brain. Science 262, 679-685.

Supekar, K., Musen, M., Menon, V., 2009. Development of large-scale functional brain networks in children. PLoS Biol 7, e1000157.

Taki, Y., Hashizume, H., Sassa, Y., Takeuchi, H., Wu, K., Asano, M., Asano, K., Fukuda, H., Kawashima, R., 2011. Correlation between gray matter density-adjusted brain perfusion and age using brain MR images of 202 healthy children. Hum Brain Mapp 32, 1973-1985.

Thatcher, R.W., 1994. Cyclic cortical reorganization: Origins of human cognitive development. In: Fischer, G.D.K.W. (Ed.), Human behavior and the developing brain. Guilford Press, New York, pp. 232-266.

Thomason, M.E., Chang, C.E., Glover, G.H., Gabrieli, J.D., Greicius, M.D., Gotlib, I.H., 2008. Default-mode function and task-induced deactivation have overlapping brain substrates in children. Neuroimage 41, 1493-1503.

Tsai, Y.T., Chan, H.L., Lee, S.T., Tu, P.H., Chang, B.L., Wu, T., 2010. Significant thalamocortical coherence of sleep spindle, theta, delta, and slow oscillations in NREM sleep: recordings from the human thalamus. Neurosci Lett 485, 173-177.

Tyvaert, L., Hawco, C., Kobayashi, E., LeVan, P., Dubeau, F., Gotman, J., 2008. Different structures involved during ictal and interictal epileptic activity in malformations of cortical development: an EEG–fMRI study. Brain 131, 2042-2060.

Van Dijk, K.R., Hedden, T., Venkataraman, A., Evans, K.C., Lazar, S.W., Buckner, R.L., 2010. Intrinsic functional connectivity as a tool for human connectomics: theory, properties, and optimization. J Neurophysiol 103, 297-321.

Wackermann, J., Matousek, M., 1998. From the 'EEG age' to a rational scale of brain electric maturation. Electroencephalogr Clin Neurophysiol 107, 415-421.

Whitford, T.J., Rennie, C.J., Grieve, S.M., Clark, C.R., Gordon, E., Williams, L.M., 2007. Brain maturation in adolescence: concurrent changes in neuroanatomy and neurophysiology. Hum Brain Mapp 28, 228-237.

Yang, H., Long, X.Y., Yang, Y., Yan, H., Zhu, C.Z., Zhou, X.P., Zang, Y.F., Gong, Q.Y., 2007. Amplitude of low frequency fluctuation within visual areas revealed by resting-state functional MRI. Neuroimage 36, 144-152.

Zang, Y.F., He, Y., Zhu, C.Z., Cao, Q.J., Sui, M.Q., Liang, M., Tian, L.X., Jiang, T.Z., Wang, Y.F., 2007. Altered baseline brain activity in children with ADHD revealed by resting-state functional MRI. Brain Dev 29, 83-91.

Zuo, X.N., Di Martino, A., Kelly, C., Shehzad, Z.E., Gee, D.G., Klein, D.F., Castellanos, F.X., Biswal, B.B., Milham, M.P., 2010. The oscillating brain: complex and reliable. Neuroimage 49, 1432-1445.

4.8 Supplementary material

Supplementary Table S1. Table of anatomic labels corresponding to ANOVA results (Fig. 2.2). Anatomic label corresponds to the peak voxel of the cluster. Maximally 3 peak voxels of a cluster are listed.

Cluste size	Peak F-value	MNI-coordinate (x, y, z)	Region (Brodmann Area)
Group			
90	10.5	(15, -84, 15)	r Cuneus (18)
Condition			
96	37.25	(-27, -9, -21)	l Amygdala
2628	31.96	(27, -12, 75)	r Superior Frontal G. (6)
	28.71	(12, -24, 81)	No lable
	27.13	(24, -24, 78)	r Precentral G. (6)
193	28.6	(24, -15, -24)	r Parahippocampal G. (28)
78	24.1	(15, -69, 39)	r Precuneus (7)
203	23.59	(-15, -45, -3)	l Lingual G. (19)
42	18.97	(-36, 54, 18)	l Superior Frontal G. (10)
128	18.7	(12, -51, -3)	r Culmen
	15.13	(12, -39, -6)	r Culmen
224	17.23	(39, -21, 15)	r Insula (13)
	16.9	(63, -18, 6)	r Superior Temporal G. (22)
	16.32	(39, -6, 12)	r Insula (13)
59	16.77	(0, -21, 24)	l Cingulate G. (23)
	14.95	(3, -33, 18)	r Posterior Cingulate (23)
27	15.34	(33, 51, 33)	r Superior Frontal G. (9)
Frequency			
29118	17.05	(18, -84, 3)	r Cuneus (17)
	17.01	(-21, -30, 69)	l Precentral G. (4)
	16.44	(9, 6, 48)	r Medial Frontal G. (32)
51	7.32	(24, -9, -27)	r Parahippocampal G. (35)
37	5.31	(-33, 57, 6)	l Middle Frontal G. (10)
Group x Frequency			
29	3.92	(57, -60, 6)	r Middle Temporal G. (39)
26	3.32	(-15, -66, 3)	l Lingual G. (19)
Condition x Frequency			
2453	9.23	(9, -30, 69)	r Medial Frontal G. (6)
	8.08	(-9, -21, 75)	l Superior Frontal G. (6)
	7.64	(-3, -27, 69)	l Medial Frontal G. (6)
86	8.16	(33, 18, 6)	r Claustrum
163	8.13	(33, 45, 36)	r Superior Frontal G. (9)
	5.21	(39, 51, 24)	r Middle Frontal G. (10)
138	6.96	(15, -6, 9)	r Thalamus
	5.02	(-12, -9, 9)	l Thalamus
	4.53	(0, -18, 6)	l Thalamus
685	6.68	(9, -78, 24)	r Cuneus (18)
	6.42	(-6, -99, 3)	l Cuneus (18)
	6.32	(18, -78, 30)	r Cuneus (7)
69	6.63	(0, 60, 30)	l Superior Frontal G. (9)
94	6.44	(60, -36, 42)	r Inferior Parietal L. (40)
	5.47	(57, -39, 54)	r Postcentral G. (40)
138	6.42	(-66, -33, 6)	l Superior Temporal G. (22)
	5.9	(-54, -39, 12)	l Superior Temporal G. (22)
101	5.94	(-51, 6, 3)	l Superior Temporal G. (22)
	5.72	(-33, 15, 6)	l Claustrum

table continues on next page

table continued from the previous page

Cluste size	**Peak F-value**	**MNI-coordinate (x, y, z)**	**Region (Brodmann Area)**
77	5.86	(-33, 42, 18)	l Middle Frontal G. (10)
	5.8	(-33, 48, 36)	l Superior Frontal G. (9)
98	5.86	(6, 18, 36)	r Cingulate G. (32)
	5.71	(6, 15, 45)	r Cingulate G. (32)
45	5.8	(12, -27, 39)	r Cingulate G. (31)
113	5.65	(66, -24, -3)	r Superior Temporal G. (21)
	5.23	(48, -27, 0)	r Superior Temporal G. (22)
	5.19	(63, -12, -6)	r Superior Temporal G. (21)
294	5.56	(-6, -51, 3)	l Posterior Cingulate (29)
	5.37	(-6, -48, 24)	l Posterior Cingulate (23)
	5.18	(18, -48, -6)	r Lingual G. (19)
99	5.53	(-18, -81, 30)	l Cuneus (7)
	4.57	(-24, -84, 15)	l Cuneus (18)
	4.5	(-21, -75, 21)	l Precuneus (31)
98	5.22	(-48, -63, 33)	l Angular G. (39)
	5.1	(-48, -54, 21)	l Supramarginal G. (40)
Group x Condition x Frequency			
28	3.57	(6, 57, -9)	r Medial Frontal G. (10)
	3.35	(6, 60, 3)	r Medial Frontal G.

Supplementary Table S2. Table of anatomic labels corresponding to group differences of EEG-BOLD coupling (Fig. 2.3B). The table is ordered by group difference, condition, frequency and contrast direction. Anatomic label corresponds to the peak voxel of the cluster. Maximally 3 peak voxels of a cluster are listed.

Cluste size	Peak T-value	MNI-coordinate (x, y, z)	Region (Brodmann Area)
		Children <> Adults	
Children < Adults EO Theta			
49	3.7	(-6, -84, 21)	l Cuneus (18)
Children > Adults EO Theta			
30	3.75	(45, 30, 45)	r Middle Frontal G. (8)
Children > Adults EO Beta2			
102	4.11	(-60, -54, 33)	l Supramarginal G. (40)
Children < Adults EC Alpha2			
31	3.55	(-6, -9, 3)	l Thalamus
Children > Adults EC Alpha2			
85	3.91	(-42, -12, 36)	l Precentral G. (6)
	3.81	(-51, -12, 39)	l Precentral G. (6)
114	3.82	(54, -9, 54)	r Precentral G. (6)
	3.81	(48, -9, 45)	r Precentral G. (6)
	3.29	(63, -3, 30)	r Precentral G. (6)
170	3.65	(-15, -66, 3)	l Lingual G. (19)
	3.65	(-21, -87, -3)	l Lingual G. (17)
	3.34	(-18, -87, 9)	l Cuneus (17)
Children < Adults EC Beta1			
107	4.36	(21, 15, 63)	r Superior Frontal G. (6)
57	3.98	(-15, 12, 57)	l Superior Frontal G. (6)
	3.68	(-21, 3, 54)	l Medial Frontal G. (6)
	3.16	(-30, 9, 60)	l Middle Frontal G. (6)
118	3.84	(9, -3, 3)	r Thalamus
	3.71	(-9, -6, 0)	l Thalamus
	3.69	(-12, 0, 9)	l Caudate Body
27	3.38	(-21, 9, -12)	l Lentiform Nucleus
	3.24	(-24, 6, -3)	l Lentiform Nucleus
Children > Adults EC Beta1			
43	3.79	(-42, -12, 33)	l Precentral G. (6)
Children > Adults EC Beta2			
50	4.08	(-57, -54, 45)	l Inferior Parietal L. (40)
	3.96	(-51, -57, 51)	l Inferior Parietal L. (40)
27	3.75	(48, 36, -12)	r Inferior Frontal G. (47)
	3.42	(51, 39, 0)	r Inferior Frontal G. (46)
27	3.51	(6, 36, 39)	r Medial Frontal G. (6)
		Children <> Adolescents	
Children < Adolescents EO Alpha2			
30	3.91	(-3, -45, 15)	l Posterior Cingulate (29)
Children > Adolescents EO Beta1			

table continues on next page

table continued from the previous page

Cluste size	Peak T-value	MNI-coordinate (x, y, z)	Region (Brodmann Area)
40	3.46	(-6, -84, -9)	l Lingual G. (18)
	3.36	(-18, -90, -6)	l Lingual G. (17)
Children > Adolescents EO Beta2			
60	3.9	(12, -84, -9)	r Lingual G. (18)
107	3.67	(-18, -90, -6)	l Lingual G. (17)
	3.63	(-30, -93, 0)	l Middle Occipital G. (18)
	3.39	(-15, -99, 15)	l Cuneus (18)
Children > Adolescents EC Alpha1			
101	4.22	(-45, -42, 12)	l Superior Temporal G. (41)
	3.37	(-48, -60, 9)	l Middle Temporal G. (39)
Children > Adolescents EC Alpha2			
1652	4.84	(-27, -93, -6)	l Inferior Occipital G. (18)
	4.74	(27, -93, 0)	r Middle Occipital G. (18)
	4.29	(24, -60, -3)	r Lingual G. (19)
565	4.69	(6, -27, 60)	r Medial Frontal G. (6)
	4.17	(-12, -33, 66)	l Precentral G. (4)
	3.91	(12, -33, 75)	r Precentral G. (4)
390	4.62	(-12, -51, -6)	l Culmen
	3.68	(-15, -69, -12)	l Lingual G. (18)
230	4.29	(-66, -30, 3)	l Superior Temporal G. (22)
	4.15	(-57, -39, 9)	l Superior Temporal G. (22)
	3.58	(-60, -9, -12)	l Middle Temporal G. (21)
224	4.19	(60, -18, -9)	r Middle Temporal G. (21)
	4.17	(51, -24, -9)	r Superior Temporal G. (21)
	3.73	(63, -6, -15)	r Middle Temporal G. (21)
180	4.07	(51, -9, 39)	r Precentral G. (6)
	3.8	(63, -6, 36)	r Precentral G. (6)
	3.71	(33, -15, 45)	r Middle Frontal G. (6)
89	3.9	(-54, -12, 36)	l Precentral G. (6)
	3.35	(-39, -21, 36)	l Precentral G. (4)
31	3.5	(-45, -60, 9)	l Middle Temporal G. (39)
	3.35	(-51, -66, 15)	l Middle Temporal G. (19)
Children < Adolescents EC Beta1			
41	3.72	(0, -6, 0)	l Thalamus
	3.5	(0, -18, 3)	l Thalamus
	3.24	(-9, -12, 12)	l Thalamus
Children > Adolescents EC Beta1			
737	4.56	(15, -84, 18)	r Cuneus (18)
	4.11	(27, -60, -3)	r Lingual G. (19)
	3.71	(18, -63, -15)	r Culmen
153	3.86	(-39, -21, 36)	l Precentral G. (4)
	3.79	(-54, -6, 21)	l Precentral G. (4)
	3.27	(-48, -21, 48)	l Postcentral G. (3)
108	3.83	(63, -6, 33)	r Precentral G. (6)
	3.76	(51, -12, 36)	r Precentral G. (6)
106	3.63	(-18, -54, -9)	l Parahippocampal G. (19)
	3.62	(-18, -66, -12)	l Lingual G. (19)
59	3.61	(51, -27, -12)	r Middle Temporal G. (21)
	3.57	(60, -27, -9)	r Middle Temporal G. (21)
	3.17	(60, -15, -12)	r Middle Temporal G. (21)
36	3.55	(45, -36, 3)	r Superior Temporal G. (41)
	3.47	(48, -42, 15)	r Insula (13)

table continues on next page

table continued from the previous page

Cluste size	Peak T-value	MNI-coordinate (x, y, z)	Region (Brodmann Area)
27	3.44	(-18, -66, 9)	l Posterior Cingulate (30)
	3.15	(-12, -72, 15)	l Cuneus (18)
Children < Adolescents EC Beta2			
84	4.12	(0, -3, 3)	l Thalamus
	3.63	(6, -30, 3)	r Thalamus
	3.59	(-3, -30, 6)	l Thalamus
Children > Adolescents EC Beta2			
193	4.64	(-57, -6, 21)	l Precentral G. (4)
	3.89	(-60, -9, 33)	l Precentral G. (6)
	3.73	(-39, -18, 36)	l Precentral G. (6)
1422	4.61	(-12, -48, -6)	l Culmen
	4.6	(24, -60, -3)	r Lingual G. (19)
	4.51	(12, -84, 15)	r Cuneus (18)
47	4.55	(45, -9, 63)	r Precentral G. (6)
	3.71	(33, -15, 72)	r Precentral G. (6)
583	4.43	(66, -15, 18)	r Postcentral G. (43)
	4.42	(51, 0, 18)	r Inferior Frontal G. (44)
	3.92	(54, -12, 21)	r Postcentral G. (43)
		Adolescents <> Adults	
Adolescents < Adults EO Delta			
32	3.86	(-45, 9, 54)	l Middle Frontal G. (6)
68	3.82	(-6, 63, 15)	l Medial Frontal G. (10)
	3.8	(-6, 63, 27)	l Superior Frontal G. (10)
46	3.69	(-42, -63, 48)	l Superior Parietal L. (7)
Adolescents > Adults EO Alpha1			
50	4.12	(42, -54, 45)	r Inferior Parietal L. (40)
	3.76	(39, -63, 60)	r Superior Parietal L. (7)
Adolescents < AdultsEO Beta1			
60	4.05	(21, -81, 12)	r Cuneus (17)
147	4.01	(15, -87, -9)	r Lingual G. (18)
	3.58	(33, -87, -9)	r Inferior Occipital G. (18)
	3.55	(33, -78, -15)	r Fusiform G. (19)
265	3.95	(-24, -93, 6)	l Middle Occipital G. (18)
	3.83	(-6, -84, -9)	l Lingual G. (18)
	3.82	(-18, -99, 12)	l Middle Occipital G. (18)
67	3.88	(27, -48, 72)	r Postcentral G. (5)
	3.75	(15, -42, 78)	No lable
29	3.7	(-24, -45, 75)	l Postcentral G. (5)
	3.57	(-30, -39, 63)	l Postcentral G. (3)
Adolescents < Adults EC Alpha2			
29	3.83	(-12, -42, -6)	l Culmen
Adolescents < Adults EC Beta1			
27	3.49	(9, -42, 60)	r Paracentral L. (5)
Adolescents < Adults EC Beta2			
53	3.86	(66, -15, 12)	r Transverse Temporal G. (42)
53	3.44	(3, -93, 15)	r Cuneus (18)

table continues on next page

table continued from the previous page

Cluste size	**Peak T-value**	**MNI-coordinate (x, y, z)**	**Region (Brodmann Area)**
	3.37	(9, -87, 15)	r Cuneus (18)

Supplementary Table S3. Table of anatomic labels corresponding to maturation-independent EEG-BOLD signal correlations (Fig. 2.4A and B). Table is ordered by condition, frequency and correlation sign. Anatomic label corresponds to the peak voxel of the cluster. Maximally 3 peak voxels of a cluster are listed.

Cluste size	Peak T-value	MNI-coordinate (x, y, z)	Region (Brodmann Area)
EO Delta positive			
471	4.76	(9, 6, 48)	r Medial Frontal G. (32)
	4.71	(3, 21, 30)	r Anterior Cingulate (24)
65	4.54	(0, -63, -15)	l Culmen
	3.81	(9, -57, -18)	r Declive
44	3.9	(39, 9, 12)	r Insula (13)
	3.23	(57, 3, 6)	r Superior Temporal G. (22)
26	3.61	(-54, -6, 15)	l Precentral G. (4)
	3.25	(-57, 0, 9)	l Precentral G. (6)
25	3.47	(51, -33, 24)	r Inferior Parietal L. (40)
EO Delta negative			
129	5.83	(-48, 42, -6)	l Inferior Frontal G. (47)
563	5.11	(-45, -51, 42)	l Inferior Parietal L. (40)
	4.15	(-24, -78, 48)	l Superior Parietal L. (7)
	3.79	(-30, -84, 36)	l Precuneus (19)
788	4.98	(27, -78, 54)	r Precuneus (7)
	4.95	(45, -57, 36)	r Inferior Parietal L. (40)
	4.21	(30, -84, 45)	r Precuneus (19)
415	4.56	(24, 24, 60)	r Superior Frontal G. (6)
	4.39	(48, 33, 21)	r Middle Frontal G. (46)
	4.34	(51, 24, 33)	r Middle Frontal G. (9)
139	4.32	(39, 42, -9)	r Middle Frontal G. (47)
	4.19	(48, 48, -3)	r Inferior Frontal G. (10)
	3.91	(42, 54, 0)	r Middle Frontal G. (10)
274	4.08	(-18, 27, 57)	l Superior Frontal G. (6)
	4.08	(-51, 24, 27)	l Middle Frontal G. (46)
	4.06	(-48, 15, 48)	l Middle Frontal G. (8)
EO Theta positive			
213	6.56	(-3, -63, -15)	l Culmen
	6.45	(6, -63, -15)	r Culmen
5378	6.09	(-36, -12, 24)	l Insula (13)
	5.96	(-54, -6, 15)	l Precentral G. (4)
	5.75	(12, 9, 45)	r Cingulate G. (32)
195	4.23	(18, -27, 81)	No lable
	4.01	(27, -21, 75)	r Precentral G. (6)
	3.92	(21, -15, 78)	r Superior Frontal G. (6)
49	4.08	(-24, -9, -18)	l Amygdala
139	4.04	(39, -54, 0)	r Temporal Lobe Sub-Gyral
	3.96	(36, -63, 3)	r Occipital Lobe Sub-Gyral
	3.8	(36, -36, -3)	r Caudate Tail
EO Theat negative			
2298	7.01	(-51, -60, 36)	l Supramarginal G. (40)
	6.2	(-3, -33, 39)	l Cingulate G. (31)
	5.98	(-42, -63, 54)	l Superior Parietal L. (7)
1639	5.68	(-45, 18, 48)	l Middle Frontal G. (8)
	5.59	(-24, 24, 60)	l Superior Frontal G. (8)
	5.41	(-30, 21, 54)	l Superior Frontal G. (8)
34	3.97	(48, 39, -9)	r Middle Frontal G. (47)
EO Alpha1 positive			

table continues on next page

table continued from the previous page

Cluste size	Peak T-value	MNI-coordinate (x, y, z)	Region (Brodmann Area)
45	5.13	(-27, -9, -21)	l Amygdala
61	4.49	(24, -12, -21)	r Parahippocampal G. (28)
EO Alpha1 negative			
2198	6.59	(-12, -81, 51)	l Precuneus (7)
	6.31	(15, -75, 48)	r Precuneus (7)
	5.92	(9, -69, 63)	r Precuneus (7)
101	5.5	(-60, -42, 36)	l Inferior Parietal L. (40)
309	4.57	(-39, 24, 0)	l Inferior Frontal G. (47)
	4.23	(-39, 45, 12)	l Middle Frontal G. (10)
	3.33	(-45, 9, 9)	l Precentral G. (44)
189	4.43	(9, -33, 45)	r Paracentral L. (31)
	3.56	(6, -36, 21)	r Posterior Cingulate (23)
	3.5	(-6, -33, 42)	l Cingulate G. (31)
247	4.35	(9, -87, 6)	r Cuneus (17)
	4.17	(18, -75, -12)	r Lingual G. (18)
	3.82	(-6, -96, 0)	l Cuneus (17)
36	3.79	(-48, 30, 33)	l Middle Frontal G. (9)
	3.33	(-33, 48, 36)	l Superior Frontal G. (9)
72	3.71	(51, 42, 9)	r Inferior Frontal G. (46)
	3.65	(45, 51, -3)	r Middle Frontal G. (10)
45	3.66	(48, 15, 9)	r Precentral G. (44)
	3.25	(33, 18, 6)	r Claustrum
63	3.64	(-57, -60, 3)	l Middle Temporal G. (21)
	3.63	(-48, -69, -6)	l Inferior Temporal G. (37)
28	3.6	(-33, -51, 48)	l Superior Parietal L. (7)
EO Alpha2 negative			
3404	7.18	(12, -78, 48)	r Precuneus (7)
	6.09	(-9, -81, 51)	l Precuneus (7)
	5.98	(27, -87, 30)	r Cuneus (19)
902	6.17	(33, 48, 36)	r Superior Frontal G. (9)
	5.64	(39, 54, 24)	r Middle Frontal G. (10)
	5.14	(30, 21, 6)	r Claustrum
442	5.73	(57, -39, 42)	r Inferior Parietal L. (40)
	5.04	(51, -42, 60)	r Inferior Parietal L. (40)
413	5.36	(-33, 48, 36)	l Superior Frontal G. (9)
	5.36	(-36, 51, 21)	l Middle Frontal G. (10)
	3.68	(-51, 24, 36)	l Middle Frontal G. (9)
183	5.09	(45, 6, 51)	r Middle Frontal G. (6)
250	5.08	(12, -33, 45)	r Cingulate G. (31)
	3.72	(-6, -18, 33)	l Cingulate G. (23)
294	4.64	(-42, 12, 12)	l Insula (13)
	4.43	(-33, 18, 3)	l Claustrum
	3.79	(-30, 27, 6)	l Inferior Frontal G. (45)
75	4.31	(-63, -42, 30)	l Inferior Parietal L. (40)
	4.27	(-54, -39, 45)	l Inferior Parietal L. (40)
133	4.06	(6, 18, 51)	r Medial Frontal G. (8)
	4.04	(6, 18, 33)	r Cingulate G. (24)
EO Beat1 negative			
8742	8.46	(-21, -75, 45)	l Precuneus (7)
	7.92	(30, -72, 36)	r Precuneus (19)
	7.86	(30, -60, 51)	r Superior Parietal L. (7)
2317	7.76	(-51, 18, 36)	l Middle Frontal G. (9)
	6.1	(-45, 45, 0)	l Inferior Frontal G. (10)
	5.84	(-30, 6, 54)	l Middle Frontal G. (6)

table continues on next page

table continued from the previous page

Cluste size	Peak T-value	MNI-coordinate (x, y, z)	Region (Brodmann Area)
1858	6.3	(30, 12, 63)	r Middle Frontal G. (6)
	5.9	(51, 39, 18)	r Middle Frontal G. (46)
	5.79	(51, 21, 36)	r Middle Frontal G. (9)
25	3.95	(18, -30, 0)	r Thalamus
EO Beat2 negative			
455	5.49	(-15, -69, 39)	l Precuneus (7)
	3.6	(-30, -78, 27)	l Superior Occipital G. (39)
	3.43	(-30, -90, 21)	l Cuneus (19)
930	5.24	(15, -72, 45)	r Precuneus (7)
	4.64	(33, -84, 21)	r Middle Occipital G. (19)
	4.56	(30, -63, 36)	r Angular G. (39)
203	4.25	(6, -87, 3)	r Cuneus (17)
	3.39	(12, -102, 9)	r Cuneus (18)
323	4.21	(6, -36, 24)	r Posterior Cingulate (23)
	4.12	(-6, -27, 27)	l Cingulate G. (23)
	3.9	(9, -24, 27)	r Cingulate G. (23)
52	3.85	(-45, 33, 36)	l Middle Frontal G. (9)
	3.25	(-51, 18, 36)	l Middle Frontal G. (9)
48	3.59	(-33, -51, 45)	l Inferior Parietal L. (40)
EC Delta positive			
395	5.25	(3, 18, 33)	r Cingulate G. (32)
	4.78	(9, 6, 39)	r Cingulate G. (24)
	4.24	(-18, 12, 27)	l Caudate Body
212	4.71	(0, 0, 0)	r Anterior Cingulate (25)
	3.56	(12, -6, 9)	r Thalamus
	3.45	(-6, -9, 15)	l Thalamus
43	4.25	(-36, 9, 9)	l Insula (13)
66	3.97	(33, 12, 6)	r Claustrum
	3.3	(27, 30, 9)	r Insula (45)
35	3.83	(6, -27, -18)	r Midbrain
	3.37	(-3, -27, -21)	l Midbrain
40	3.82	(-21, 42, -6)	l Anterior Cingulate (32)
	3.27	(-24, 30, 9)	l Claustrum
EC Delta negative			
74	3.83	(42, -33, 42)	r Inferior Parietal L. (40)
	3.13	(51, -21, 45)	r Postcentral G. (3)
45	3.74	(36, -48, 66)	r Postcentral G. (5)
	3.67	(30, -54, 69)	r Superior Parietal L. (7)
81	3.68	(-30, -36, 45)	l Postcentral G. (3)
	3.47	(-39, -39, 54)	l Inferior Parietal L. (40)
	3.23	(-36, -30, 39)	l Postcentral G. (2)
56	3.67	(6, -27, 63)	r Medial Frontal G. (6)
	3.52	(9, -24, 75)	r Medial Frontal G. (6)
EC Theta positive			
3621	5.73	(-21, -27, 66)	l Precentral G. (4)
	5.72	(21, -24, 63)	r Precentral G. (4)
	5.46	(-33, -21, 72)	l Precentral G. (6)
87	4.39	(24, -99, 3)	r Middle Occipital G. (18)
	3.51	(21, -99, 18)	r Cuneus (19)
61	4.32	(-30, -72, 9)	l Posterior Cingulate (30)
77	4.29	(15, -57, -18)	r Declive
	3.77	(6, -66, -12)	r Culmen
	3.49	(-3, -66, -12)	l Culmen of Vermis

table continues on next page

table continued from the previous page

Cluste size	Peak T-value	MNI-coordinate (x, y, z)	Region (Brodmann Area)
112	4.25	(-21, 24, 18)	l Caudate Body
	3.81	(-21, 33, 6)	l Frontal Lobe Sub-Gyral
	3.79	(-24, 39, -3)	l Middle Frontal G. (11)
139	3.91	(-12, -99, 24)	l Cuneus (19)
	3.65	(-15, -99, 12)	l Middle Occipital G. (18)
39	3.78	(33, -72, 9)	r Temporal Lobe Sub-Gyral
EC Theat negative			
118	4.47	(45, 18, 42)	r Precentral G. (9)
258	4.46	(-51, -51, 45)	l Inferior Parietal L. (40)
	4.29	(-39, -60, 60)	l Superior Parietal L. (7)
	3.86	(-27, -81, 48)	l Superior Parietal L. (7)
276	4.33	(12, 30, 63)	r Superior Frontal G. (6)
	4.2	(24, 24, 57)	r Superior Frontal G. (8)
	3.91	(0, 33, 45)	l Medial Frontal G. (8)
112	4.21	(-45, 18, 45)	l Middle Frontal G. (8)
	3.81	(-27, 24, 57)	l Superior Frontal G. (8)
25	4.1	(-60, -57, -6)	l Inferior Temporal G. (37)
	3.39	(-60, -45, -9)	l Middle Temporal G. (21)
68	3.77	(54, -51, 45)	r Inferior Parietal L. (40)
	3.59	(57, -48, 36)	r Supramarginal G. (40)
28	3.48	(39, -66, 57)	r Superior Parietal L. (7)
EC Alpha1 positive			
30	3.59	(-24, -39, 21)	l Caudate Tail
EC Alpha1 negative			
932	5.34	(-3, -72, 57)	l Superior Parietal L. (7)
	5.31	(-6, -54, 72)	l Postcentral G. (7)
	4.78	(9, -75, 57)	r Superior Parietal L. (7)
103	4.83	(-42, -48, 63)	l Postcentral G. (5)
83	4.01	(42, -78, 30)	r Angular G. (39)
41	3.98	(15, -33, -6)	r Parahippocampal G. (30)
52	3.89	(57, -54, 9)	r Superior Temporal G. (22)
	3.19	(63, -57, -3)	r Middle Temporal G. (21)
38	3.73	(42, -45, 57)	r Inferior Parietal L. (40)
34	3.64	(-48, 27, 15)	l Inferior Frontal G. (46)
EC Alpha2 positive			
334	6.96	(0, -6, 3)	l Thalamus
EC Alpha2 negative			
19832	7.23	(24, -75, 27)	r Precuneus (31)
	7.22	(15, -78, 21)	r Cuneus (18)
	6.82	(21, -45, -6)	r Parahippocampal G. (19)
150	4.27	(57, 30, 12)	r Inferior Frontal G. (46)
EC Beta1 positive			
412	6.64	(0, -6, 3)	l Thalamus
	4.72	(12, -9, 12)	r Thalamus
	3.58	(-27, -12, 27)	l Extra-Nuclear
62	4.74	(-24, -45, 24)	l Cingulate G. (31)
EC Beat1 negative			
23338	8.18	(-39, -42, 60)	l Postcentral G. (2)
	7.41	(-21, -78, 48)	l Precuneus (7)
	7.19	(39, -33, 42)	r Inferior Parietal L. (40)

table continues on next page

table continued from the previous page

Cluste size	**Peak T-value**	**MNI-coordinate (x, y, z)**	**Region (Brodmann Area)**
38	3.93	(-12, 63, 9)	l Medial Frontal G. (10)
28	3.88	(-33, 0, -24)	l Amygdala
46	3.73	(12, 66, 15)	r Medial Frontal G. (10)
EC Beta2 positive			
558	6.19	(-3, -6, 0)	l Thalamus
	5.47	(-12, -12, 12)	l Thalamus
	5.45	(0, -18, 6)	l Thalamus
EC Beta2 negative			
17534	6.86	(6, -33, 63)	r Paracentral L. (6)
	6.82	(27, -12, 72)	r Superior Frontal G. (6)
	6.66	(21, -75, 27)	r Precuneus (31)
48	4.14	(27, -12, -30)	r Parahippocampal G. (35)
	4.12	(24, 0, -30)	r Amygdala
28	3.48	(-21, -30, -9)	l Parahippocampal G. (27)
	3.37	(-30, -18, -21)	l Hippocampus
	3.34	(-21, -21, -15)	l Parahippocampal G. (35)

5 General Discussion

Adolescence, the transition from childhood to adulthood is a critical maturational stage as has been noted across cultures and centuries (Paus et al., 2008; Walker, 2002). It marks the transition from dependence on a caregiver to being a self-sufficient member of society, involving the development of cognitive, emotional and social competences. It is also a period characterized by risk-taking behavior, substance abuse and delinquency (Casey et al., 2005; Casey et al., 2008) and increasing incidence of several classes of psychiatric illness, including anxiety and mood disorders, psychosis, eating disorders and personality disorders (Paus et al., 2008). Many major neuropsychiatrc disorders are thought to arise out of deviations from normal brain development, suggesting a neurodevelopmental basis for these disorders (Gogtay and Thompson, 2010).

Much has been written about structural changes in the adolescent brain such as the trajectory of the major brain compartments, white matter and gray matter, as reviewed in the introduction section. Also functional aspects of neuronal maturation were reviewed such as changes in electrophysiology, hemodynamics and metabolism. In this thesis we focused on EEG and fMRI-BOLD signal changes, two methods that dominate the field of non-invasive, functional human neuroscience. We made use of the recent advantages to simultaneously record EEG and fMRI, which allows to study the functional coupling of the two signals (Mulert and Lemieux, 2010). EEG and BOLD signal represent complementary aspects of neuronal activity and their coupling reflects a distinct feature of brain function (Laufs, 2008). So far, the EEG–BOLD signal coupling has not been investigated in the developmental context, hence promised new insights and potentially novel markers of brain maturation. Specifically we focused on the major maturational phenomenon, the age related decrease of low frequency EEG power (Clarke et al., 2001; Gasser et al., 1988; Gibbs and Knott, 1949; Gmehlin et al., 2010; Matousek and Petersen, 1973; Matsuura et al., 1985). This effect is not only a robust major outcome of decades of neurodevelopmental research, it has also been related to structural brain development (Buchmann et al., 2010; Feinberg and Campbell, 2010; Whitford et al., 2007) and cognitive maturation (Case, 1992; John et al., 1980; Thatcher, 1994; Wackermann and Matousek, 1998). The study of functional correlates of the EEG power is promising as EEG power has been shown to be frequency specific coupled to distinct and meaningful fMRI brain networks (Goldman et al., 2002; Laufs, 2008; Mantini et al., 2007).

5.1 EEG–BOLD correlations during (post-)adolescent brain maturation

The first study focused on late brain maturation or post-adolescent maturation between the age of 15 and 25 years. The study aimed to capture brain maturation at a specifically late stage, which is usually neglected as a maturational step for its own. Most research focus on earlier maturation when the developmental effects are strongest. Even when post-adolescent age ranges are included, the linear and curvilinear regression slopes are mainly driven by the younger subjects and relatively insensitive to changes in specific, short periods (Lüchinger et al., 2011). The more subtle, later changes are obscured unless studied in a smaller age range confined to the specific post-adolescent transition. An early publication of the data was desirable as the approach of characterizing brain maturation by EEG–BOLD signal coupling was novel.

The main result of the study was that the EEG–BOLD signal did not differ between adolescents and adults, although EEG power decrease continued beyond mid-adolescence. This result suggested that the EEG–BOLD signal coupling is largely independent from the EEG amplitudes and that the basic EEG–BOLD signal coupling pattern reflect a distinct aspect of resting brain activity that is established before EEG oscillations reach full maturity. To clarify at which developmental stage the mature pattern of EEG–BOLD coupling emerges younger subjects were included in the subsequent study.

Apart from the developmental aspect, the first study also contributes to the knowledge of resting EEG–BOLD signal coupling. (i) This was the first study to demonstrate the major pattern of EEG–BOLD coupling (default mode network, attention network and thalamocortical network) within a single measurement. This was achieved by the eyes-open / eyes-closed design and the parallel analysis of six major EEG frequency bands. (ii) The EEG–BOLD coupling patterns were robust as the independent groups of adults and adolescents showed very similar patterns across conditions and frequencies. Further, the results were robust in terms of statistical significance, allowing to report the random-effects statistics at a conservative threshold ($p < 0.001$) in addition to rigorous control for multiple comparisons using the family-wise-error approach. This robustness was surprising as EEG–BOLD correlations pattern were reported somewhat inconsistent (iii) The comparison between separate frequency band correlations and the partial correlations (common model analysis) allowed to directly compare the different approaches. This issue has been debated in the field (de Munck et al., 2009; Kilner et al., 2005; Rosa et al., 2010). (iv) The EEG–BOLD coupling patterns reported here, reflected global EEG activity (global spectral power, GSP) rather than local components (e.g. posterior alpha, frontal midline theta) which were commonly used in previous studies. The implementation of global activity was motivated by the global topography of EEG maturation. Our results suggest that the EEG coupling to DMN, attention- and thalamocortical network is well reflected in diffuse, global distributed EEG activity and not only restricted in local components. The additional correlation analyses with frontal midline theta/delta, posterior alpha and central beta traces revealed no substantial change in coupling patterns. (v) The use of two different resting state conditions (EO

and EC) allowed not only a comprehensive covering of previously reported EEG–BOLD signal coupling patterns but aimed to test the existence of different resting states. While EO and EC conditions were not compared explicitly by statistical tests, the distinct coupling patterns between the two conditions suggests that there is not a simple answer to the "search of a baseline of brain activity" (Gusnard and Raichle, 2001), a quest that gained much interest in the last decade in the imaging community (Biswal et al., 2010). It also indicates that such a simple thing like opening /closing the eyes affects brain state regulation much more profoundly that one would possibly expect. Worth mentioning, the EEG–BOLD coupling reported here reflects the maintenance of resting state (the EO/EC blocks lasted 2.5 min) and not shorter intervals (e.g. 20s) applied in other studies mainly to induce alpha blocking. (vi) EEG–BOLD signal coupling has only been studied in healthy adults so far, but has not been used to compare other conditions such as pathology, immaturity, aging, sleep, sedation and so on. This study is the first to use EEG–BOLD signal coupling as distinct aspect of brain function to describe deviations from healthy, mature brain function.

In summary, these finding demonstrated the usefulness of the study design and analyses in general and were retained in the subsequent study. However, besides the inclusion of younger participants, another important extension was applied in the succeeding study. EEG power reflects baseline activity in absolute terms. In contrast, the fMRI-BOLD signal is a relative measure that needs to be contrasted to a baseline (Friston et al., 1996; Morcom and Fletcher, 2007). In this first study, maturation effects in the BOLD signal (independent from EEG) were approximated using classical fMRI condition subtracting (EO <> EC). However, the difference between EO and EC condition is very different from baseline activity as it is reflected by EEG power. Hence, it remained elusive how the baseline resting state BOLD signal activity develops. Therefore, the subsequent study omitted classical fMRI method and instead applied spectral power analysis of the BOLD signal (Zang et al., 2007; Zou et al., 2008) in direct analogy to EEG power.

5.2 EEG–BOLD coupling and normalized BOLD power indicate maturational changes in thalamocortical functioning

The decrease of EEG oscillatory activity is most prominent early in the course of brain development. Therefore, the EEG–BOLD signal coupling in children (10 years) promised to reveal maturational change that was not identified in the first approach in adolescents (15 years). However, such a direct substrate was not identified in the second study. The EEG–BOLD signal coupling did not differ in frequency-, condition- or topographic-specific correspondence to the maturational, mainly low frequency EEG power reduction, neither between adults and adolescents nor between adolescents and children. This result corroborated the former conclusion that the EEG–BOLD coupling is largely independent from the EEG's oscillatory amplitude. The basic EEG–BOLD coupling patterns are

established at the age of 10 years while the EEG pattern matures up into young adulthood. Nevertheless, a maturational change in the EEG–BOLD signal coupling was identified. The eyes-closed high frequency (10 - 30 Hz) thalamocortical network – the hallmark resting state coupling pattern – was not evident in children. Our results indicated that this pattern matures between childhood and adolescence. This change in the EEG–BOLD coupling was not directly related to the maturational EEG power reduction. It was in restricted to one condition (EC) and to higher frequencies while EEG maturation was state-independent (EO and EC) and pronounced in low frequencies. The thalamocortical coupling pattern demonstrates that frequency-specific EEG synchronization co-varies with thalamic activity (positive correlations) and with the deactivation of primary sensory areas (negative correlations). Most likely this coupling directly shows the arousal regulation of the thalamus and the thalamocortical circuits (Feige et al., 2005; Goldman et al., 2002; Moosmann et al., 2003). The thalamus innervates large portions of the cortex and regulates the brain state by means of arousal, vigilance and alertness (Llinas and Steriade, 2006). This role of the thalamocortical activity matches the functional connotation of the alpha EEG oscillation which elicited this coupling pattern as alpha indicates an idling state of the brain and the transient synchronization and desynchronization indicate shifts in arousal (Barry et al., 2009; Barry et al., 2007). The thalamocortical coupling pattern was evident in adults and adolescents but not in children, suggesting that a certain aspect of thalamocortical function and arousal regulation is in an immature state in children and reaches maturity during adolescence.

Converging evidence for thalamic maturation was revealed by normalized BOLD signal power. Relative to the global BOLD signal fluctuations, the thalamic activity fluctuations continuously increased with age. Possibly this neuronal maturation refers to behavioral and cognitive maturation. Children differ to adults in the ability to maintain prolonged mental focus and are more prone to sensory and motor distraction. These abilities may be associated with the thalamic and thalamocortical involvement in arousal regulation. Taken together, the EEG–BOLD signal coupling did not reveal a direct functional substrate of the maturational low frequency EEG power decrease but yielded an immature thalamocortical coupling pattern in children that suggest the maturation of brain state regulatory mechanisms.

5.3 Absolute amplitudes of BOLD signal fluctuations feature a novel marker of brain maturation

As an extension to the first study, we compared EEG maturation to BOLD signal maturation in terms of absolute amplitudes. This appeared as the most logical and direct approach in terms of equivalent measures but has not been done before. The spontaneous fluctuating BOLD signal reflects the energy demand of the brain at rest (Raichle, 2006) and this activity was averaged within the low frequency range (0.01 - 0.08 Hz) (Biswal et al., 1995; Yang et al., 2007) which is believed to mainly reflect neuronal activity (Cordes et al., 2001). We found the resting BOLD signal amplitudes to decrease as a curvilinear function of age in almost all brain regions. This finding marked the discovery of a novel

marker for brain maturation and reflected a direct correspondence to the maturational EEG power decrease. Moreover the activity attenuation of BOLD signal fluctuations is in line with other markers of brain maturation which show similar decreasing trajectories. We supposed that the reduction of gray matter and synaptic density during adolescence does not only lead to reduced metabolic demand and oscillatory scalp amplitudes as suggested before (Boord et al., 2007; Feinberg and Campbell, 2010; Feinberg et al., 1990), but also to decreased amplitudes of spontaneous fluctuating BOLD signal. Moreover, the BOLD power maturation paralleled the aforementioned neurophysiological indicators not only temporally but also spatially as it appeared as a global phenomenon, affecting the entire brain. This is also the case for gray matter loss, glucose metabolism and – as indicated by our results – EEG power maturation.

5.4 Conclusion

This thesis presents novel approaches to study non-invasively functional human brain maturation. Resting state EEG–BOLD signal coupling, resulting from simultaneous EEG–fMRI recordings, revealed the cortical and subcortical functional correlates of scalp oscillatory activity, namely the coupling to major resting state networks. EEG–BOLD signal coupling reflects a distinct aspect of resting brain activity and was used the first time to study brain activity deviant from the healthy, adult state. Also to the first time, the spontaneous fluctuating fMRI-BOLD signal was calculated in terms of absolute spectral power to study brain maturation.

EEG power decreased strongly between late childhood and early adulthood indicating a functional reorganization in the developing brain. This maturational electrophysiological reorganization was not accompanied by corresponding changes in the temporally co-activated fMRI-BOLD signal. Nevertheless, EEG–BOLD coupling indicated maturation of a thalamocortical network in state-dependent higher frequencies. This was identified as a potential neuronal substrate of EEG power maturation as thalamocortical activity is well known to generate low frequency scalp activity. A direct correspondence to EEG power maturation was identified in BOLD power as the two neuronal measures showed parallel non-linearly decreasing trajectories with age, consistent with structural and metabolic trajectories of brain maturation.

By identifying these markers of brain maturation, this thesis added novel and significant findings to the existing literature. These findings provide a fruitful ground for future research towards a better understanding of brain maturation. A good understanding of healthy brain development is the basis to identify lags and deviations from the normal maturational trajectories. Diagnostic tools and clinical applications may arise from such research.

5.5 References

Barry, R.J., Clarke, A.R., Johnstone, S.J., Brown, C.R., 2009. EEG differences in children between eyes-closed and eyes-open resting conditions. Clin Neurophysiol 120, 1806-1811.

Barry, R.J., Clarke, A.R., Johnstone, S.J., Magee, C.A., Rushby, J.A., 2007. EEG differences between eyes-closed and eyes-open resting conditions. Clin Neurophysiol 118, 2765-2773.

Biswal, B., Yetkin, F.Z., Haughton, V.M., Hyde, J.S., 1995. Functional connectivity in the motor cortex of resting human brain using echo-planar MRI. Magn Reson Med 34, 537-541.

Biswal, B.B., Mennes, M., Zuo, X.N., Gohel, S., Kelly, C., Smith, S.M., Beckmann, C.F., Adelstein, J.S., Buckner, R.L., Colcombe, S., Dogonowski, A.M., Ernst, M., Fair, D., Hampson, M., Hoptman, M.J., Hyde, J.S., Kiviniemi, V.J., Kotter, R., Li, S.J., Lin, C.P., Lowe, M.J., Mackay, C., Madden, D.J., Madsen, K.H., Margulies, D.S., Mayberg, H.S., McMahon, K., Monk, C.S., Mostofsky, S.H., Nagel, B.J., Pekar, J.J., Peltier, S.J., Petersen, S.E., Riedl, V., Rombouts, S.A., Rypma, B., Schlaggar, B.L., Schmidt, S., Seidler, R.D., Siegle, G.J., Sorg, C., Teng, G.J., Veijola, J., Villringer, A., Walter, M., Wang, L., Weng, X.C., Whitfield-Gabrieli, S., Williamson, P., Windischberger, C., Zang, Y.F., Zhang, H.Y., Castellanos, F.X., Milham, M.P., 2010. Toward discovery science of human brain function. Proc Natl Acad Sci U S A 107, 4734-4739.

Boord, P.R., Rennie, C.J., Williams, L.M., 2007. Integrating "brain" and "body" measures: correlations between EEG and metabolic changes over the human lifespan. J Integr Neurosci 6, 205-218.

Buchmann, A., Ringli, M., Kurth, S., Schaerer, M., Geiger, A., Jenni, O.G., Huber, R., 2010. EEG sleep slow-wave activity as a mirror of cortical maturation. Cereb Cortex 21, 607-615.

Case, R., 1992. The role of the frontal lobes in the regulation of cognitive development. Brain Cogn 20, 51-73.

Casey, B.J., Galvan, A., Hare, T.A., 2005. Changes in cerebral functional organization during cognitive development. Curr Opin Neurobiol 15, 239-244.

Casey, B.J., Getz, S., Galvan, A., 2008. The adolescent brain. Dev Rev 28, 62-77.

Clarke, A.R., Barry, R.J., McCarthy, R., Selikowitz, M., 2001. Age and sex effects in the EEG: development of the normal child. Clin Neurophysiol 112, 806-814.

Cordes, D., Haughton, V.M., Arfanakis, K., Carew, J.D., Turski, P.A., Moritz, C.H., Quigley, M.A., Meyerand, M.E., 2001. Frequencies contributing to functional connectivity in the cerebral cortex in "resting-state" data. AJNR Am J Neuroradiol 22, 1326-1333.

de Munck, J.C., Goncalves, S.I., Mammoliti, R., Heethaar, R.M., Lopes da Silva, F.H., 2009. Interactions between different EEG frequency bands and their effect on alpha-fMRI correlations. Neuroimage 47, 69-76.

Feige, B., Scheffler, K., Esposito, F., Di Salle, F., Hennig, J., Seifritz, E., 2005. Cortical and subcortical correlates of electroencephalographic alpha rhythm modulation. J Neurophysiol 93, 2864-2872.

Feinberg, I., Campbell, I.G., 2010. Sleep EEG changes during adolescence: an index of a fundamental brain reorganization. Brain Cogn 72, 56-65.

Feinberg, I., Thode, H.C., Jr., Chugani, H.T., March, J.D., 1990. Gamma distribution model describes maturational curves for delta wave amplitude, cortical metabolic rate and synaptic density. J Theor Biol 142, 149-161.

Friston, K.J., Price, C.J., Fletcher, P., Moore, C., Frackowiak, R.S., Dolan, R.J., 1996. The trouble with cognitive subtraction. Neuroimage 4, 97-104.

Gasser, T., Verleger, R., Bacher, P., Sroka, L., 1988. Development of the EEG of school-age children and adolescents. I. Analysis of band power. Electroencephalogr Clin Neurophysiol 69, 91-99.

Gibbs, F.A., Knott, J.R., 1949. Growth of the electrical activity of the cortex. Electroencephalogr Clin Neurophysiol 1, 223-229.

Gmehlin, D., Thomas, C., Weisbrod, M., Walther, S., Pfuller, U., Resch, F., Oelkers-Ax, R., 2010. Individual analysis of EEG background-activity within school age: impact of age and sex within a longitudinal data set. Int J Dev Neurosci.

Gogtay, N., Thompson, P.M., 2010. Mapping gray matter development: implications for typical development and vulnerability to psychopathology. Brain Cogn 72, 6-15.

Goldman, R.I., Stern, J.M., Engel, J., Jr., Cohen, M.S., 2002. Simultaneous EEG and fMRI of the alpha rhythm. Neuroreport 13, 2487-2492.

Gusnard, D.A., Raichle, M.E., 2001. Searching for a baseline: functional imaging and the resting human brain. Nat Rev Neurosci 2, 685-694.

John, E.R., Ahn, H., Prichep, L., Trepetin, M., Brown, D., Kaye, H., 1980. Developmental equations for the electroencephalogram. Science 210, 1255-1258.

Kilner, J.M., Mattout, J., Henson, R., Friston, K.J., 2005. Hemodynamic correlates of EEG: a heuristic. Neuroimage 28, 280-286.

Laufs, H., 2008. Endogenous brain oscillations and related networks detected by surface EEG-combined fMRI. Hum Brain Mapp 29, 762-769.

Llinas, R.R., Steriade, M., 2006. Bursting of thalamic neurons and states of vigilance. J Neurophysiol 95, 3297-3308.

Lüchinger, R., Michels, L., Martin, E., Brandeis, D., 2011. EEG–BOLD correlations during (post-)adolescent brain maturation. Neuroimage 56, 1493-1505.

Mantini, D., Perrucci, M.G., Del Gratta, C., Romani, G.L., Corbetta, M., 2007. Electrophysiological signatures of

resting state networks in the human brain. Proc Natl Acad Sci U S A 104, 13170-13175.
Matousek, M., Petersen, I., 1973. Automatic evaluation of EEG background activity by means of age-dependent EEG quotients. Electroencephalogr Clin Neurophysiol 35, 603-612.
Matsuura, M., Yamamoto, K., Fukuzawa, H., Okubo, Y., Uesugi, H., Moriiwa, M., Kojima, T., Shimazono, Y., 1985. Age development and sex differences of various EEG elements in healthy children and adults–quantification by a computerized wave form recognition method. Electroencephalogr Clin Neurophysiol 60, 394-406.
Moosmann, M., Ritter, P., Krastel, I., Brink, A., Thees, S., Blankenburg, F., Taskin, B., Obrig, H., Villringer, A., 2003. Correlates of alpha rhythm in functional magnetic resonance imaging and near infrared spectroscopy. Neuroimage 20, 145-158.
Morcom, A.M., Fletcher, P.C., 2007. Does the brain have a baseline? Why we should be resisting a rest. Neuroimage 37, 1073-1082.
Mulert, C., Lemieux, L., 2010. EEG–fMRI. Physiological Basis, Technique, and Applications. Springer, Berlin Heidelberg.
Paus, T., Keshavan, M., Giedd, J.N., 2008. Why do many psychiatric disorders emerge during adolescence? Nat Rev Neurosci 9, 947-957.
Raichle, M.E., 2006. Neuroscience. The brain's dark energy. Science 314, 1249-1250.
Rosa, M.J., Kilner, J., Blankenburg, F., Josephs, O., Penny, W., 2010. Estimating the transfer function from neuronal activity to BOLD using simultaneous EEG–fMRI. Neuroimage 49, 1496-1509.
Thatcher, R.W., 1994. Cyclic cortical reorganization: Origins of human cognitive development. In: Fischer, G.D.K.W. (Ed.), Human behavior and the developing brain. Guilford Press, New York, pp. 232-266.
Wackermann, J., Matousek, M., 1998. From the 'EEG age' to a rational scale of brain electric maturation. Electroencephalogr Clin Neurophysiol 107, 415-421.
Walker, E.F., 2002. Adolescent Neurodevelopment and Psychopathology. Current Directions in Psychological Science 11, 24-28.
Whitford, T.J., Rennie, C.J., Grieve, S.M., Clark, C.R., Gordon, E., Williams, L.M., 2007. Brain maturation in adolescence: concurrent changes in neuroanatomy and neurophysiology. Hum Brain Mapp 28, 228-237.
Yang, H., Long, X.Y., Yang, Y., Yan, H., Zhu, C.Z., Zhou, X.P., Zang, Y.F., Gong, Q.Y., 2007. Amplitude of low frequency fluctuation within visual areas revealed by resting-state functional MRI. Neuroimage 36, 144-152.
Zang, Y.F., He, Y., Zhu, C.Z., Cao, Q.J., Sui, M.Q., Liang, M., Tian, L.X., Jiang, T.Z., Wang, Y.F., 2007. Altered baseline brain activity in children with ADHD revealed by resting-state functional MRI. Brain Dev 29, 83-91.
Zou, Q.H., Zhu, C.Z., Yang, Y., Zuo, X.N., Long, X.Y., Cao, Q.J., Wang, Y.F., Zang, Y.F., 2008. An improved approach to detection of amplitude of low-frequency fluctuation (ALFF) for resting-state fMRI: fractional ALFF. J Neurosci Methods 172, 137-141.

6 Acknowledgement

I thank Prof. Daniel Brandeis for the appointment as PhD student in the ZIHP project "Thalamocortical interaction in brain state regulation during normal development and in epilepsy" and the opportunity to accomplish this PhD thesis in his lab at the University of Zurich, Department of Child and Adolescent Psychiatry. I like to thank Prof. Dr. Daniel Brandeis and Prof. Dr. Lutz Jäncke for recommending this thesis to the Faculty of Arts of the University of Zurich.

I like to thank Prof. Daniel Brandeis and Dr. Lars Michels for their mentoring and valuable support. I like to thank Dr. Lars Michels for his great dedication directed into our teamwork and to the success of the project. I also like to thank Dr. Kerstin Bucher for her introduction and supervision in the beginning of the project. I like to thank Prof. Dr. Ernst Martin at the MR-Center of the Childrens Hospital Zurich for this most valuable cooperation.

I'd like to thank the members of the ZNZ international PhD Programme steering committee Prof. Dr. Daniel Brandeis, Prof. Dr. Martin Wolf, Prof. Dr. Ernst Martin and Prof. Dr. Lutz Jäncke for their support.

I am very grateful to the excellent infrastructure I stood to benefit from at the Department of Child and Adolescent Psychiatry and the Jugendpsychiatrischer Dienst des Kanton Zürichs, respectively. I am grateful to have joined the brain mapping team, giving me a very friendly and supportive social environment. Special thanks to Silvia Bach and Antonia Bak and their splendid company and the times we shared laughed our heads off.

Many thanks to all those who participated in our demanding recordings, especially the children and their parents. This work was only achieved due to their volunteering, their interest, patience and commitment.

7 Curriculum Vitae

Rafael Lüchinger
Feldeggstrasse 74, CH-8008
Born on the 20. September 1979, Zurich, Switzerland

Education

2008–2011	Ph.D. thesis, University of Zurich, Department of Child and Adolescent Psychiatry International Ph.D. Program in Neuroscience, Neuroscience Center Zurich
2001–2007	Master of Science, University of Zurich Psychology, Human Movement Sciences and Sport and Educational sciences
1996–2001	Matura (highschool), Kantonsschule Stadelhofen Zurich

Employment

01–03/2008	Research Assistant (Swiss Civilian Service), University Psychiatric Clinics Basel, Child and Adolescent Psychiatry Clinic
07–12/2007	Research Assistant (Swiss Civilian Service), University Hospital Zurich, Clinic of Neonatology, Biomedical Optics Research Laboratory
04–06/2006	Internship, Swiss Federal Highschool of Sport Magglingen, Sportpsychology
06–08/2005	Internship, Research Institute for Safety and Security in Transportation (RISST), School of Engineering and Applied Sciences, University of Buffalo, State University of New York, USA
2004–2006	Research Assistant, University of Zurich, Institute of Psychology, Visual Cognition Research Group
2002–2007	Tutor for research methods in experimental psychology, University of Zurich, Institute of Psychology
02–07/2006	Semester assistance, University of Zurich, Institute of Educational Sciences
02–07/2001	Assistance (Swiss Civilian Service), Zentrum für Gehör und Sprache Zürich

Zurich, March 2, 2012

Publications

Paper

Michels L, Martin E, Klaver P, Edden R, Zelaya F, Lythgoe D, Lüchinger R, Brandeis D, O'Gorman R. Frontal GABA levels change during working memory. PLoS ONE. Article accepted for publication.

Lüchinger R, Michels L, Martin E, Brandeis D. (2012). Brain state regulation during normal development: Intrinsic activity fluctuations in simultaneous EEG–fMRI. Neuroimage (60), 1426-1439.

Lüchinger R, Michels L, Martin E, Brandeis D. (2011). EEG–BOLD correlations during (post-) adolescent brain maturation. Neuroimage (56), 1493-1505.

Michels L, Bucher K, Brem S, Halder P, Lüchinger R, Liechti M, Martin E, Jeanmonod D, Kröll J, Brandeis D. (2011). Does Greater Low Frequency EEG Activity in Normal Immaturity and in Children with Epilepsy Arise in the Same Neuronal Network? Brain Topography (24), 78-89.

Michels L, Bucher K, Lüchinger R, Klaver P, Martin E, Jeanmonod D, Brandeis D. (2010). Simultaneous EEG–fMRI during a Working Memory Task: Modulations in Low and High Frequency Bands. PLoS ONE 5(4).

Lüchinger R: X-Ray Object Recognition Test, Version 2.0 (XRay ORT 2.0). Lizentiatsarbeit, Universität Zürich, Psychologisches Institut, 2007.

Talks

Lüchinger R: EEG–BOLD signal coupling and brain development. 19. German EEG/EP Mapping Meeting, Marburg, Germany, 15-17.10.2010.

Lüchinger R: fMRI Bildgebung; simultane Bildgebung. Blockkurs "EEG Felder und Hirnfunktionen", UZH / ETH. Herbstsemester 2010.

Lüchinger R: Brain maturation mirrored by co-registered electrophysiological and hemodynamic signal oscillations. Blockkurs "EEG Felder und Hirnfunktionen", UZH / ETH. Sommersemester 2011.

Lüchinger R: Einführung zu simultanem EEG–fMRI, eigene Forschungsansätzen und Resultate. Labor Vorstellung. Zentralinstitut für Seelische Gesundheit, Departement für Kinder- und Jugendpsychiatrie und Psychotherapie. Mannheim, 2010.

Posters

Lüchinger R. et. al. Frequency dependent EEG power synchronization correlates with the BOLD signal during working memory. 5th Symposium of the Zurich Center for Integrative Human Physiology (ZIHP). Universität Zürich, 2009.

Lüchinger R. et. al. Frequency dependent EEG power synchronization correlates with the BOLD signal during working memory. 9th International Congress of the European Society of Magnetic Resonance in Neuropediatrics, University Hospital Zurich, Switzerland. 2009.

Lüchinger R. et. al. Frequency dependent EEG power synchronization correlates with the BOLD signal during working memory. Symposium of the Neuroscience Center Zurich (ZNZ). 2009.

Lüchinger R. et. al. Frequency dependent EEG power synchronization correlates with the BOLD signal during working memory. 16th Annual Meeting of the Organization for Human Brain Mapping. Barcelona, Spain, 6-10.7.2010.

Lüchinger R. et. al. Investigating late brain maturation using simultaneous EEG–fMRI. 6th Symposium of the Zurich Center for Integrative Human Physiology (ZIHP). Universität Zürich, 2010.

Lüchinger R. et. al. Investigating late brain maturation using simultaneous EEG–fMRI. Symposium of the Neuroscience Center Zurich (ZNZ). 2010.

Lüchinger R. et. al. Brain maturation captured by co-registered electrophysiological (EEG) and hemodynamic (fMRI) signal fluctuations. 7th Symposium of the Zurich Center for Integrative Human Physiology (ZIHP). 2011.

Lüchinger R. et. al. Brain maturation captured by co-registered electrophysiological (EEG) and hemodynamic (fMRI) signal fluctuations. Symposium of the Neuroscience Center Zurich (ZNZ). 2011.